



**UNSW**  
A U S T R A L I A

School of Risk and Actuarial Studies  
UNSW Business School  
University of New South Wales  
Sydney, Australia

# **Longevity Risk Management: A Value-Based Longevity Index for Retirement Income Portfolios**

**Kevin Krahe**

Supervised by Dr. Jonathan Ziveyi,  
Professor Michael Sherris and Dr. Andrés Villegas

A thesis submitted in partial fulfilment of the requirements  
for the degree of Bachelor of Actuarial Studies (Honours)

November 2018

# Declaration

‘I hereby declare that this submission is my own work and to the best of my knowledge it contains no materials previously published or written by another person, or substantial proportions of material which have been accepted for the award of any other degree or diploma at UNSW or any other educational institution, except where due acknowledgement is made in the thesis. Any contribution made to the research by others, with whom I have worked at UNSW or elsewhere, is explicitly acknowledged in the thesis. I also declare that the intellectual content of this thesis is the product of my own work, except to the extent that assistance from others in the project’s design and conception or in style, presentation and linguistic expression is acknowledged.’

---

Kevin Krahe  
November, 2018

# Acknowledgements

First and foremost, I would like to express my sincere gratitude to my Honours supervisors, Dr Jonathan Ziveyi, Professor Michael Sherris, and Dr Andrés Villegas for their dedication, guidance and support throughout the year. I have learned so much under their supervision and it has been a great privilege to work alongside such outstanding mentors.

I would also like to extend my thanks to the entire team at the School of Risk and Actuarial Studies and the Australian Research Council Centre of Excellence in Population Ageing Research. Their valued feedback, suggestions and encouragement along the way have been greatly appreciated. A sincere thanks also to my fellow research students in the School of Risk and Actuarial Studies for their support and assistance.

I would like to acknowledge the generous financial support provided by the UNSW Business School, the Australian Research Council Centre of Excellence in Population Ageing Research, the Society of Actuaries, the Australian Prudential Regulatory Authority and the Reserve Bank of Australia. It has been an honour to be awarded these prestigious scholarships and work in partnership with such great organisations.

# Abstract

Retirement income providers, such as defined benefit pension funds and annuity providers, are heavily exposed to longevity risk. Some estimates suggest that each additional year of life expectancy increases pension liability values by 3 to 4 percent. As such, it is critical for retirement income providers to manage their longevity risk exposure effectively. The traditional approach to managing longevity risk involves transferring pension liabilities to reinsurers. However, reinsurers have a finite capacity for assuming longevity risk. Given the rapid growth of the world's aggregate longevity risk exposure, this limit is rapidly being approached. In recent years, the development of a longevity risk transfer market has emerged as a potential solution to greatly expand capacity for absorbing longevity risk.

To date, most longevity market transactions have been customised indemnity swaps: hedges that are customised to transfer a specific retirement income provider's pension liability to a counterparty. However, the complexity of having to analyse portfolio-specific details has made these instruments unappealing to capital markets. In contrast, standardised index-based hedges, in which cashflows are tied to some published longevity index that tracks the mortality experience of a broad population, are much simpler for investors to manage. Therefore, they have greater potential to develop sufficient market liquidity and become viable longevity risk transfer instruments. However, with cashflows determined by a broad longevity index rather than the survival experience of a specific pension pool, index hedging exposes retirement income providers to basis risk – a significant barrier to these types of transactions.

The availability of a longevity index that closely tracks the value of longevity-linked liabilities could significantly improve hedging efficiency. Such an index would have to account for the major risks facing retirement income providers: longevity risk, interest rate risk and inflation risk. The lack of such a longevity index in the market has turned retirement income providers away from index hedges under the assumption that the associated basis risk exposure would remain excessive.

Our contribution to the literature is threefold. Firstly, we construct a universal value-based longevity index whose functionality is illustrated with U.S. economic and population data. The index is defined as the expected present value of a unit of longevity and inflation-indexed income, thereby providing an index that closely

tracks longevity-linked liability values. It also facilitates the attribution of risks associated with retirement income portfolios into distinct longevity risk, inflation risk and interest rate risk components. Through the comparison of multiple different types of indices, we find that all three components have a material impact on hedging efficiency.

Our second contribution involves the robust analysis of basis risk. We present numerical tests demonstrating that our proposed hedging framework generates a material reduction in basis risk relative to standard mortality rate indices widely used in the market, such as the Life and Longevity Market Association's Lifemetrics Index, as well as survival rate indices proposed by the Institute and Faculty of Actuaries' Longevity Basis Risk Working Group.

Finally, we bridge the literature gap between continuous and discrete-time multi-population mortality models by comparing the hedge effectiveness associated with the constructed value-based longevity index under both mortality frameworks. It is found that the two modelling approaches suggest relatively similar hedging outcomes.

# Contents

<b>1</b>	<b>Introduction</b>	<b>11</b>
1.1	Background and Research Motivation . . . . .	11
1.2	Research Objectives . . . . .	18
1.2.1	Construction of a Universal Value-Based Longevity Index . . .	18
1.2.2	Decomposed Longevity Basis Risk Quantification for Hedge Comparisons . . . . .	19
1.2.3	Comparison of Continuous-Time and Discrete-Time Multi- Population Mortality Modelling Frameworks . . . . .	19
1.3	Thesis Outline . . . . .	20
<b>2</b>	<b>Literature Review</b>	<b>21</b>
2.1	The Longevity Risk Transfer Market . . . . .	21
2.1.1	Longevity-Linked Instruments . . . . .	22
2.1.2	Longevity Indices . . . . .	25
2.2	Longevity Basis Risk . . . . .	26
2.3	Multi-Population Mortality Modelling . . . . .	29
2.4	Value-Based Longevity Indices . . . . .	33
2.5	Gaps in the Literature . . . . .	35
<b>3</b>	<b>Mortality Modelling Frameworks</b>	<b>37</b>
3.1	Joint Affine Term Structure Model . . . . .	37
3.1.1	Model Specification . . . . .	37
3.1.2	Model Calibration . . . . .	39
3.1.3	Forecasting and Simulation . . . . .	41
3.2	M7-M5 Mortality Model . . . . .	45
3.2.1	Model Specification . . . . .	46
3.2.2	Model Calibration . . . . .	46
3.2.3	Forecasting and Simulation . . . . .	48
<b>4</b>	<b>Interest Rate Modelling Frameworks</b>	<b>51</b>
4.1	Nominal Interest Rate Model . . . . .	51
4.1.1	Model Specification . . . . .	51

4.1.2	Model Calibration . . . . .	52
4.1.3	Forecasting and Simulation . . . . .	55
4.2	Real Interest Rate Model . . . . .	57
4.2.1	Model Specification . . . . .	57
4.2.2	Model Calibration . . . . .	58
4.2.3	Forecasting and Simulation . . . . .	62
<b>5</b>	<b>Value-Based Longevity Index and Longevity Risk Hedging</b>	<b>63</b>
5.1	Index Construction . . . . .	63
5.2	Hedging Strategy . . . . .	66
5.3	Comparison Against Other Longevity Indices . . . . .	69
5.3.1	Survival Index . . . . .	69
5.3.2	Value-Based Longevity Index without Inflation-Indexation . . . . .	69
5.4	Basis Risk Analysis . . . . .	70
5.5	Sensitivity Analysis . . . . .	74
5.5.1	Book Size . . . . .	74
5.5.2	Discrete-Time Mortality Model . . . . .	75
5.5.3	Extending to Age 90 . . . . .	79
<b>6</b>	<b>Conclusion</b>	<b>84</b>
6.1	Key Contributions . . . . .	84
6.1.1	Construction of a Universal Value-Based Longevity Index . . . . .	84
6.1.2	Decomposed Longevity Basis Risk Quantification for Hedge Comparisons . . . . .	85
6.1.3	Comparison of Continuous-Time and Discrete-Time Multi-Population Mortality Modelling Frameworks . . . . .	85
6.2	Limitations and Areas for Future Research . . . . .	85
6.2.1	Book Population Data . . . . .	85
6.2.2	Application to Realistic Retirement Income Portfolios . . . . .	86
6.2.3	Dynamic Hedging . . . . .	86
6.2.4	Incorporation of the Longevity Risk Premium . . . . .	87
6.2.5	Further Sensitivity Analyses . . . . .	87
	<b>References</b>	<b>93</b>

# List of Figures

1.1	Longevity market worldwide trading volumes from 2007 to 2018 . . .	13
1.2	Transaction diagram for the Canada Life customised longevity swap .	16
2.1	Longevity bond cashflows . . . . .	22
2.2	Longevity swap cashflows . . . . .	24
2.3	Net q-forward payment as a function of the realised population mortality rate . . . . .	24
2.4	Net S-forward payment as a function of the realised population survival rate . . . . .	25
2.5	Xpect survival indices by pension amount (England and Wales 1935 to 1939 male cohort) . . . . .	26
2.6	Comparison of male mortality rates for the U.K. assured and E.W. national populations . . . . .	27
2.7	Overview of discrete-time multi-population mortality modelling . . .	30
2.8	Decision tree for modelling demographic basis risk as developed by the Longevity Basis Risk Working Group . . . . .	32
2.9	BlackRock's Cost of Retirement Index showing the \$ value of the index associated with twenty U.S. cohorts as at 24/10/2018 . . . . .	34
2.10	CoRI determinants . . . . .	35
3.1	Observed average force of mortality for ages 60 to 84 from 1999 to 2016 in the reference and book populations . . . . .	41
3.2	Book to reference population average force of mortality ratio for ages 60 to 84 from 1999 to 2016 . . . . .	42
3.3	Fitted average force of mortality for ages 60 to 84 from 1999 to 2016 in the reference and book populations . . . . .	42
3.4	Simulated average force of mortality for ages 60 to 84 from 2017 to 2036 in the reference and book populations . . . . .	44
3.5	Simulated survival curves for ages 60 to 84 from 2017 to 2036 in the reference and book populations . . . . .	44
3.6	Simulated survival curves for the reference population cohort aged 65 in 2017 over a 20 year simulation horizon . . . . .	45

3.7	Reference population: estimated factors and cohort effect . . . . .	47
3.8	Book population: estimated factors . . . . .	48
3.9	Reference population: estimated, forecast and simulated factors . . .	49
3.10	Forecast mortality rates for ages 65 to 84 from 2017 to 2036 for the reference and book populations . . . . .	50
4.1	Observed nominal bond yields from October 2006 to May 2018 . . . .	53
4.2	Fitted nominal bond yields from October 2006 to May 2018 . . . . .	53
4.3	Observed and fitted nominal mean yields, October 2006 to May 2018	56
4.4	Simulated nominal bond prices over a 20 year simulation horizon . . .	57
4.5	Observed real bond yields from February 2010 to May 2018 . . . . .	59
4.6	Fitted real bond yields from February 2010 to May 2018 . . . . .	59
4.7	Observed and fitted real mean yields, February 2010 to May 2018 . .	61
4.8	Simulated real bond prices over a 20 year simulation horizon . . . . .	62
5.1	Initial index value by age (joint ATSM) . . . . .	65
5.2	Forward and simulated index values, (joint ATSM) . . . . .	65
5.3	Liability present value histogram, (joint ATSM, 100,000 lives) . . . .	67
5.4	Simulated swap payments (joint ATSM) . . . . .	68
5.5	Hedged and unhedged liability present value distributions by hedging index (joint ATSM, 100,000 lives) . . . . .	71
5.6	Hedged and unhedged liability present value box and whisker plots by hedging index (joint ATSM, 100,000 lives) . . . . .	72
5.7	Longevity risk reduction: % reduction in variance (joint ATSM) . . .	74
5.8	Hedge efficiency by book size (joint ATSM) . . . . .	75
5.9	Forward and simulated index values, (M7-M5 model) . . . . .	76
5.10	Simulated swap payments (M7-M5 model) . . . . .	77
5.11	Liability present value distributions histogram, (M7-M5 model, 100,000 lives) . . . . .	78
5.12	Hedged and unhedged liability present value distributions by hedging index (M7-M5 model, 100,000 lives) . . . . .	78
5.13	Hedged and unhedged liability present value box and whisker plots by hedging index (M7-M5 model, 100,000 lives) . . . . .	79
5.14	Longevity risk reduction: % reduction in variance (M7-M5 model) . .	80
5.15	Forward and simulated index values (joint ATSM extended to age 90)	81
5.16	Simulated swap payments (joint ATSM extended to age 90) . . . . .	82
5.17	Liability present value histogram (joint ATSM extended to age 90, 100,000 lives) . . . . .	82
5.18	Hedged and unhedged liability present value distributions – inflation- linked value index (joint ATSM extended to age 90, 100,000 lives) . .	83

# List of Tables

1.1	Details of notable longevity swap transactions . . . . .	14
2.1	Longevity-linked instruments . . . . .	23
4.1	Nominal interest rate summary statistics . . . . .	54
4.2	Nominal interest rates: residual mean and standard deviation by maturity . . . . .	55
4.3	Real interest rate summary statistics . . . . .	60
4.4	Real interest rates: residual mean and standard deviation by maturity	61
5.1	Risk coverage of different longevity indices . . . . .	70
5.2	Summary statistics: hedged and unhedged liability present value outcomes by hedging index (joint ATSM, 100,000 lives) . . . . .	72
5.3	Summary statistics: hedged and unhedged liability present value outcomes by hedging index (M7-M5 model, 100,000 lives) . . . . .	77
5.4	Model hedge effective comparison (% reduction in variance, 100,000 lives) . . . . .	79

# Chapter 1

## Introduction

### 1.1 Background and Research Motivation

Over recent centuries, rising living standards, lifestyle changes and improved access to healthcare and education have driven substantial improvements in life expectancy worldwide. Indeed, Oeppen and Vaupel (2002) find that the record female life expectancy increased by 40 years between 1840 and 2000 – a rate which translates into an improvement of 15 minutes every hour. Although this is a very positive development, it does create retirement funding challenges for both governments and the private sector alike. There is also uncertainty surrounding the rate of mortality improvements in the future, creating longevity risk. The Institute and Faculty of Actuaries (2015) defines longevity risk as *“the risk that members of some reference population might live longer on average than anticipated”*.

In particular, retirement income providers, such as defined benefit pension funds and annuity providers, are heavily exposed to longevity risk. As people survive to increasingly older ages, retirement income providers are obligated to pay out lifetime income streams for potentially much longer than initially expected. Some estimates suggest that each additional year of life expectancy increases pension liability values by 3 to 4 percent (International Monetary Fund, 2012; Chang and Sherris, 2018). The world’s aggregate longevity risk exposure is growing rapidly. The Global Pension Assets Study 2018 published by Willis Towers Watson (2018) has reported that the value of defined benefit pension assets has grown by 4.5% per year over the last 20 years, and was valued at U.S.\$21.3 trillion as of February 2018. It is estimated that each year of life expectancy underestimation could potentially cost risk holders up to U.S.\$1 trillion in additional unexpected benefit payments (Joint Forum, 2013). Therefore, it is critical for retirement income providers to manage longevity risk effectively.

There are three broad approaches that retirement income providers can take to manage their longevity risk exposure. The traditional approach is to transfer liabilities to life insurance or reinsurance companies (Coughlan et al., 2011). This

can be achieved through either a pension buy-in or a pension buy-out, as described by Blake et al. (2018).

Under a pension buy-out, both the assets and liabilities associated with a retirement income portfolio are transferred to an insurer in exchange for an initial premium. The retirement income provider is indemnified of any future obligations to fund members, as the liability and its associated risks, including longevity risk, are fully transferred to the insurer. The annuitants or pension fund members are now exposed to the counterparty risk associated with the buy-out insurer rather than the original retirement income provider.

Under a pension buy-in, the retirement income provider pays an initial premium to the reinsurer and in exchange receives periodic cash flows from the reinsurance company to match its payments to the annuitants or pension fund members. The retirement income portfolio's assets and liabilities are retained on balance sheet and payments continue to be made directly to surviving members. Although pension buy-ins eliminate longevity risk, the retirement income provider remains exposed to the counterparty risk of the reinsurer.

However, reinsurers have a limited capacity and appetite for assuming longevity risk (Wadsworth, 2005). Given the substantial growth in global longevity risk exposure, this limit is rapidly being approached, as noted by Barrieu et al. (2012) as well as the Joint Forum (2013). Indeed, Graziani (2014) has found that the potential worldwide demand for longevity risk transfer exceeds the supply capacity of the global insurance industry by more than ten times. Furthermore, regulations such as Solvency II have further enhanced the demand for longevity reinsurance as a means of reducing solvency capital requirements (Xu et al., 2017).

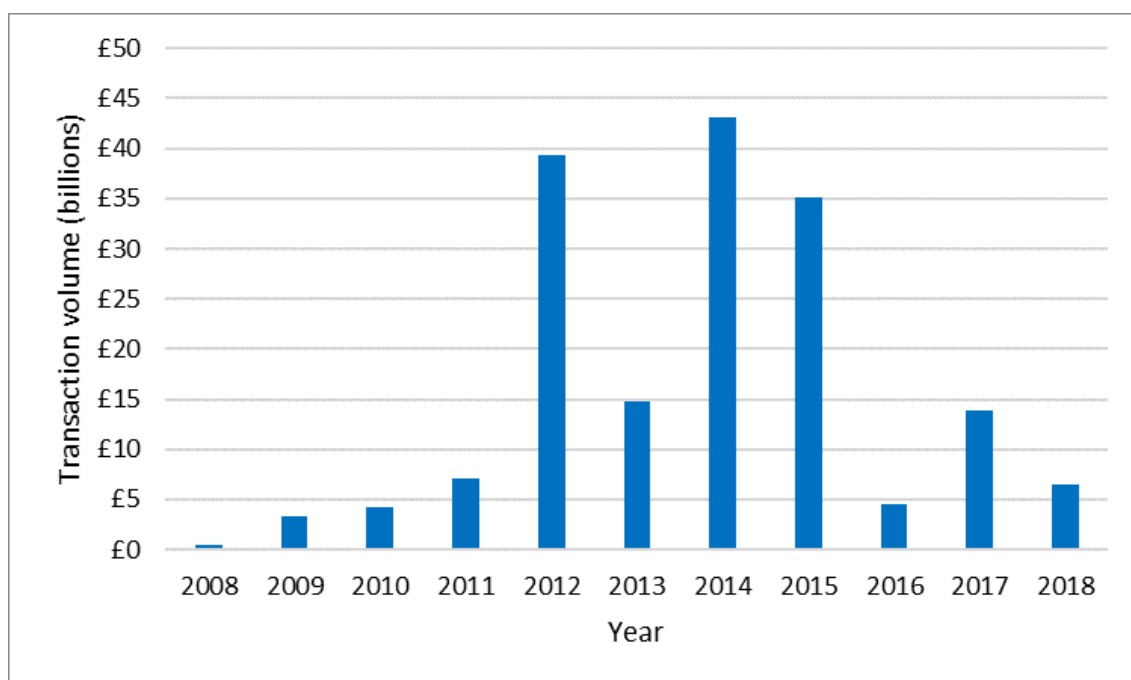
Large financial institutions which sell both retirement income products and life insurance policies are able to partially offset the longevity risk exposure of their pension liability by means of natural hedging (Cox and Lin, 2007; Loeys et al., 2007). Retirement income portfolios have a negative exposure to longevity risk since their liability values increase as survival rates improve. Conversely, life insurance portfolios have positive longevity risk exposure as increasing longevity serves to reduce the amount paid out in death benefits (Chang and Sherris, 2018). Therefore, life insurers that sell both types of products can exploit the negative correlation between the two lines of business to manage the longevity risk exposure arising from annuity pools. However, Li and Haberman (2015) show that natural hedging can be ineffective due to demographic differences between annuity members and life insurance policyholders. Furthermore, smaller life insurers lack the sufficient scale to be able adequately manage their risk exposure through natural hedging.

In recent years, the development of a longevity risk transfer market has emerged as a potential solution, with the development of various mortality and longevity-

linked indices, instruments and derivative securities. Although still in its relatively early stages, the development of a liquid longevity risk transfer market has the potential to revolutionise the management of longevity risk. Given the size and depth of global capital markets, the notion of traded longevity risk greatly expands the overall global capacity for absorbing risks relating to retirement income portfolios. (Coughlan, 2009; Xu et al., 2017). Such alternative risk transfer mechanisms have been developed in other financial services sectors, such as catastrophe bonds in general insurance (Lee and Yu, 2007) and mortgage-backed securities in the banking industry (Dunn and McConnell, 1981).

The first capital market longevity transaction was completed in January 2008 when the U.K. pension insurer Lucida executed an index-based hedge using q-forwards tied to J.P. Morgan’s Lifemetrics Index<sup>1</sup> for England and Wales (Coughlan, 2009). In 2010, a coalition of global investment banks, insurers and reinsurers established the Life and Longevity Markets Association (LLMA)<sup>2</sup>, aiming to develop a market for the trading of various mortality and longevity-linked instruments. Key developments in the longevity risk transfer market have also been described in the literature (see, for example, Tan et al., 2015). Despite still being in its relatively early stages of development, the market has grown significantly since 2008, as shown in Figure 1.1, although transaction volumes in recent years have moderated.

**Figure 1.1:** Longevity market worldwide trading volumes from 2007 to 2018



Source: Artemis (2018)

<sup>1</sup><https://llma.org/index/index-description/>

<sup>2</sup><https://llma.org/>

**Table 1.1:** Details of notable longevity swap transactions

Pension Fund	Provider(s)	Solution(s)	Amount	Date
Delta Lloyd	RGA Re	Index-based longevity swap	€12 billion	Jun 2015
Aegon	Canada Life Re	Longevity swap and reinsurance	€6 billion	Jul 2015
Manweb (Scottish Power)	Abbey Life	Longevity swap	£1 billion	Aug 2016
AXA France	RGA Re	Longevity swap and reinsurance	€1.3 billion	Nov 2016
Pension Insurance Corporation	SCOR	Longevity swap and reinsurance	£1 billion	Jul 2017
British Airways Pension Scheme	Partner Re, Canada Life Re	Longevity swap and reinsurance	£1.6 billion	Aug 2017
National Grid	Zurich	Longevity swap	£2 billion	May 2018
Aviva	Prudential Insurance Company of America	Longevity reinsurance	U.S.\$1.4 billion	Aug 2018

Source: Artemis (2018)

From an investment perspective, the development of a longevity risk transfer market creates new asset classes and diversification opportunities. Market consensus is that the correlation between longevity trends and the returns on traditional asset classes is very limited or zero (Ribeiro and di Pietro, 2009; Anderson and Baxter, 2017). Therefore, longevity and mortality-linked instruments offer investors an opportunity to earn a longevity risk premium in exchange for accepting risks that integrate efficiently into existing portfolios, thereby expanding the set of feasible investment opportunities and improving risk-return dynamics in line with modern portfolio theory (Markowitz, 1952).

However, although the longevity risk transfer market has grown strongly, it is still dwarfed by the retirement income industry's exposure to longevity risk. For example, U.K. pension funds are estimated to have an aggregate longevity risk exposure valued at over £2 trillion (Barrieu et al., 2012). The total value of U.K. longevity swaps executed in 2015 of £10 billion represents less than 0.5% of this exposure (Li et al., 2017).

To date, there have been approximately 82 pure longevity transactions. These transactions are documented by the risk transfer and capital market database Artemis (2018)<sup>3</sup>, with several major transactions in recent years detailed in Table 1.1.

There are two broad categories of capital market longevity transfer solutions by

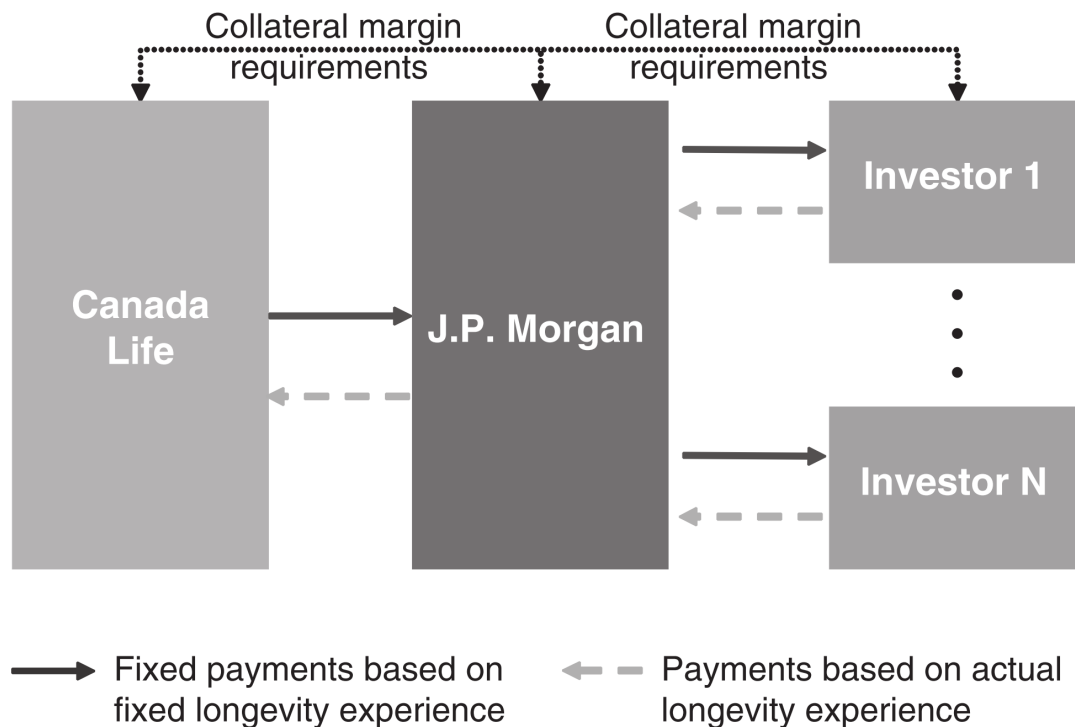
<sup>3</sup>[www.artemis.bm/library/longevity\\_swaps\\_risk\\_transfers.html](http://www.artemis.bm/library/longevity_swaps_risk_transfers.html)

which retirement income providers can hedge their exposure to unexpected changes in future mortality rates: customised indemnity-based hedges (indemnity hedges) and standardised index-based hedges (index hedges). Both generally take the form of some swap instrument whereby the hedger pays the fixed leg based on some predetermined best estimate value (that is, expected longevity experience) plus a risk premium, while the counterparty pays the floating leg based on realised mortality experience over time (Coughlan, 2009).

To date, most longevity risk transfer market transactions have been customised or “bespoke” indemnity swaps: customised over-the-counter hedges that transfer a retirement income provider’s specific longevity risk exposure to a counterparty (Anderson and Baxter, 2017). That is, the survival experience over time of the members and any other beneficiaries within the exposure will determine the cash-flows associated with the hedging instrument, with the pension fund or annuity provider retaining zero residual financial exposure. This type of survivor swap involves the hedger paying the expected annuity amounts to the counterparty which in return pays the actual realised payments to surviving members or annuitants over time. The counterparty may be the end investor, or may pass on the exposure to other investors and financial institutions. There is no basis risk associated with the hedge for the retirement income provider as the counterparty effectively assumes all obligations arising from the exposure. From an economic perspective, an indemnity hedge is identical to the traditional approach of transferring the annuity book to a life insurer or reinsurer, however in the format of a capital market instrument (Coughlan, 2009).

Figure 1.2 shows the structure and parties involved in the first ever indemnity hedge transaction, which took place in July 2008 when the U.K.’s Canada Life arranged a fully collateralised 40 year survivor swap with J.P. Morgan worth £500 million. As shown in Figure 1.2, J.P. Morgan subsequently transferred the exposure to a group of hedge funds and capital market investors (Trading Risk, 2008). The largest longevity market transaction completed to date also took the form of a customised hedge: in June 2014, the British Telecom Pension Scheme entered into a £16 billion indemnity swap with the Prudential Insurance Company of America, a deal which covered more than 25% of the pension fund’s total longevity risk exposure (Artemis, 2014).

The major drawback to indemnity hedges is that these transactions require the disclosure and analysis of fund-specific details on the portfolio being hedged. Details such as the portfolio’s particular demographic composition, mortality experience and benefit structure need to be made available to any counterparties for both pricing and hedge settlement purposes (Coughlan, 2009). This makes it substantially more complex and costly for capital markets to analyse, value and manage customised

**Figure 1.2:** Transaction diagram for the Canada Life customised longevity swap

Source: J.P. Morgan; Coughlan (2009)

longevity hedging instruments, thereby discouraging potential investors and inhibiting the development of market liquidity. This in turn can make it cost prohibitive for retirement income providers to hedge their longevity risk exposure in this manner.

An index hedge, however, is based on the mortality experience over time of some underlying reference population as represented by a published longevity index. For example, the Lifemetrics Index (J.P. Morgan, 2007) provides population-level life expectancies and mortality rates for various countries. Index hedges are generally structured as q-forwards whereby the retirement income provider pays the expected mortality rate of the reference population plus a longevity risk premium at some specified future time point, while the counterparty pays the realised mortality rate (as published by the specified longevity index) at that time. As outlined previously, the first ever capital market longevity transaction was completed in January 2008 when the U.K. pension insurer Lucida executed an index-based hedge using q-forwards tied to the Lifemetrics Index for England and Wales (Coughlan, 2009). In February 2012, Dutch life insurer Aegon arranged a €12 billion index hedge with Deutsche Bank in which the national population of the Netherlands was used as the underlying reference population (Li et al., 2017).

In contrast to indemnity hedges, index hedges do not require the analysis of portfolio-specific details; cashflows only depend on population-level mortality expe-

rience as represented by the published longevity index which makes it much simpler for investors to understand and manage the associated risks. Therefore, these instruments have a much greater potential to develop sufficient market liquidity over time and become viable longevity risk transfer vehicles. Furthermore, index hedges are substantially less credit intensive than indemnity hedges, are easier to unwind or adjust over time if needed and provide for greater transparency (Villegas et al., 2017). They also represent the only viable approach to hedging the entire longevity risk exposure of larger pension funds (Coughlan, 2009) and are the most appropriate instruments for hedging the risks arising from retirement income portfolios with deferred income elements (Coughlan, 2009a). However, despite the many advantages associated with index-based longevity hedging, several barriers have prevented the market from embracing these types of standardised transactions. These barriers essentially relate to the fact that index-based hedges cannot hedge the specific mortality experience of a given annuity book or pension fund because, by definition, payments are determined with respect to the mortality experience of a broad reference population as represented by a published longevity index (Coughlan et al., 2007). Therefore, while index hedges can reduce a retirement income provider's longevity risk exposure, it cannot completely indemnify them of the exposure; that is, these instruments are subject to longevity basis risk. Given the dominance of customised hedging transactions observed to date in the longevity risk transfer market, the basis risk issue has evidently proved a significant deterrent to the use of index-based longevity hedges (Li et al., 2015).

To date, the few index-based longevity hedging transactions have referenced longevity indices linked to national life tables such as the Lifemetrics Index and the Xpect-Club Vita Index (Deutsche Börse, 2012). However, it is insufficient to only focus on longevity risk since retirement income providers also retain material exposure to interest rate and inflation risk (Towers Watson, 2013). The failure of major indices to incorporate these risks have deterred retirement income providers from pursuing index hedges under the assumption that the basis risk exposure would remain significant. However, the availability of a longevity index that closely tracks the value of longevity-linked liabilities could significantly reduce basis risk (Sweeting, 2010; Wills and Sherris, 2010). This notion motivated the development of value-based longevity indices by Sherris (2009) – indices which are constructed to track the expected present value of a unit of longevity-indexed income. As demonstrated in Chang and Sherris (2018), value-based longevity indices are associated with improved hedge outcomes and reduced levels of longevity basis risk relative to mortality rate indices. These findings have the potential to revitalise the demand for index-based hedging solutions.

Furthermore, in order for index hedges to gain industry acceptance as viable

longevity risk management vehicles, retirement income providers must be able to effectively assess hedge efficiency in the context of their individual portfolios. This requires a flexible yet robust methodology for quantifying the longevity basis risk exposure associated with a given longevity index for a given retirement income portfolio (Haberman et al., 2014; Villegas et al., 2017; Li et al., 2017).

This brings us to our research, which aims to address the aforementioned barriers to index-based longevity hedging as a means of incentivising and accelerating the transition towards the standardised transfer of longevity risk. To this end, our research is ultimately guided by the goal of promoting the capital market as a viable vehicle for absorbing the risks arising from the management of retirement income portfolios.

## 1.2 Research Objectives

There are three objectives that our research aims to accomplish. These objectives represent important original contributions to the literature while also retaining the practically-focused motivation of supporting the progression towards the index-based hedging of risks arising from retirement income portfolios such as annuity books and defined benefit pension schemes.

### 1.2.1 Construction of a Universal Value-Based Longevity Index

Our first research objective is to construct a universal value-based longevity index and illustrate its functionality with the aid of U.S. economic and population data. Inspired by Sherris (2009), the index will be defined as the expected present value of a unit of longevity and inflation-indexed income, thereby incorporating both interest rate and inflation risk unlike other value-based longevity indices constructed in the literature which only consider interest rate risk. The index will also be split by gender – a distinguishing feature from BlackRock’s Cost of Retirement Indices<sup>4</sup>. This contribution will address the first key barrier to index-based longevity hedging (that is, the availability of an index that closely tracks the value of longevity-linked liabilities).

Furthermore, although the three main aspects of risk inherent in standard retirement income portfolios have been identified in the literature (see, for example, Towers Watson, 2013), there has been little in terms of quantifying the relative impact of each risk factor. The construction of the aforementioned value-based

---

<sup>4</sup><https://www.blackrock.com/cori/fact-sheets>

longevity index can therefore facilitate an additional contribution to the literature through the attribution of risk arising from retirement income portfolios into distinct longevity risk, interest rate risk and inflation risk components.

### **1.2.2 Decomposed Longevity Basis Risk Quantification for Hedge Comparisons**

Our second major research objective is to quantify the residual basis risk exposure arising from standardised hedges tied to the constructed value-based longevity index using the decomposed framework proposed by the Longevity Basis Risk Working Group (LBRWG) (Haberman et al., 2014; Villegas et al., 2017; Li et al., 2017). This method separates longevity basis risk into its constituent components, allowing for a more holistic and thorough evaluation. By applying this framework to our universal value-based longevity index and demonstrating the reduction in basis risk relative to standard mortality rate indices, we will contribute towards the second major barrier to index-based longevity hedging described above (that is, the minimisation and robust quantification of longevity basis risk). Furthermore, to date, no work in the literature has applied the LBRWG's decomposed basis risk quantification framework to a value-based longevity index, marking another important literature gap that we expect to fill.

### **1.2.3 Comparison of Continuous-Time and Discrete-Time Multi-Population Mortality Modelling Frameworks**

Our base research methodology entails a continuous-time multi-population mortality modelling approach. However, we will also repeat the index construction process and basis risk analysis within a discrete-time mortality modelling framework. This will facilitate the comparison of hedge effectiveness under the two different mortality modelling regimes. To date, no such comparison has been made in the longevity risk transfer market literature. Furthermore, this contribution will also support the assessment of model risk on hedge outcomes.

Ultimately by making these contributions to the literature, our research has the potential to incentivise and accelerate the transition towards index-based longevity hedging. This is of critical importance since index-based longevity hedging represents arguably the most realistic prospect for a viable and liquid longevity risk transfer market, given all of the complexities associated with indemnity-based longevity hedges.

## 1.3 Thesis Outline

The remainder of this thesis is organised as follows. Chapter 2 reviews the literature on the key events in the longevity risk transfer market to date, including the development of longevity-linked instruments and indices, the conception of value-based longevity indices, as well as longevity basis risk quantification techniques such as the use of continuous and discrete-time multi-population mortality models. Chapter 3 describes the estimation, forecasting and simulation of the continuous and discrete-time mortality modelling framework adopted in this thesis. The modelling of the nominal and real term structure of interest rates is covered in Chapter 4. Chapter 5 describes the design of the proposed value-based longevity index and the process for calibrating and evaluating hedges tied to the constructed index. Furthermore, we also present a range of sensitivity analyses, including the comparison of hedge effectiveness for various longevity indices under different mortality modelling frameworks. Chapter 6 concludes the thesis by reiterating the fundamental contributions of our research, the limitations of our findings as well as the scope for future research to extend and build upon our contributions to the literature.

# Chapter 2

## Literature Review

In this chapter, we review the literature detailing the development of the longevity risk transfer market, including the range of mortality and longevity-linked securities and derivatives available as well as the major longevity indices, in Section 2.1. As alluded to in Chapter 1, basis risk is a critical issue when it comes to index-based longevity hedging. Therefore, Section 2.2 explores basis risk in substantial depth, both in terms of its conceptual decomposition as well as how each of its constituent components can be modelled and quantified by retirement income providers. In Section 2.3, we review the development of multi-population mortality models – stochastic actuarial models that project how the mortality rates of several populations may evolve over time. Section 2.4 summarises the literature on value-based longevity indices, including the motivation for their development, industry innovations and their effectiveness in index hedging applications. Finally, we identify the gaps in the existing literature that our research is able to address in Section 2.5.

### 2.1 The Longevity Risk Transfer Market

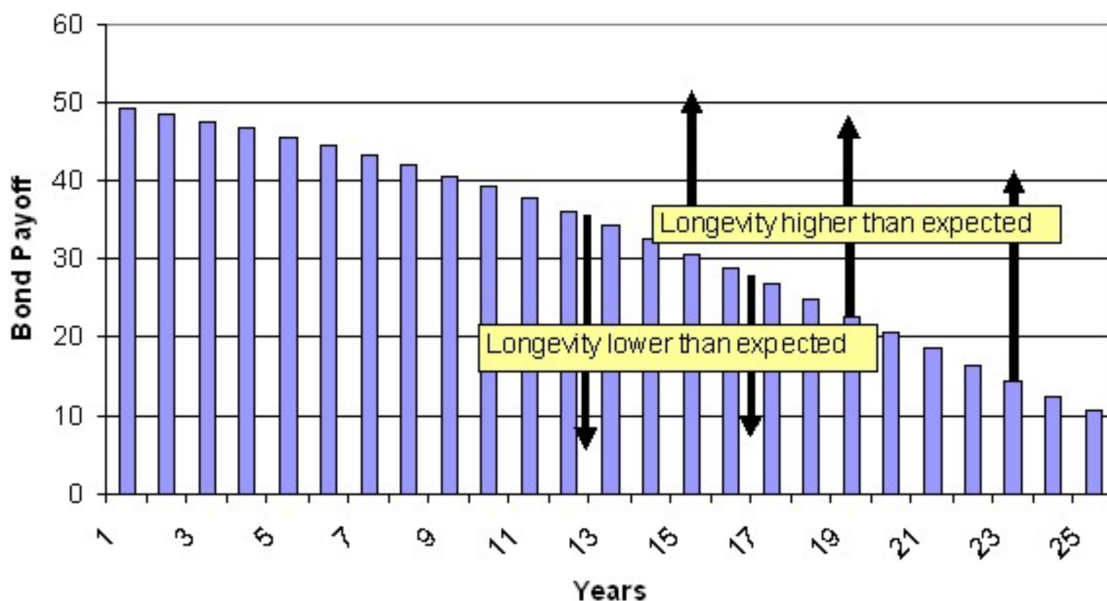
Although still in its initial stages, the development of a liquid market for hedgers and investors to actively trade mortality and longevity-linked securities and derivatives has the potential to revolutionise the management of longevity risk. Given the size and depth of capital markets, the concept of longevity risk trading greatly expands the overall capacity for absorbing global longevity risk exposure (Blake et al., 2009). Pension funds and annuity providers can reduce their counterparty risk exposure by using collateralised instruments (that is, longevity derivatives such as survivor swaps) and by diversifying their counterparty base beyond just life insurers and reinsurers. Furthermore, unlike insurance-based solutions, traded longevity-linked instruments have the potential to be highly liquid and therefore unwound with investors or institutions other than the original counterparty (Coughlan, 2009).

### 2.1.1 Longevity-Linked Instruments

There are various instruments and securities available in the longevity market as detailed in Table 2.1 (Li et al., 2017).

Longevity bonds (Blake and Burrows, 2001) remain the simplest of these securities, paying out periodic coupons, the size of which are indexed to the percentage of the underlying reference population still alive on the date of coupon payment as depicted in Figure 2.1.

**Figure 2.1:** Longevity bond cashflows



Source: Wehrhahn (2005)

Longevity (or survivor) swaps (Dowd, 2003; Dowd et al., 2006) represent a derivative form of longevity bonds, exchanging a stream of fixed future cashflows for a floating stream indexed to the realised survival experience of the reference population as shown in Figure 2.2. Such structures have the distinct advantages of providing greater flexibility and not requiring retirement income providers to modify their asset allocations in response to a significant upfront capital investment as is the case when purchasing longevity bonds (Coughlan, 2009). Indeed, longevity swaps represent the most commonly traded instrument type in the current longevity risk transfer market (Xu et al., 2017).

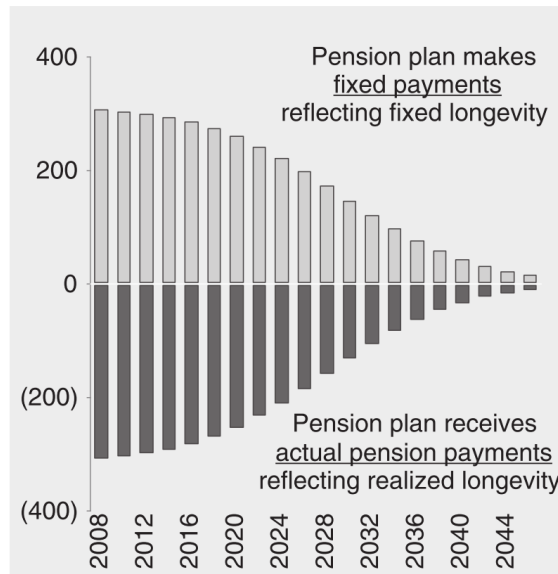
The majority of the existing literature has proposed simpler derivative structures, involving only a single exchange payments at a given future date. For example, Coughlan et al. (2007) describe the q-forward contract – a transaction in which the hedger receives the net difference between the realised and forward mortality rates of the reference population at the payment date (Figure 2.4).

**Table 2.1:** Longevity-linked instruments

<b>Instrument</b>	<b>Proposed</b>	<b>Description</b>
Longevity nond	Blake and Burrows (2001); Dowd (2003)	Coupon sizes are linked to the percentage of the reference population who are still alive (i.e. survivor index) on the coupon payment dates, in which the survivor index at time $t$ is calculated as ${}_t p_{65} = (1 - q_{65,0})(1 - q_{66,1}) \dots (1 - q_{65+t-1,t-1})$ and $q_{x,t}$ is the mortality rate of the reference population observed in year $t$
Longevity swap	Dowd (2003); Dowd et al. (2006)	Two series of future cash flows are exchanged, one of which is linked to the percentage of the reference population who are still alive (i.e. survivor index) on the payment dates, and the other series is fixed at time 0
q-forward	Coughlan et al. (2007)	To a fixed rate receiver, a payoff of $(q_{x,t}^{forward} - q_{x,t})$ is made after $T + 1$ years (maturity), in which $q_{x,t}^{forward}$ is the forward mortality rate set at time 0 and $q_{x,t}$ is the actual mortality rate of the reference population observed in year $T$ ; for a floating rate receiver, the payoff is $(q_{x,t} - q_{x,t}^{forward})$ instead
S-forward	Life and Longevity Markets Association (2010)	The payoffs are similar to those of the q-forward, with the mortality rate being replaced by the percentage of the reference population who are still alive (i.e. survivor index) on maturity
K-forward	Chan et al. (2014); Tan et al. (2014)	To a fixed rate receiver, a payoff of $(K_{t,i}^{forward} - K_{t,i})$ is made after $T + 1$ years (maturity), in which $(K_{t,i}$ is the $i^{\text{th}}$ CBD model parameter as the $i^{\text{th}}$ type of mortality index in year $t$ ), $K_{t,i}^{forward}$ is the forward mortality index set at time 0 and $K_{t,i}$ is the mortality index calculated from the actual observations of the reference population in year $T$ ; for a floating rate receiver, the payoff is $(K_{t,i} - K_{t,i}^{forward})$ instead
Mortality option	Cairns et al. (2008)	To a call holder, a payoff of $\max(q_{x,t} - q_{x,t}^{strike}, 0)$ is made after $T + 1$ years (maturity), in which $q_{x,t}^{strike}$ is a fixed rate set at time 0 and $q_{x,t}$ is the actual mortality rate of the reference population observed in year $T$ ; for a put holder, the payoff is $\max(q_{x,t}^{strike} - q_{x,t}, 0)$ instead
Survivor option	Dowd (2003)	The payoffs are similar to those of the mortality option, with the mortality rate being replaced by the percentage of the reference population who are still alive (i.e. survivor index) on maturity

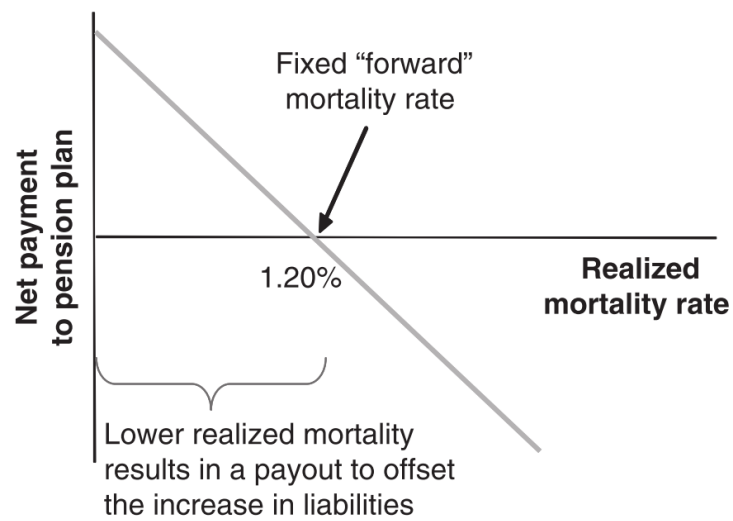
Source: Adapted from Li et al. (2017)

**Figure 2.2:** Longevity swap cashflows



Source: J.P. Morgan; Coughlan (2009)

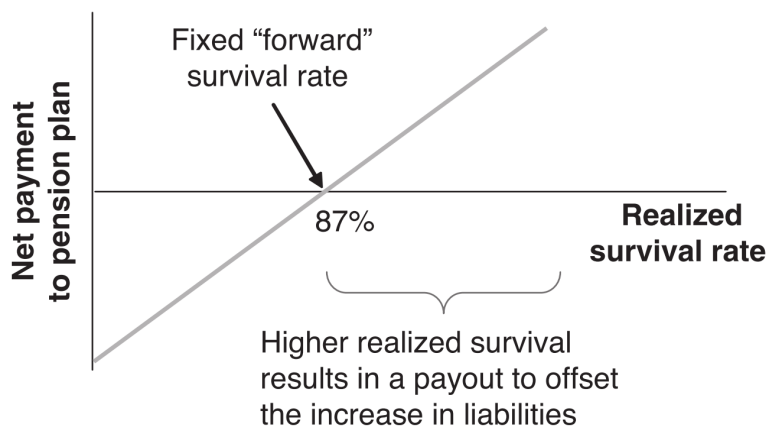
**Figure 2.3:** Net q-forward payment as a function of the realised population mortality rate



Source: J.P. Morgan; Coughlan (2009)

Similarly, the Life and Longevity Markets Association (2010) propose the trading of S-forwards; derivatives which are similar in structure to q-forwards but where the swap settlement is determined by survival rather than mortality rates.

**Figure 2.4:** Net S-forward payment as a function of the realised population survival rate



Source: J.P. Morgan; Coughlan (2009)

### 2.1.2 Longevity Indices

A key requirement for the use of any of the above standardised capital market longevity hedging instruments is a published index to underlie the derivative. It is critical that any longevity index is transparent, objective and can serve as an unbiased point of reference for all participants in the longevity risk transfer market (Loeys et al., 2007; Sweeting, 2010). There are numerous existing longevity indices, as described in Coughlan (2009) and Chang and Sherris (2018).

Credit Suisse launched the first longevity index in December 2005 based on U.S. population-level mortality data. The index included current, historical and projected mortality rates (Coughlan, 2009).

J.P. Morgan (2007) launched the Lifemetrics Index<sup>1</sup> which provides male and female period life expectancies, crude central mortality rates and graduated initial mortality rates for the U.S., England and Wales, the Netherlands and Germany (Coughlan et al., 2007). In 2010, the management of the Lifemetrics Index was assumed by the LLMA (Chang and Sherris, 2018).

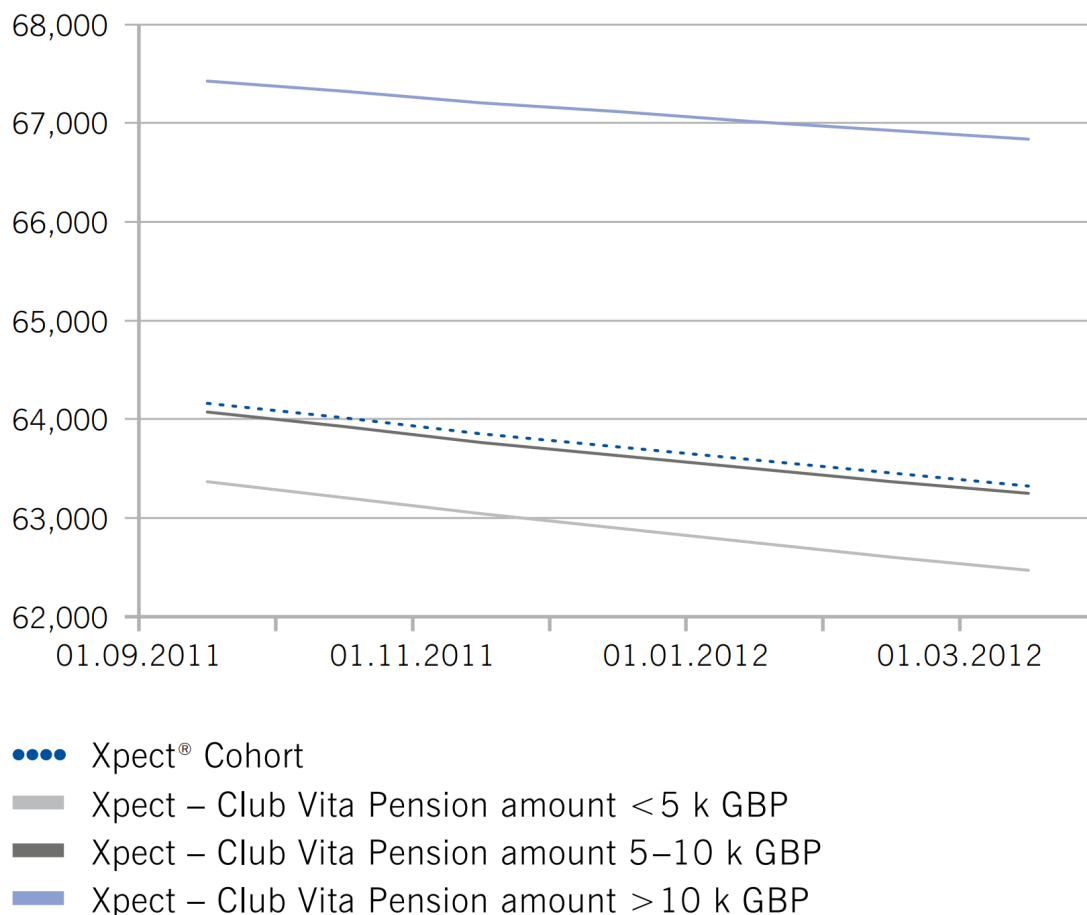
Deutsche Börse launched the Xpect-Club Vita Index<sup>2</sup> for Germany, the Netherlands and England and Wales in March 2008 (Xu et al., 2017). The Club Vita

<sup>1</sup><https://llma.org/index/index-description/>

<sup>2</sup><http://www.xpect-index.com>

indices also differentiate survival experience by the pension amount received as a proxy for different socio-economic classes (see Figure 2.5).

**Figure 2.5:** Xpect survival indices by pension amount (England and Wales 1935 to 1939 male cohort)



Source: Deutsche Börse (2012)

## 2.2 Longevity Basis Risk

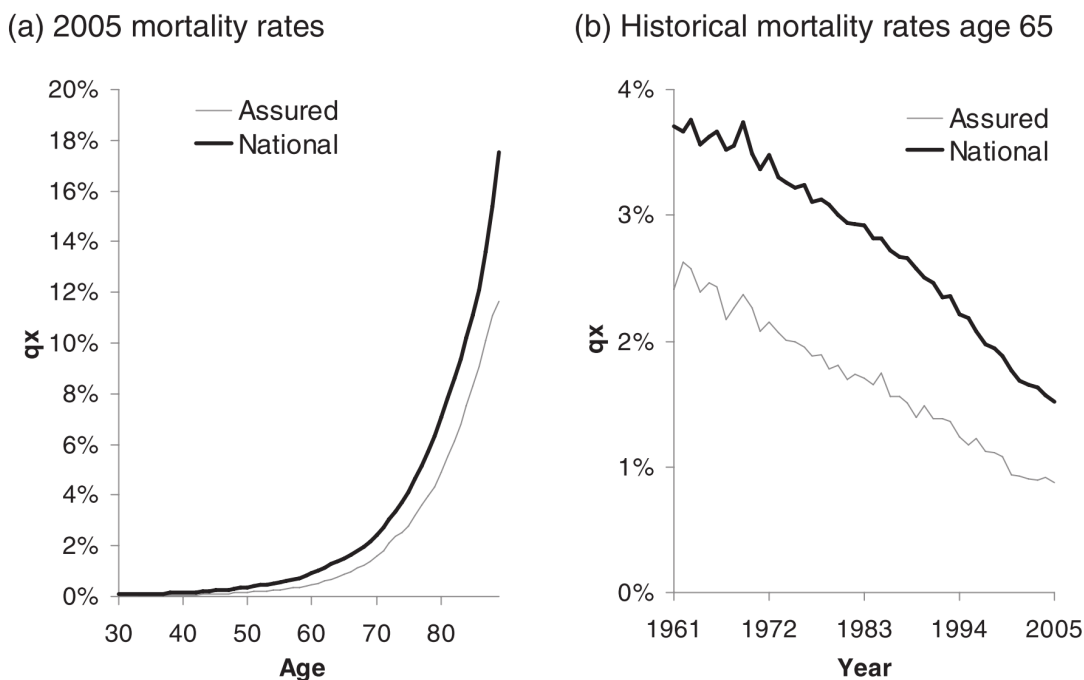
As outlined in Chapter 1, longevity basis risk remains a major barrier to index-based longevity hedging (Villegas et al., 2017). Index hedges cannot hedge the specific mortality experience of a given retirement income portfolio as, by definition, payments are determined with respect to the mortality experience of a broad reference population as represented by a published longevity index (Coughlan et al., 2007).

Longevity basis risk associated with standardised longevity hedging instruments can be decomposed into three distinct components (Mosher and Sagoo, 2011), namely

demographic basis risk, structuring basis risk and sampling basis risk.

1. Demographic basis risk: the composition of the retirement income portfolio can have significant socio-economic or demographic differences from the broader population underlying the referenced longevity index. For example, members within a retirement income portfolio may be wealthier on average than the national population, which may cause their future mortality experience to deviate from the average across the population. Indeed, Coughlan et al. (2011) compare the mortality trends of the national population of England and Wales (E.W.) to a sub-population of U.K. individuals who hold life insurance policies.

**Figure 2.6:** Comparison of male mortality rates for the U.K. assured and E.W. national populations



Source: Coughlan et al. (2011)

It is evident from Figure 2.6 that the assured population has significantly lower mortality rates than the national average at all ages beyond 35 (a). Furthermore, although the mortality rates of both populations have consistently trended downwards over time, assured mortality rates have perennially been lower than the national population (b). Therefore, a hedging instrument indexed to population-level longevity outcomes would be imperfect in such a scenario.

2. Structuring basis risk: the timing of cashflows from the hedging instrument will, in general, differ from the payments made by the retirement income

provider to their surviving members or annuitants. For example, retirement income benefits might be paid monthly or fortnightly to pension fund members, whereas the swap agreement might only be settled annually. Alternatively, the maturity of the hedging instrument may be significantly shorter than the run-off horizon of the retirement income portfolio (Haberman et al., 2014).

3. Sampling basis risk: due to the finite number of individual lives within retirement income portfolios, the longevity outcomes experienced by the pool of members or annuitants is subject to sampling variability. Even for two populations which are demographically identical, there will inevitably be random variation about expected mortality outcomes. However, sampling basis risk can be diversified away by increasing the number of individual lives within the exposure.

An organisation called the Longevity Basis Risk Working Group (LBRWG) has noted that, in addition to the prevalence of longevity basis risk, the lack of a robust framework for quantifying longevity basis risk has further impeded the appetite for standardised index-based longevity hedging solutions. To date the LBRWG has published Phase 1 (Haberman et al., 2014) and Phase 2 (Li et al., 2017) technical reports as well as work by Villegas et al. (2017). The fundamental aim of these publications is to:

*“develop a readily-applicable methodology for quantifying the basis risk arising from the use of population-based mortality indices for managing the longevity risk inherent in specific blocks of pension benefits or annuitant liabilities.”*

The LBRWG builds on the decomposition of longevity basis risk proposed in Mosher and Sagoo (2011) by developing techniques to quantify each of three individual components. In particular, demographic basis risk is modelled through multi-population mortality modelling frameworks (see Section 2.3), structuring basis risk is incorporated using numerical optimisation procedures, while random sampling techniques are implemented to account for sampling basis risk.

The Longevity Risk Reduction (LRR) metric is a key indicator used to evaluate hedge effectiveness (Coughlan et al., 2011; Li et al., 2017). LRR is based on the percentage reduction in portfolio risk, as represented by a given risk measure (for example, variance). Note that some authors reference the LRR metric using alternate terms such as “hedge efficiency” (Chang and Sherris, 2018). The LRR is defined as

$$\text{Longevity Risk Reduction} = \left(1 - \frac{\rho(\text{Hedged Portfolio})}{\rho(\text{Unhedged Portfolio})}\right) \times 100\%, \quad (2.1)$$

where  $\rho(\text{Unhedged Portfolio})$  and  $\rho(\text{Hedged Portfolio})$  refer to some selected risk measure of the present value of the retirement income provider’s net position before

and after the hedge has been applied, respectively. There are various risk measures that have been adopted in the literature for LRR calculations including variance (Li and Hardy, 2011; Cairns et al., 2014), Value-at-Risk (Li et al., 2017) and expected shortfall (Ngai and Sherris, 2011). As Li et al. (2017) highlight, given that various solvency regulations, such as Solvency II’s Solvency Capital Requirement, refer to the Value-at-Risk in their capital guidelines, it may be of particular interest for retirement income providers to adopt this risk measure in their LRR calculations.

Other researchers instead convey visual longevity basis risk metrics such as net liability value histograms (Coughlan et al., 2011) as well as Mahalanobis distance (Chan et al., 2016; Xu et al., 2017).

## 2.3 Multi-Population Mortality Modelling

The modelling of demographic basis risk requires the use of a multi-population mortality modelling framework (Li et al., 2015). As noted by Pretty Sagoo, the Chair of the LLMA and IFoA Joint Longevity Basis Risk Working Group as part of the LBRWG Phase 1 report (Haberman et al., 2014):

*“To be able to assess demographic basis risk, the required model needs to be able to capture the mortality trends in both the reference population backing the hedging instrument and in the population of the portfolio being hedged.”*

Multi-population mortality models are fitted to the mortality data of multiple different populations, modelling their relationship over time and projecting the joint mortality outcomes of the different populations into the future, thereby capturing mortality dependence structures.

Most multi-population mortality models described in the literature are constructed in a discrete time mortality modelling framework. These models are typically based on the notion of coherent forecasts as proposed by Li and Lee (2005). A multi-population mortality model is coherent if the mortality rate projections of the multiple related populations do not diverge indefinitely in the long run – an idea that has been mathematically formalised in Cairns et al. (2011) who stated that the ratio of projected mortality rates should become stable for long term forecasts.

Villegas et al. (2017) provide a comprehensive overview of the “universe” of discrete-time multi-population mortality models, as depicted in Figure 2.7.

There are three main categories of discrete-time multi-population mortality models:

1. Lee-Carter extensions that are based on the form of the Lee-Carter model (Lee and Carter, 1992).

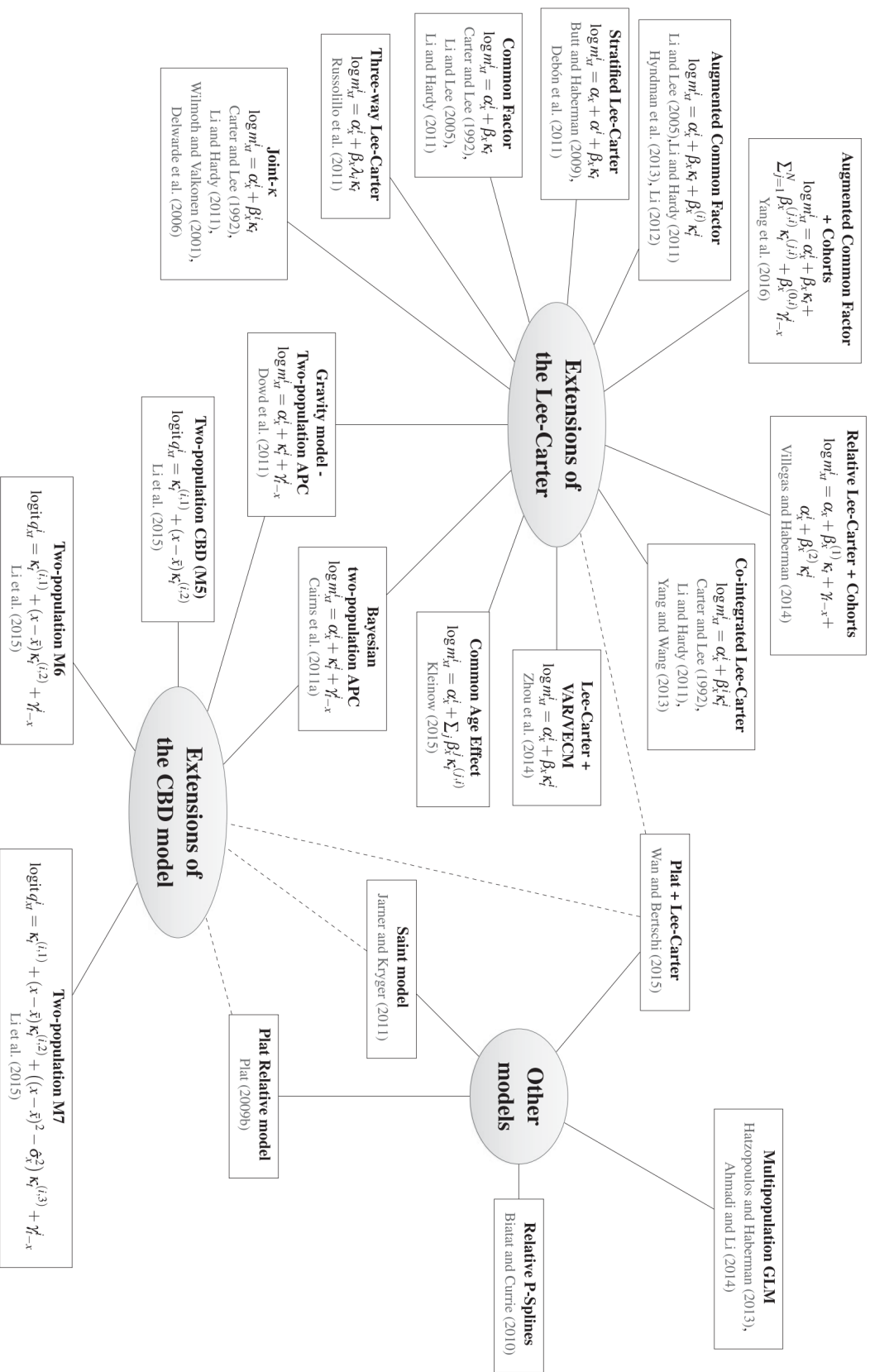


Figure 2.7: Overview of discrete-time multi-population mortality modelling

Source: Villegas et al. (2017)

2. Cairns-Blake-Dowd (CBD) extensions that are based on the form of the CBD model (Cairns et al., 2006).
3. Other models: discrete-time multi-population mortality models that do not fit into either of the first two categories.

Of this large set of models, the LBRWG recommends that retirement income providers use a decision tree framework to select the most appropriate multi-population mortality modelling methodology, based on the specific characteristics of the exposed portfolio (see Figure 2.8). In particular, only three broad modelling approaches need to be considered: the M7-M5 model (a multi-population extension of the CBD model), the Common Age Effect (CAE) plus Cohorts model (a multi-population extension of the Lee Carter model) and the characterisation approach (for retirement income portfolios with less than 8 years of reliable data or fewer than 25,000 lives) which involves fitting either the M7-M5 or CAE plus cohorts model to a book population which approximates the demographic composition of the retirement income portfolio. Full details of these modelling techniques are provided in Haberman et al. (2014) and Li et al. (2017).

However, as noted in Xu et al. (2017), a continuous-time multi-population mortality model is more flexible for applications combining mortality and financial modelling elements. Despite this, the literature on continuous-time multi-population mortality modelling is much less developed. The only such model constructed in the affine framework is the joint affine term structure model developed in Xu et al. (2017). This model is inspired by multi-country affine term structure interest rate models which have shown to be flexible, tractable and have a good empirical fit (see, for example, Egorov et al., 2011), as well as the fact that single-population affine term structure mortality models have been shown to capture mortality trends well (see, for example, Blackburn and Sherris, 2013). Three latent time-varying factors are incorporated into the joint ATSM: a single “common” factor which impacts the mortality dynamics of both populations as well as two “local” factors which only impact the mortality of the associated local populations.



## 2.4 Value-Based Longevity Indices

To date, index-based longevity hedging transactions have referenced longevity indices linked to national life tables such as the Lifemetrics Index and the Xpect-Club Vita Index. However, as articulated in Chapter 1, the failure of such indices to incorporate the other major risk factors associated with retirement income portfolios, such as interest rate and inflation risk (Towers Watson, 2013), has deterred providers from such hedges under the assumption that the basis risk exposure would remain significant. This notion motivated the development of value-based longevity indices in Sherris (2009) – indices which are constructed to track the expected present value of a unit of longevity-indexed income.

In 2013, the global asset manager BlackRock launched the Cost of Retirement Index (CoRI)<sup>3</sup>. Twenty U.S. cohorts are represented across the CoRI – one for each year in which an individual attains age 65 from 2006 to 2025. These correspond to the cohorts born in years 1941 to 1960 (Xu et al., 2017). BlackRock (2018) describes the CoRI as follows:

*“The CoRI Indexes seek to track the estimated cost of a dollar of future retirement income. By one dollar of future retirement income, we mean one dollar per year beginning at age 65, lasting as long as you live. For example, a CoRI Index level of \$13.54 means that a dollar of life contingent income beginning at age 65 (or now if 65 and older) would cost \$13.54 today.”*

The CoRI also includes an annual cost-of-living adjustment to preserve retirees’ real purchasing power over time. Recent CoRI levels across the different cohorts are presented in Figure 2.9.

The CoRI is a function of five different factors (see Figure 2.10). In addition to longevity risk, interest rate risk and inflation risk, the CoRI also accounts for the market price of longevity risk based on the current pricing of retirement income products by providers. Therefore, the CoRI would not be an appropriate longevity index to underlie standardised capital market longevity hedging instruments. As described by Sweeting (2010), longevity indices must be calculated in an objective and transparent manner. Since retirement income providers are able to directly influence the CoRI through their pricing policies, the index would not be perceived as an independent, objective representation of longevity outcomes if used for index-hedging purposes.

Xu et al. (2017) construct value-based longevity indices based on the national populations of Australia, the U.K., the Netherlands and France. They subsequently design an index-based hedging strategy in which an Australian retirement income portfolio is hedged using the U.K. index, as well as a strategy in which a Dutch

---

<sup>3</sup><https://www.blackrock.com/cori/fact-sheets>

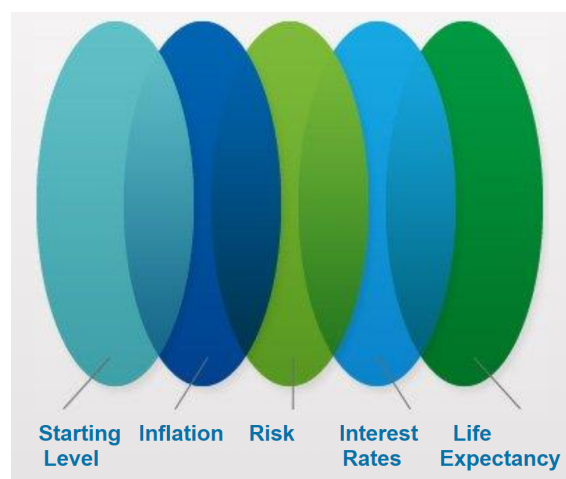
**Figure 2.9:** BlackRock's Cost of Retirement Index showing the \$ value of the index associated with twenty U.S. cohorts as at 24/10/2018

<b>Current Age</b>	<b>CoRI Index Name</b>	<b>Index Level*</b>
74	CoRI Index 2009	\$13.83
73	CoRI Index 2010	\$14.46
72	CoRI Index 2011	\$15.10
71	CoRI Index 2012	\$15.74
70	CoRI Index 2013	\$16.38
69	CoRI Index 2014	\$17.03
68	CoRI Index 2015	\$17.69
67	CoRI Index 2016	\$18.32
66	CoRI Index 2017	\$18.97
65	CoRI Index 2018	\$19.62
64	CoRI Index 2019	\$19.74
63	CoRI Index 2020	\$19.05
62	CoRI Index 2021	\$18.42
61	CoRI Index 2022	\$17.78
60	CoRI Index 2023	\$17.19
59	CoRI Index 2024	\$16.61
58	CoRI Index 2025	\$15.95
57	CoRI Index 2026	\$15.20
56	CoRI Index 2027	\$14.76
55	CoRI Index 2028	\$14.30

Source: BlackRock (2018)

portfolio is hedged against the French index. The authors find that basis risk is significantly lower in the Netherlands-France example; a differential that they attribute to the common interest rate between the two countries. This demonstrates that interest rate risk is a material element in the hedging framework, implying that value-based longevity indices have the capacity to improve hedge outcomes through their potential to incorporate interest rate risk in addition to longevity risk.

Indeed, value-based longevity indices have the capacity to integrate all of the major risk factors associated with the provision of retirement income products (Wills and Sherris, 2010): longevity risk, interest rate risk and inflation risk (Towers Watson, 2013). Therefore, such indices should intuitively be associated with lower levels of basis risk relative to mortality rate indices (for example, the Lifemetrics Index and the Xpect-Club Vita Index) when used to underlie standardised longevity hedging

**Figure 2.10:** CoRI determinants

Source: BlackRock (2018)

transactions. Chang and Sherris (2018) test this hypothesis by comparing the the longevity basis risk of two different hedge transactions:

- an index swap contract on a value-based longevity index representing the expected present value of a standardised annual payment of a unit of longevity-indexed income to a group of Australian males aged 65 years, and
- an S-forward based on the population survival rate of the national cohort of 65 year old males.

The authors find that the basis risk exposure associated with the value-based longevity index is significantly lower than that of the S-forward contract across all book sizes. In particular, the relative out-performance of the former is substantially greater for larger retirement income portfolios where sampling basis risk lacks the requisite leverage to materially impact hedge outcomes. While this analysis did not incorporate demographic basis risk nor inflation-indexation of retirement benefits, it demonstrates the potential for value-based longevity indices to significantly improve standardised longevity hedging outcomes. This, in turn, has the capacity to stimulate further growth and development in the longevity risk transfer market.

## 2.5 Gaps in the Literature

While various value-based longevity indices have been proposed and constructed in the literature, to date none have incorporated all three of the major risk factors associated with retirement income portfolios (that is, longevity risk, interest rate risk and inflation risk). We expect to fill this literature gap. Furthermore, by constructing such an index, the attribution of risk among these three elements can

be estimated; to date no such decomposition has appeared in the literature to our knowledge.

Additionally, while various authors have assessed the basis risk associated with value-based longevity indices, none have engaged the holistic, decomposed quantification framework developed by the LBRWG. For example, Xu et al. (2017) account for demographic basis risk in their analysis, while Chang and Sherris (2018) incorporate sampling basis risk. By assessing all constituent components of longevity basis risk, our research can fill an important literature gap and contribute towards the robust evaluation of index-based longevity hedging. Finally, while multi-population mortality modelling frameworks have been developed, no work has compared the hedging outcomes associated with the two different frameworks – a contribution which will additionally facilitate the assessment of model risk on hedge outcomes.

# Chapter 3

## Mortality Modelling Frameworks

This chapter describes the mortality modelling techniques adopted in this thesis. Section 3.1 details a joint affine term structure model; a continuous-time multi-population mortality model that utilises concepts from the financial literature to describe the relationship between the reference and book populations in an affine framework. In Section 3.2, we calibrate and forecast a discrete-time multi-population mortality model called the M7-M5 model, a model used extensively by the LBRWG.

### 3.1 Joint Affine Term Structure Model

This section details the development of a multi-factor joint affine term structure model (ATSM) for mortality, as developed in Xu et al. (2017). The model consists of two populations: a “reference” population (R) which refers to the population underlying the value-based longevity index, as well as a “book” population (B) which refers to the portfolio to be hedged against the value-based longevity index. For example, B could consist of members of a defined benefit pension fund or a pool of lifetime annuity recipients.

#### 3.1.1 Model Specification

Three latent time-varying factors are incorporated into the modelling framework:

- a “local” factor  $R_{x,t}$  which only impacts the mortality dynamics of the reference population R,
- a “local” factor  $B_{x,t}$  which only impacts the mortality dynamics of the book population B, and
- a “common” factor  $C_{x,t}$  which affects the mortality of both the reference population R as well as the book population B and thereby captures the dependence in mortality experience.

The full mathematical details on the joint ATSM can be found in Xu et al. (2017). Starting from a given age  $x$  at initial time  $t$ , the average mortality intensities of the two populations are modelled as affine functions of the time-varying factors

$$\bar{\mu}_{x,t}^R = \delta_{R,0} + \delta_{R,1}C_{x,t} + \delta_{R,2}R_{x,t}, \quad (3.1)$$

$$\bar{\mu}_{x,t}^B = \delta_{B,0} + \delta_{B,1}C_{x,t} + \delta_{B,2}B_{x,t}. \quad (3.2)$$

As in Xu et al. (2017), the factors are assumed to evolve independently. This implies that the common factor does not depend on the local factors, which allows the joint ATSM to be decomposed into two single-population term structure mortality models (Egorov et al., 2011).

Due to the incompleteness of the longevity market, Xu et al. (2017) define a best-estimate measure  $\bar{Q}$ , fixed to observed mortality. However, because we assume that the market price of longevity risk is zero, factor dynamics under the risk neutral measure  $Q$ , which are needed for pricing purposes, are identical to the best estimate measure  $\bar{Q}$ . Factor dynamics under the risk neutral measure  $Q$  are

$$\begin{bmatrix} dC_{x,t} \\ dR_{x,t} \\ dB_{x,t} \end{bmatrix} = - \begin{bmatrix} \phi_1 & 0 & 0 \\ 0 & \phi_2 & 0 \\ 0 & 0 & \phi_3 \end{bmatrix} \begin{bmatrix} C_{x,t} \\ R_{x,t} \\ B_{x,t} \end{bmatrix} dt + \begin{bmatrix} \sigma_1 & 0 & 0 \\ 0 & \sigma_2 & 0 \\ 0 & 0 & \sigma_3 \end{bmatrix} \begin{bmatrix} dW_t^{Q,C} \\ dW_t^{Q,R} \\ dW_t^{Q,B} \end{bmatrix}, \quad (3.3)$$

where

- $\phi_1, \phi_2, \phi_3, \sigma_1, \sigma_2$  and  $\sigma_3$  are parameters, and
- $W_t^{Q,C}, W_t^{Q,R}$  and  $W_t^{Q,B}$  are Wiener processes under the risk neutral measure.

Under the real-world measure  $P$ , the factors evolve as

$$\begin{bmatrix} dC_{x,t} \\ dR_{x,t} \\ dB_{x,t} \end{bmatrix} = - \begin{bmatrix} \psi_1 & 0 & 0 \\ 0 & \psi_2 & 0 \\ 0 & 0 & \psi_3 \end{bmatrix} \begin{bmatrix} C_{x,t} \\ R_{x,t} \\ B_{x,t} \end{bmatrix} dt + \begin{bmatrix} \sigma_1 & 0 & 0 \\ 0 & \sigma_2 & 0 \\ 0 & 0 & \sigma_3 \end{bmatrix} \begin{bmatrix} dW_t^{P,C} \\ dW_t^{P,R} \\ dW_t^{P,B} \end{bmatrix}, \quad (3.4)$$

where

- $\psi_1, \psi_2, \psi_3, \sigma_1, \sigma_2$  and  $\sigma_3$  are parameters, and
- $W_t^{P,C}, W_t^{P,R}$  and  $W_t^{P,B}$  are Wiener processes under the real-world measure.

Xu et al. (2017) show that under this framework the survival probabilities of the reference and book populations are respectively given by

$$S^R(x, t, T) = e^{B_1(t,T)C_{x,t} + B_2(t,T)R_{x,t} + A^R(t,T)}, \quad (3.5)$$

$$S^B(x, t, T) = e^{B_1(t,T)C_{x,t} + B_3(t,T)B_{x,t} + A^B(t,T)}, \quad (3.6)$$

where

$$B_j(t, T) = -\frac{1 - e^{-\phi_j(T-t)}}{\phi_j} \quad \text{for } j = 1, 2, 3,$$

$$A^R(t, T) = \frac{1}{2} \sum_{j=1,2} \frac{\sigma_j^2}{\phi_j^3} \left[ \frac{1}{2} (1 - e^{-2\phi_j(T-t)}) - 2(1 - e^{-\phi_j(T-t)}) + \phi_j(T-t) \right],$$

$$A^B(t, T) = \frac{1}{2} \sum_{j=1,3} \frac{\sigma_j^2}{\phi_j^3} \left[ \frac{1}{2} (1 - e^{-2\phi_j(T-t)}) - 2(1 - e^{-\phi_j(T-t)}) + \phi_j(T-t) \right].$$

The average force of mortality curve for the reference and book populations respectively are

$$\begin{aligned} \bar{\mu}_{x,t}^R(T) &= -\frac{1}{T-t} \log[S^R(x, t, T)] \\ &= -\frac{1}{T-t} [B_1(t, T)C_{x,t} + B_2(t, T)R_{x,t} + A_t^R(t, T)] \\ &= \frac{1 - e^{-\phi_1(T-t)}}{\phi_1(T-t)} C_{x,t} + \frac{1 - e^{-\phi_2(T-t)}}{\phi_2(T-t)} R_{x,t} - \frac{A_t^R(t, T)}{T-t}, \end{aligned} \quad (3.7)$$

$$\begin{aligned} \bar{\mu}_{x,t}^B(T) &= -\frac{1}{T-t} \log[S^B(x, t, T)] \\ &= -\frac{1}{T-t} [B_1(t, T)C_{x,t} + B_3(t, T)B_{x,t} + A_t^B(t, T)] \\ &= \frac{1 - e^{-\phi_1(T-t)}}{\phi_1(T-t)} C_{x,t} + \frac{1 - e^{-\phi_3(T-t)}}{\phi_3(T-t)} B_{x,t} - \frac{A_t^B(t, T)}{T-t}. \end{aligned} \quad (3.8)$$

### 3.1.2 Model Calibration

The model can be written in state space form and can therefore be estimated using the Kalman filter (Kalman, 1960). In particular, the state space form consists of a measurement equation, which specifies the relationship between the average mortality intensities  $\bar{\mu}_{x,t}$  and the factors  $R_{x,t}$ ,  $B_{x,t}$  and  $C_{x,t}$ , as well as a state transition equation which describes the time series dynamics of the latent time-varying factors. For the joint ATSM, Xu et al. (2017) show that the measurement equation is

$$\bar{\mu}_{x,t} = B\vec{X}_t - \vec{A} + \vec{\epsilon}_t, \quad \vec{\epsilon}_t \sim N_{2k}(\vec{0}, H), \quad (3.9)$$

where

$$\vec{\mu}_{x,t} = \begin{bmatrix} \bar{\mu}_{x,t}^R(\tau_1) \\ \vdots \\ \bar{\mu}_{x,t}^R(\tau_k) \\ \bar{\mu}_{x,t}^B(\tau_1) \\ \vdots \\ \bar{\mu}_{x,t}^B(\tau_k) \end{bmatrix}, \quad B = \begin{bmatrix} \frac{1-e^{-\phi_1\tau_1}}{\phi_1\tau_1} & \frac{1-e^{-\phi_2\tau_1}}{\phi_2\tau_1} & 0 \\ \vdots & \vdots & \vdots \\ \frac{1-e^{-\phi_1\tau_k}}{\phi_1\tau_k} & \frac{1-e^{-\phi_2\tau_k}}{\phi_2\tau_k} & 0 \\ \frac{1-e^{-\phi_1\tau_1}}{\phi_1\tau_1} & 0 & \frac{1-e^{-\phi_3\tau_1}}{\phi_3\tau_1} \\ \vdots & \vdots & \vdots \\ \frac{1-e^{-\phi_1\tau_k}}{\phi_1\tau_k} & 0 & \frac{1-e^{-\phi_3\tau_k}}{\phi_3\tau_k} \end{bmatrix}, \quad X_t = \begin{bmatrix} C_t \\ R_t \\ B_t \end{bmatrix},$$

$$A = \begin{bmatrix} \frac{1}{2\tau_1} \sum_{i=1,2} \frac{\sigma_i^2}{\phi_i^3} \left[ \frac{1}{2}(1 - e^{-2\phi_i\tau_1}) - 2(1 - e^{-\phi_i\tau_1}) + \phi_i\tau_1 \right] \\ \vdots \\ \frac{1}{2\tau_k} \sum_{i=1,2} \frac{\sigma_i^2}{\phi_i^3} \left[ \frac{1}{2}(1 - e^{-2\phi_i\tau_k}) - 2(1 - e^{-\phi_i\tau_k}) + \phi_i\tau_k \right] \\ \frac{1}{2\tau_1} \sum_{i=1,3} \frac{\sigma_i^2}{\phi_i^3} \left[ \frac{1}{2}(1 - e^{-2\phi_i\tau_1}) - 2(1 - e^{-\phi_i\tau_1}) + \phi_i\tau_1 \right] \\ \vdots \\ \frac{1}{2\tau_k} \sum_{i=1,3} \frac{\sigma_i^2}{\phi_i^3} \left[ \frac{1}{2}(1 - e^{-2\phi_i\tau_k}) - 2(1 - e^{-\phi_i\tau_k}) + \phi_i\tau_k \right] \end{bmatrix},$$

$H$  is the (diagonal) covariance matrix of the normal error terms and  $k$  is the number of ages in the mortality dataset.

The state transition equation is given by

$$\vec{X}_t = \Psi \vec{X}_{t-1} + \vec{\eta}_t, \quad \vec{\eta}_t \sim N_3(\vec{0}, Q), \quad (3.10)$$

where

$$\Psi = \begin{bmatrix} e^{-\psi_1} & 0 & 0 \\ 0 & e^{-\psi_2} & 0 \\ 0 & 0 & e^{-\psi_3} \end{bmatrix}, \quad Q = \begin{bmatrix} \frac{\sigma_1^2}{2\psi_1}(1 - e^{-2\psi_1}) & 0 & 0 \\ 0 & \frac{\sigma_2^2}{2\psi_2}(1 - e^{-2\psi_2}) & 0 \\ 0 & 0 & \frac{\sigma_3^2}{2\psi_3}(1 - e^{-2\psi_3}) \end{bmatrix}.$$

We calibrate the reference population component using U.S. male population-level mortality data sourced from the Human Mortality Database (HMD)<sup>1</sup>. The HMD publishes population-level deaths and exposure data over the period from 1933 to 2016 for the U.S.

However, we have not been able to obtain time series deaths and exposure data for U.S. annuity holders. Therefore, we construct a synthetic book population which is assumed to approximate the demographics of a typical retirement income portfolio. The Centers for Disease Control and Prevention (CDC)<sup>2</sup> publishes state-level mortality data over the period 1999 to 2016. To construct a proxy retirement income portfolio population, we aggregate the exposure and deaths data of the annually-updated set of states in the highest U.S. income quintile. This aggregation is based

<sup>1</sup>[www.mortality.org/](http://www.mortality.org/)

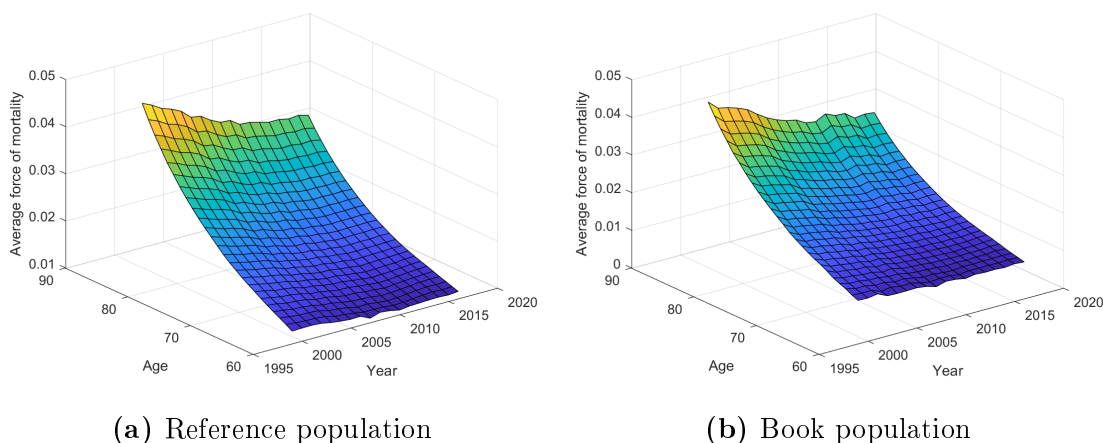
<sup>2</sup><https://www.cdc.gov/>

on state-level average household income statistics as published by the Small Area Income and Poverty Estimates Program (SAIPE)<sup>3</sup>.

Single-year single-age deaths and exposure data for males ages 60 to 84 between 1999 and 2016 (that is, the overlapping period between the two data sources) are used to fit the joint mortality model.

The average force of mortality for the reference and book populations over the in-sample period is shown in Figure 3.1. Both populations clearly exhibit mortality improvement over time, and it appears that the book population tends to have lower mortality rates relative to the reference population. This is confirmed by examining the ratio of the average force of mortality in the book population to that of the reference population in Figure 3.2 where all values are lower than 1 across all years and age ranges. Furthermore, the general downward trend in the ratio over time suggests that faster rates of mortality improvement have been observed in the book population over the in-sample period.

**Figure 3.1:** Observed average force of mortality for ages 60 to 84 from 1999 to 2016 in the reference and book populations



The joint ATSM is calibrated by fitting the observed average force of mortality data to the model average force of mortality expressions detailed in Equations (3.7) and (3.8). The Kalman filtering maximum likelihood estimation produces the fitted values as shown in Figure 3.3. It appears that the model has effectively captured the key features of the observed data.

### 3.1.3 Forecasting and Simulation

Having estimated the model, we then forecast and simulate the future average force of mortality and the associated survival probabilities over a 20 year time horizon. The forecasting of survival probabilities is achieved as follows:

<sup>3</sup><https://www.census.gov/en.html>

**Figure 3.2:** Book to reference population average force of mortality ratio for ages 60 to 84 from 1999 to 2016

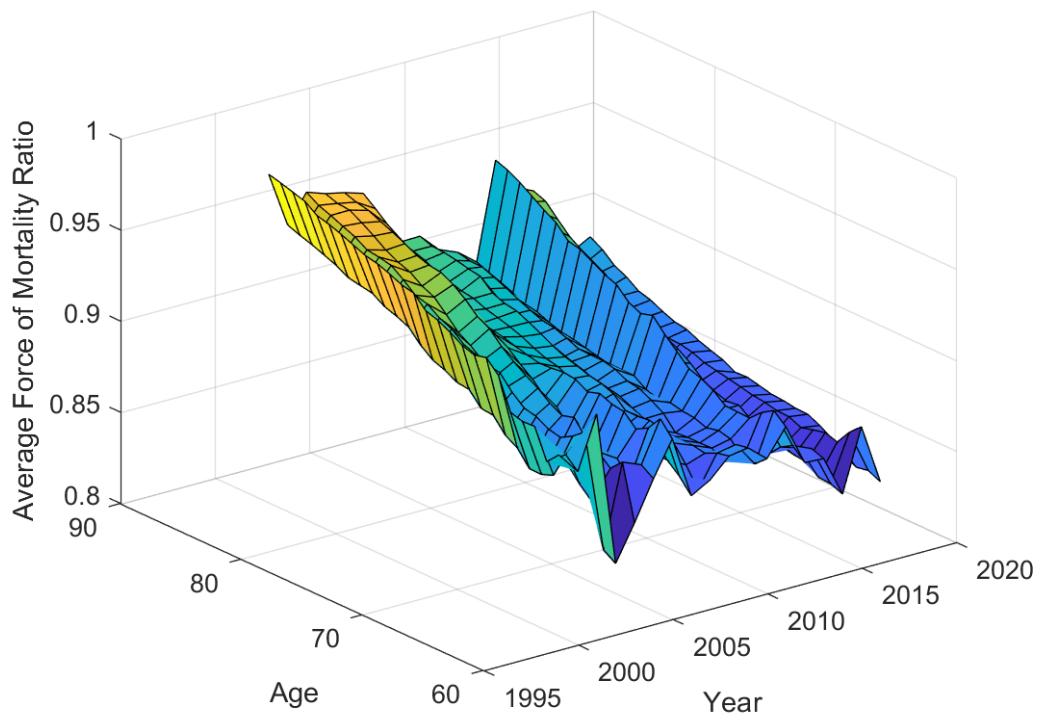
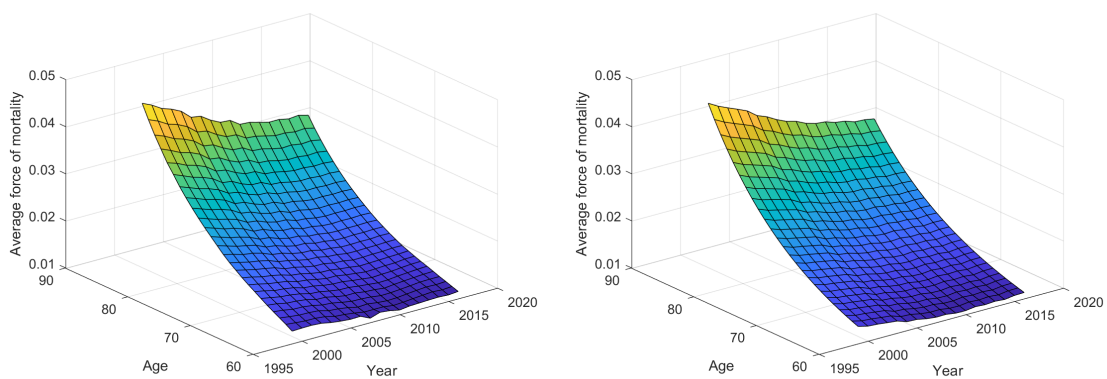


**Figure 3.3:** Fitted average force of mortality for ages 60 to 84 from 1999 to 2016 in the reference and book populations



(a) Reference population

(b) Book population

1. Forecast the common, reference and book factors  $C_{x,t}^F$ ,  $R_{x,t}^F$ ,  $B_{x,t}^F$  for years  $t = 1, 2, \dots, 20$  from the estimated joint ATSM.
2. Substitute the forecast factors into the average force of mortality functions to forecast the average force of mortality.

$$\bar{\mu}_{x,t}^{R,F}(T) = \frac{1 - e^{-\phi_1(T-t)}}{\phi_1(T-t)} C_{x,t}^F + \frac{1 - e^{-\phi_2(T-t)}}{\phi_2(T-t)} R_{x,t}^F - \frac{A_t^R(t, T)}{T-t}, \quad (3.11)$$

$$\bar{\mu}_{x,t}^{B,F}(T) = \frac{1 - e^{-\phi_1(T-t)}}{\phi_1(T-t)} C_{x,t}^F + \frac{1 - e^{-\phi_3(T-t)}}{\phi_3(T-t)} B_{x,t}^F - \frac{A_t^B(t, T)}{T-t}. \quad (3.12)$$

3. Compute the associated survival probability forecasts:

$$S^{R,F}(x, t, T) = e^{(-\bar{\mu}_{x,t}^{R,F}(T)(T-t))}, \quad (3.13)$$

$$S^{B,F}(x, t, T) = e^{(-\bar{\mu}_{x,t}^{B,F}(T)(T-t))}. \quad (3.14)$$

The simulation of survival probabilities follows a similar procedure.

1. Simulate the common, reference and book factors  $C_{x,t}^{[i]}$ ,  $R_{x,t}^{[i]}$ ,  $B_{x,t}^{[i]}$  for years  $t = 1, 2, \dots, 20$  and for simulation paths  $i = 1, 2, \dots, 5000$  from the estimated joint ATSM.
2. Substitute the simulated factors into the average force of mortality functions to simulate the average force of mortality.

$$\bar{\mu}_{x,t}^{R,[i]}(T) = \frac{1 - e^{-\phi_1(T-t)}}{\phi_1(T-t)} C_{x,t}^{[i]} + \frac{1 - e^{-\phi_2(T-t)}}{\phi_2(T-t)} R_{x,t}^{[i]} - \frac{A_t^R(t, T)}{T-t}, \quad (3.15)$$

$$\bar{\mu}_{x,t}^{B,[i]}(T) = \frac{1 - e^{-\phi_1(T-t)}}{\phi_1(T-t)} C_{x,t}^{[i]} + \frac{1 - e^{-\phi_3(T-t)}}{\phi_3(T-t)} B_{x,t}^{[i]} - \frac{A_t^B(t, T)}{T-t}. \quad (3.16)$$

3. Compute the associated survival probability simulations:

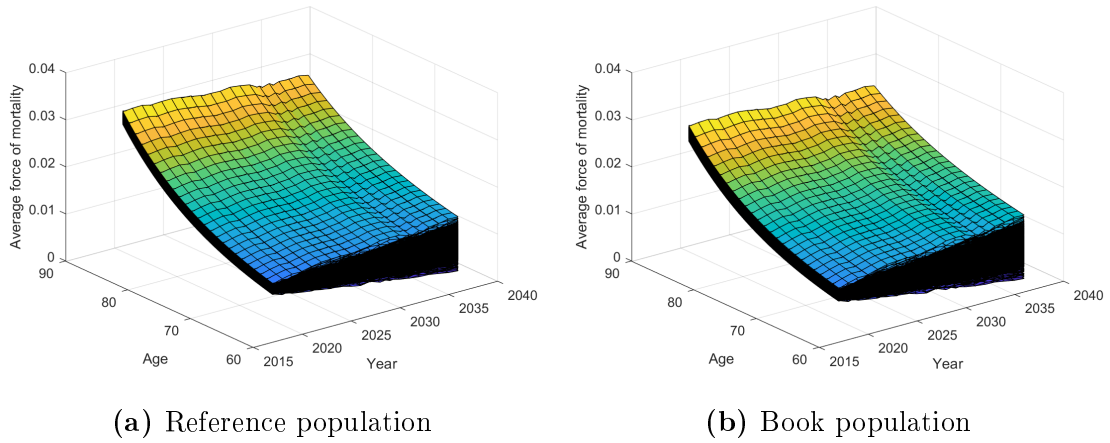
$$S^{R,[i]}(x, t, T) = e^{(-\bar{\mu}_{x,t}^{R,[i]}(T)(T-t))}, \quad (3.17)$$

$$S^{B,[i]}(x, t, T) = e^{(-\bar{\mu}_{x,t}^{B,[i]}(T)(T-t))}. \quad (3.18)$$

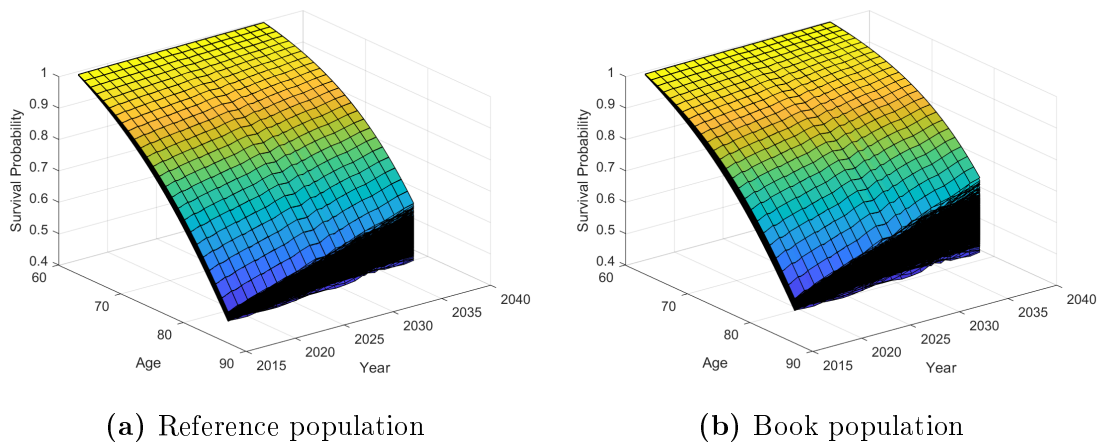
Indeed, one of the key advantages associated with the affine term structure mortality modelling framework is the availability of explicit closed-form solutions for survival probabilities which can be expressed as a function of the underlying factors.

Figure 3.4 shows 5,000 simulations for the average force of mortality over a 20 year simulation horizon for both the reference and book populations. The corresponding simulated population survival curves are shown in Figure 3.5. From the simulated survival curves, two observations are immediately apparent: the average

**Figure 3.4:** Simulated average force of mortality for ages 60 to 84 from 2017 to 2036 in the reference and book populations



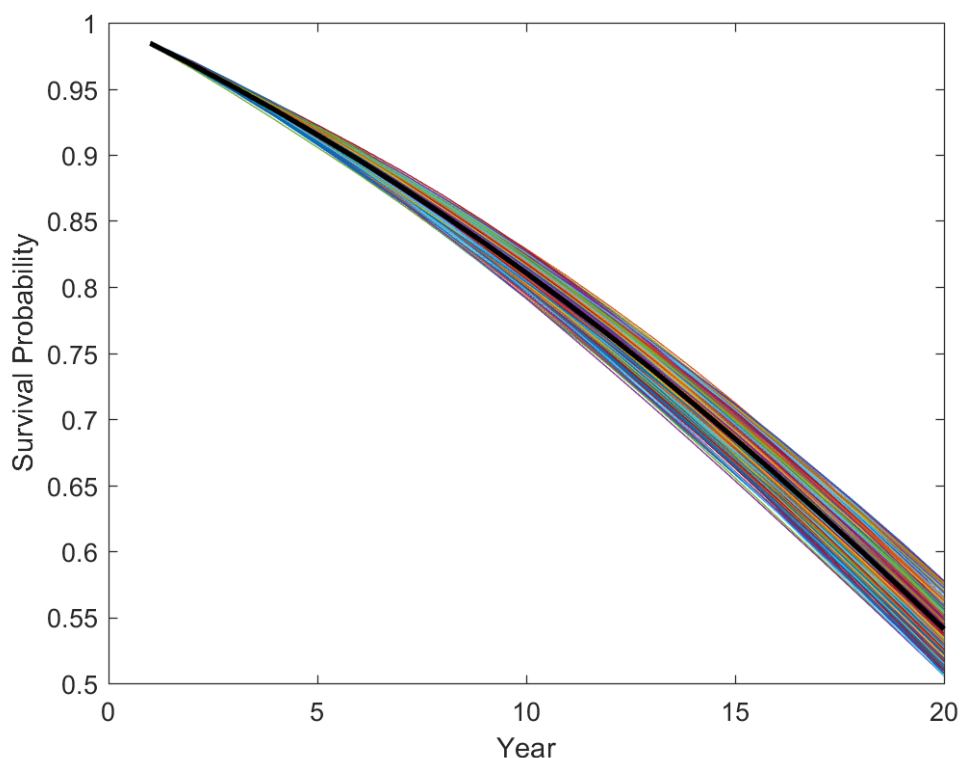
**Figure 3.5:** Simulated survival curves for ages 60 to 84 from 2017 to 2036 in the reference and book populations



survival probabilities for all ages improve over time, and the variability in survival outcomes increases for longer simulation horizons (that is, there is greater uncertainty in survival probabilities for simulations further into the future).

We also present the simulated survival curves for the reference population cohort aged 65 in 2017 in Figure 3.6. This plot exhibits the variability of survival probabilities over time around the central forecast.

**Figure 3.6:** Simulated survival curves for the reference population cohort aged 65 in 2017 over a 20 year simulation horizon



## 3.2 M7-M5 Mortality Model

We base the discrete-time multi-population mortality modelling approach on the framework described by the LBRWG (Haberman et al., 2014; Villegas et al., 2017; Li et al., 2017). In particular, based on the LBRWG's framework, the M7-M5 model is adopted. This model allows for inter-age mortality correlations and is appropriate for basis risk assessments for annuity portfolios that have at least 25,000 lives, 8 years of reliable data, a stable demographic mix and do not have book specific cohort effects.

### 3.2.1 Model Specification

The M7 model (Cairns et al., 2009) is used for reference population component, that is

$$\text{logit}(q_{x,t}^R) = \kappa_{t,1}^R + (x - \bar{x})\kappa_{t,2}^R + ((x - \bar{x})^2 - \sigma_x^2)\kappa_{t,3}^R + \gamma_{t-x}^R, \quad (3.19)$$

where

- $q_{x,t}^R$  is the year  $t$  age  $x$  mortality rate in the reference population,
- $\kappa_{t,1}^R$ ,  $\kappa_{t,2}^R$  and  $\kappa_{t,3}^R$  are latent-time varying factors corresponding to the mortality curve's level, slope and curvature respectively,
- $\gamma_{t-x}^R$  is the cohort effect for those born in year  $t - x$ , and
- $\bar{x}$  and  $\sigma_x^2$  denote the sample age mean and sample age variance respectively.

The difference between the book and reference population mortality rates is modelled as

$$\text{logit}(q_{x,t}^B) - \text{logit}(q_{x,t}^R) = \kappa_{t,1}^B + (x - \bar{x})\kappa_{t,2}^B, \quad (3.20)$$

where

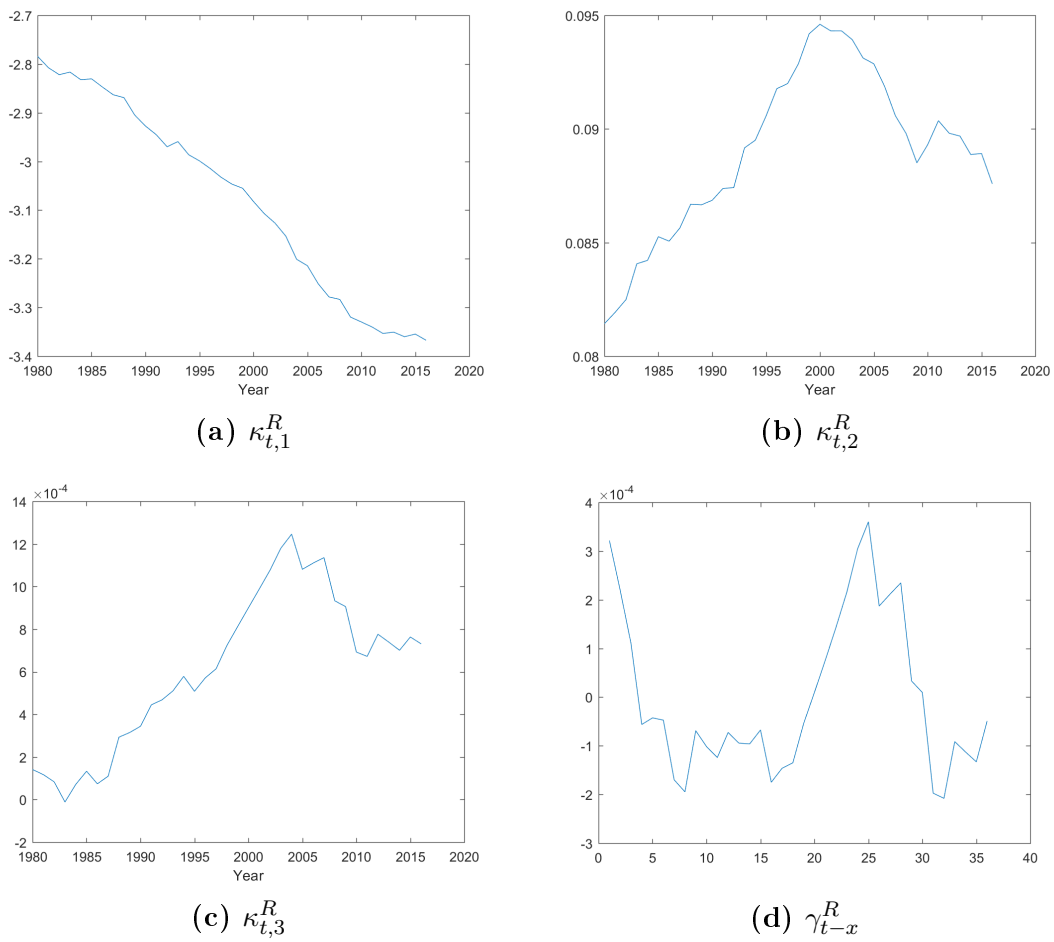
- $q_{x,t}^B$  is year  $t$  age  $x$  mortality rate in the book population,
- $\kappa_{t,1}^B$  and  $\kappa_{t,2}^B$  are latent-time varying factors explaining the difference in logit mortality rates, and
- $\bar{x}$  is the sample age mean.

### 3.2.2 Model Calibration

The discrete-time M7-M5 model is estimated in two distinct stages. Firstly, single-year single-age U.S. population-level deaths and exposure data from 1980 to 2016 for males aged 60 to 84 sourced from the HMD are used to estimate the reference population component of the model (that is the single-population M7 model). The estimated latent time-varying mortality factors and the cohort effect term are shown in Figure 3.7.

From Figure 3.7, it is apparent that:

- the level of the reference population mortality curve  $\kappa_{t,1}^R$  has been steadily decreasing over time reflecting declining mortality rates (Figure 3.7a),
- the age effects of mortality as represented by the slope  $\kappa_{t,2}^R$  and curvature  $\kappa_{t,3}^R$  terms seem to have undergone a trend shift since the early 2000's (Figures 3.7b and 3.7c), and

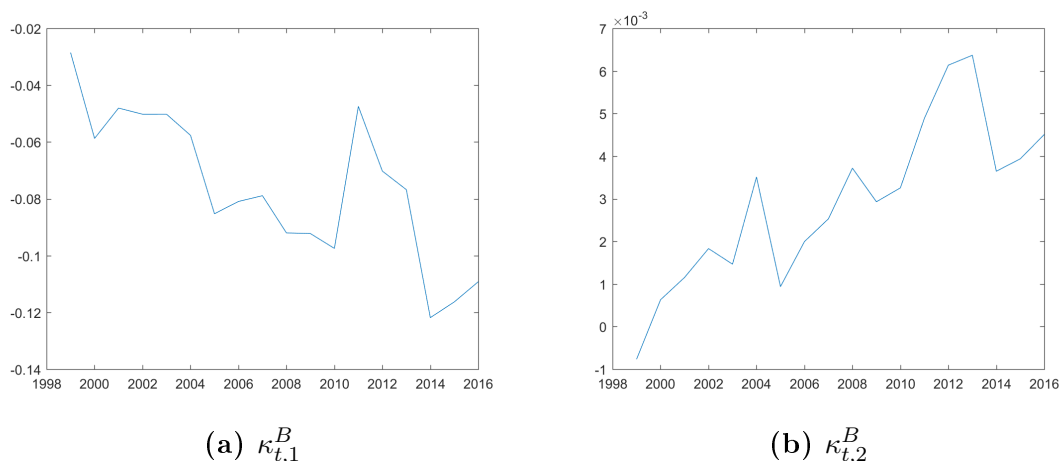
**Figure 3.7:** Reference population: estimated factors and cohort effect

- there is a clearly discernible cohort effect in the mortality rates (Figure 3.7d).

The book population's mortality dataset is constructed in the same manner as described in Subsection 3.1.2 for the continuous-time mortality model (that is, the annually-updated set of states in the highest household income quintile comprise the book population). Calibration of the mortality rate difference between the reference and book populations is based on single-year single-age deaths and exposure data for males aged 60 to 84 spanning the years 1999 to 2016 (that is, the overlapping period between the two populations' data sources).

The estimated mortality difference factors are shown in Figure 3.8. In particular, the negative values of  $\kappa_{t,1}^B$  in Figure 3.8a reflect the lower mortality rates in the book population relative to the reference population. Additionally, the downward trend in  $\kappa_{t,1}^B$  also suggests that faster rates of mortality improvement have been observed in the book population over the in-sample period. This is consistent with the downward trending book to reference population average force of mortality ratio plotted in Figure 3.2.

**Figure 3.8:** Book population: estimated factors



### 3.2.3 Forecasting and Simulation

To generate future mortality rate forecasts and simulations in the reference population, the factors  $\kappa_{t,1}^R$ ,  $\kappa_{t,2}^R$  and  $\kappa_{t,3}^R$  are modelled as a multivariate random walk with drift

$$\begin{bmatrix} \kappa_{t,1}^R \\ \kappa_{t,2}^R \\ \kappa_{t,3}^R \end{bmatrix} = \begin{bmatrix} \mu_1^R \\ \mu_2^R \\ \mu_3^R \end{bmatrix} + \begin{bmatrix} \kappa_{t-1,1}^R \\ \kappa_{t-1,2}^R \\ \kappa_{t-1,3}^R \end{bmatrix} + \begin{bmatrix} \epsilon_{t,1}^R \\ \epsilon_{t,2}^R \\ \epsilon_{t,3}^R \end{bmatrix}, \quad \begin{bmatrix} \epsilon_{t,1}^R \\ \epsilon_{t,2}^R \\ \epsilon_{t,3}^R \end{bmatrix} \sim N_3(\vec{0}, \Sigma) \quad (3.21)$$

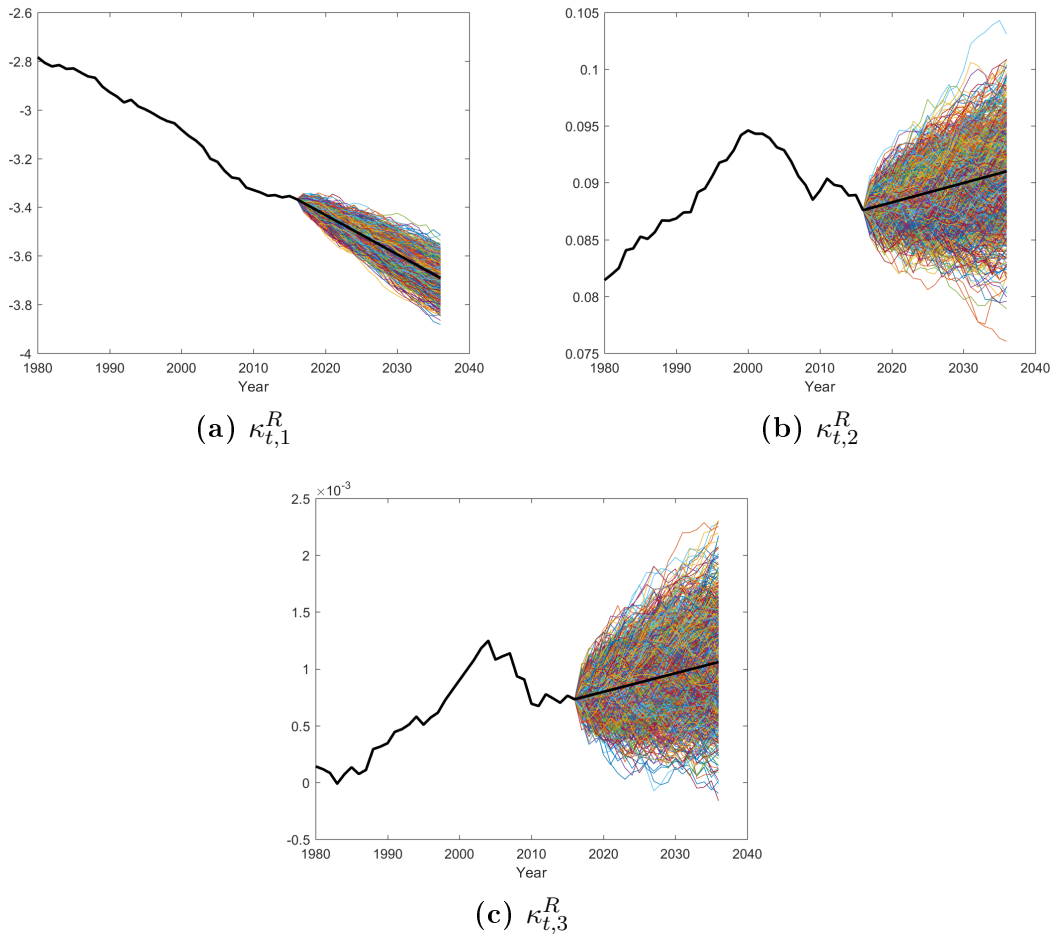
where

- $\mu_1^R$ ,  $\mu_2^R$ , and  $\mu_3^R$  are the drift parameters, and
- $\epsilon_{t,1}^R$ ,  $\epsilon_{t,2}^R$  and  $\epsilon_{t,3}^R$  are error terms that follow a multivariate normal distribution with a mean vector  $\vec{0}$  and a covariance matrix  $\Sigma$ .

Under this framework, the variability in future factor values increases with greater forecast horizons as shown in Figure 3.9, indicating that the variability in future mortality rates likewise increases for simulations further into the future.

The cohort effect  $\gamma_{t-x}^R$  is modelled as an autoregressive integrated moving average process, ARIMA (1,1,0).

**Figure 3.9:** Reference population: estimated, forecast and simulated factors



To generate future mortality rate projections for the book population, the factors  $\kappa_{t,1}^B$  and  $\kappa_{t,2}^B$  are modelled as a first order vector auto-regression process, VAR(1)

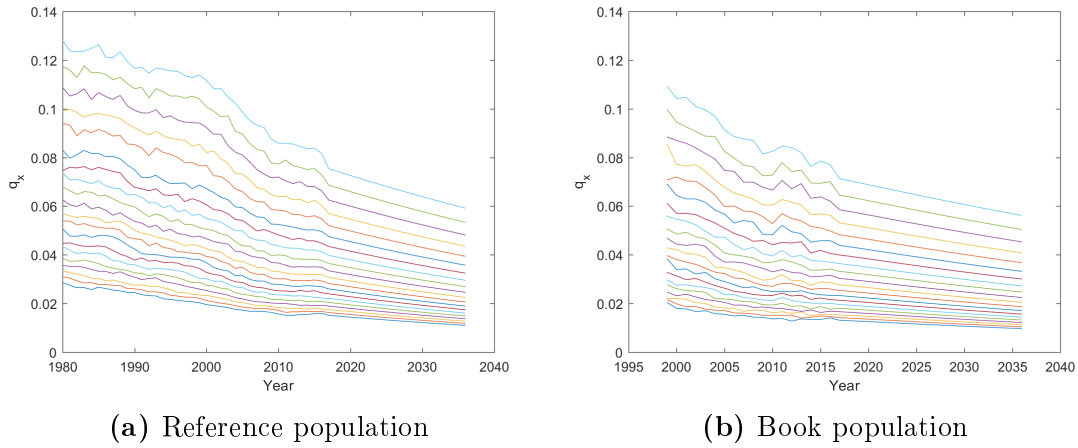
$$\begin{bmatrix} \kappa_{t,1}^B \\ \kappa_{t,2}^B \end{bmatrix} = \begin{bmatrix} \phi_1^B \\ \phi_2^B \end{bmatrix} + \begin{bmatrix} \phi_{1,1}^B & \phi_{1,2}^B \\ \phi_{2,1}^B & \phi_{2,2}^B \end{bmatrix} \begin{bmatrix} \kappa_{t-1,1}^B \\ \kappa_{t-1,2}^B \end{bmatrix} + \begin{bmatrix} \epsilon_{t,1}^B \\ \epsilon_{t,2}^B \end{bmatrix}, \quad \begin{bmatrix} \epsilon_{t,1}^B \\ \epsilon_{t,2}^B \end{bmatrix} \sim N_2(\vec{0}, \Phi) \quad (3.22)$$

where

- $\phi_1^B, \phi_2^B, \phi_{1,1}^B, \phi_{1,2}^B, \phi_{2,1}^B$  and  $\phi_{2,2}^B$  are model parameters, and
- $\epsilon_{t,1}^B$  and  $\epsilon_{t,2}^B$  are error terms that follow a multivariate normal distribution with a mean vector  $\vec{0}$  and a covariance matrix  $\Phi$ . We also assume independence between these error terms and those of the reference population time series model.

The forecast mortality rates for the reference population  $q_{x,t}^R$  and book population  $q_{x,t}^B$  for ages 65 to 84 over a 20 year forecast horizon are plotted in Figure 3.10. It is apparent from these plots that the model forecasts improving mortality rates over time in both populations.

**Figure 3.10:** Forecast mortality rates for ages 65 to 84 from 2017 to 2036 for the reference and book populations



In this chapter, we have detailed the specification, estimation, forecasting and simulation of both a discrete-time and a continuous-time multi-population mortality model. The outputs from these models facilitate the construction of the value-based longevity index and the assessment of basis risk when hedging retirement income portfolios using financial instruments that reference the constructed index.

# Chapter 4

## Interest Rate Modelling Frameworks

In this chapter, we develop two separate interest rate models: a nominal interest rate model (N) and a real interest rate model (R). The discounting of future cashflows is required both to construct the value-based longevity index as well as to assess the basis risk exposure. In particular, we adopt the affine dynamic Nelson Siegel (DNS) interest rate model with independent factors, as developed by Diebold and Li (2006). We assume that the interest rate modelling process is independent of mortality and longevity trends – a common assumption in the literature (Biffis, 2005; Xu et al., 2017). Section 4.1 presents the estimation results and future simulations and forecasts for the nominal interest rate model, while Section 4.2 details the development of the real interest rate model.

### 4.1 Nominal Interest Rate Model

#### 4.1.1 Model Specification

The nominal interest rate model incorporates three latent time-varying factors:

- $L_t^N$ : a level factor for the nominal yield curve,
- $S_t^N$ : a slope factor for the nominal yield curve, and
- $C_t^N$ : a curvature factor for the nominal yield curve.

The risk neutral  $Q$  dynamics of the factors are

$$\begin{bmatrix} dL_t^N \\ dS_t^N \\ dC_t^N \end{bmatrix} = - \begin{bmatrix} 0 & 0 & 0 \\ 0 & \lambda^N & -\lambda^N \\ 0 & 0 & -\lambda^N \end{bmatrix} \begin{bmatrix} L_t^N \\ S_t^N \\ C_t^N \end{bmatrix} dt + \begin{bmatrix} \sigma_1^N & 0 & 0 \\ 0 & \sigma_2^N & 0 \\ 0 & 0 & \sigma_3^N \end{bmatrix} \begin{bmatrix} dW_t^{Q,L^N} \\ dW_t^{Q,S^N} \\ dW_t^{Q,C^N} \end{bmatrix}, \quad (4.1)$$

where

- $\lambda^N$  is the Nelson Siegel parameter,

- $\sigma_1^N$ ,  $\sigma_2^N$  and  $\sigma_3^N$  are the factor volatility parameters, and
- $W_t^{Q,L^N}$ ,  $W_t^{Q,S^N}$  and  $W_t^{Q,C^N}$  are Wiener processes under the risk neutral measure.

Invoking the Girsanov theorem (Girsanov, 1960), the real-world measure  $P$  factor dynamics are shown to be

$$\begin{bmatrix} dL_t^N \\ dS_t^N \\ dC_t^N \end{bmatrix} = \begin{bmatrix} k_1^N & 0 & 0 \\ 0 & k_2^N & 0 \\ 0 & 0 & k_3^N \end{bmatrix} \begin{bmatrix} \theta_{1,N} \\ \theta_{2,N} \\ \theta_{3,N} \end{bmatrix} - \begin{bmatrix} L_t^N \\ S_t^N \\ C_t^N \end{bmatrix} dt + \begin{bmatrix} \sigma_1^N & 0 & 0 \\ 0 & \sigma_2^N & 0 \\ 0 & 0 & \sigma_3^N \end{bmatrix} \begin{bmatrix} dW_t^{P,L^N} \\ dW_t^{P,S^N} \\ dW_t^{P,C^N} \end{bmatrix}, \quad (4.2)$$

where

- $k_1^N$ ,  $k_2^N$ ,  $k_3^N$ ,  $\theta_1^N$ ,  $\theta_2^N$  and  $\theta_3^N$  are parameters, and
- $W_t^{P,L^N}$ ,  $W_t^{P,S^N}$  and  $W_t^{P,C^N}$  are Wiener processes under the real-world measure.

Given these model dynamics, the zero coupon nominal bond yield at time  $t$  with  $\tau$  months maturity is given by the yield function

$$y_t^N(\tau) = L_t^N + S_t^N \left( \frac{1 - e^{-\lambda^N \tau}}{\lambda^N \tau} \right) + C_t^N \left( \frac{1 - e^{-\lambda^N \tau}}{\lambda^N \tau} - e^{-\lambda^N \tau} \right). \quad (4.3)$$

### 4.1.2 Model Calibration

To calibrate the nominal DNS interest rate model, we use monthly nominal yield observations as published by the U.S. Department of the Treasury<sup>1</sup>. In particular, we fit the period from October 2006 to May 2018 because this provides complete data for the following eleven maturity terms: 1 month, 3 months, 6 months, 1 year, 2 years, 3 years, 5 years, 7 years, 10 years, 20 years and 30 years.

The empirical data is presented in Figure 4.1. In general, the yield curve appears to be upward sloping with respect to maturity over the in-sample period. There also appears to be higher volatility in the short-term interest rates relative to the long-term rates. The summary statistics for the empirical nominal yield rates are provided in Table 4.1.

As with the joint ATSM, the DNS interest rate model can be expressed in state space form in terms of a measurement equation and a state transition equation. Therefore, it can be estimated using the Kalman filter (Kalman, 1960). The measurement equation is

$$\vec{y}_t^N = B^N \vec{X}_t^N + \vec{\epsilon}_t^N, \quad \vec{\epsilon}_t^N \sim N_n(\vec{0}, H^N), \quad (4.4)$$

<sup>1</sup><https://home.treasury.gov/>

**Figure 4.1:** Observed nominal bond yields from October 2006 to May 2018

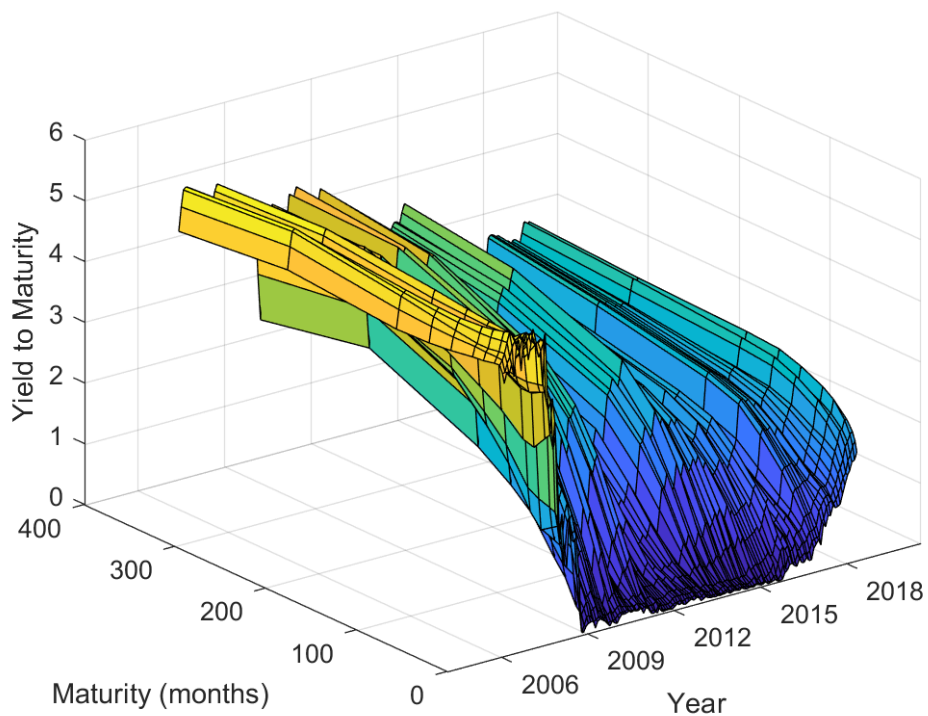


**Figure 4.2:** Fitted nominal bond yields from October 2006 to May 2018

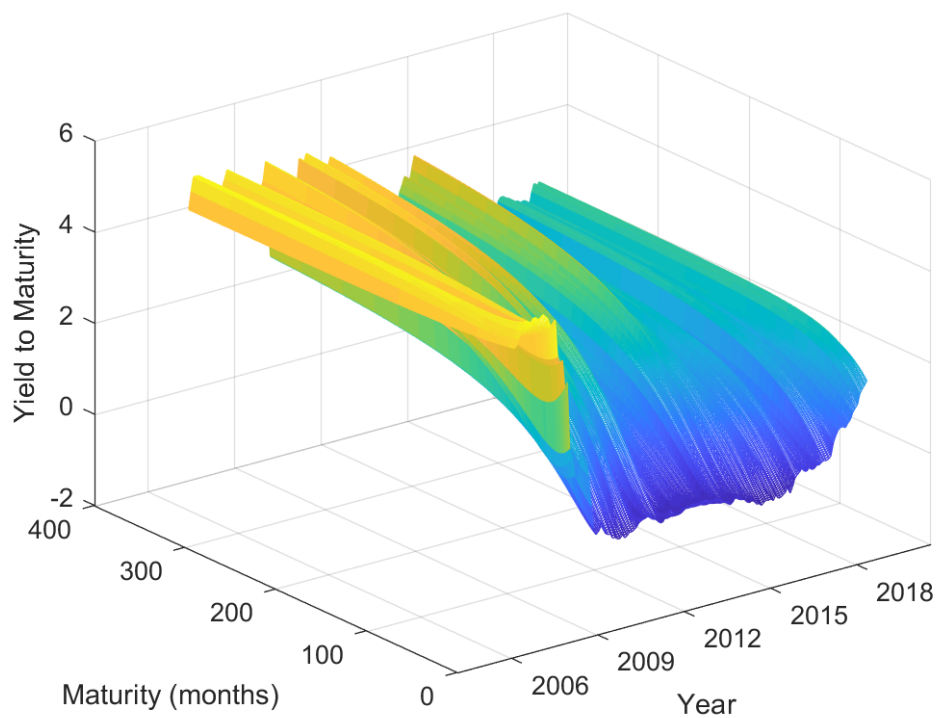


**Table 4.1:** Nominal interest rate summary statistics

Maturity (months)	Mean	Standard Deviation	Min	Max
1	0.98	1.63	0.00	5.24
3	1.04	1.65	0.00	5.16
6	1.14	1.67	0.03	5.24
12	1.23	1.61	0.09	5.21
24	1.43	1.47	0.20	5.16
36	1.66	1.37	0.30	5.13
60	2.14	1.21	0.59	5.10
84	2.54	1.09	0.98	5.11
120	2.91	1.00	1.46	5.15
240	3.46	0.97	1.78	5.35
360	3.63	0.83	2.18	5.21

where

$$\vec{y}_t^N = \begin{bmatrix} y_t^N(\tau_1) \\ \vdots \\ y_t^N(\tau_n) \end{bmatrix}, \quad B^N = \begin{bmatrix} 1 & \frac{1-e^{-\lambda^N \tau_1}}{\lambda^N \tau_1} & \frac{1-e^{-\lambda^N \tau_1}}{\lambda^N \tau_1} - e^{-\lambda^N \tau_1} \\ \vdots & \vdots & \vdots \\ 1 & \frac{1-e^{-\lambda^N \tau_n}}{\lambda^N \tau_n} & \frac{1-e^{-\lambda^N \tau_n}}{\lambda^N \tau_n} - e^{-\lambda^N \tau_n} \end{bmatrix}, \quad \vec{X}_t^N = \begin{bmatrix} L_t^N \\ S_t^N \\ C_t^N \end{bmatrix},$$

$$\vec{\epsilon}_t^N = \begin{bmatrix} \epsilon_t^N(\tau_1) \\ \vdots \\ \epsilon_t^N(\tau_n) \end{bmatrix},$$

$H^N$  is the (diagonal) covariance matrix of the normal error terms and  $n = 11$  observed maturities.

The state transition equation is given by

$$[\vec{X}_t^N - \vec{\theta}^N] = \kappa^N [\vec{X}_{t-1}^N - \vec{\theta}^N] - \vec{\eta}_t, \quad \vec{\eta}_t \sim N_3(\vec{0}, Q^N), \quad (4.5)$$

where

$$\vec{\theta}^N = \begin{bmatrix} \theta_L^N \\ \theta_S^N \\ \theta_C^N \end{bmatrix}, \quad \kappa^N = \begin{bmatrix} e^{-\kappa_1^N \Delta t} & 0 & 0 \\ 0 & e^{-\kappa_2^N \Delta t} & 0 \\ 0 & 0 & e^{-\kappa_3^N \Delta t} \end{bmatrix},$$

$$Q^N = \begin{bmatrix} \frac{\sigma_1^2(1-e^{-2\kappa_1^N \Delta t})}{2\kappa_1^N} & 0 & 0 \\ 0 & \frac{\sigma_2^2(1-e^{-2\kappa_2^N \Delta t})}{2\kappa_2^N} & 0 \\ 0 & 0 & \frac{\sigma_3^2(1-e^{-2\kappa_3^N \Delta t})}{2\kappa_3^N} \end{bmatrix}$$

and  $\Delta t = \frac{1}{12}$  (for monthly data).

We apply the Kalman filtering technique to the observed nominal bond yield data and obtain an estimated Nelson Siegel parameter of  $\lambda^N = 0.042$ . The fitted

yields are presented in Figure 4.2 and appear to broadly capture the key features of the observed interest rate data.

The mean and standard deviations of the model residuals by maturity are provided in Table 4.2. It appears that the model exhibits a better fit to the observed data for maturities beyond 3 months. Given that our basis risk analysis is based on maturities ranging from 1 year to 20 years, the model gives a satisfactory fitting performance over the most relevant maturities. Figure 4.3 compares the observed and empirical mean yield curves and confirms the satisfactory overall fit of the estimated interest rate model.

**Table 4.2:** Nominal interest rates: residual mean and standard deviation by maturity

Maturity (months)	Mean (bps)	Standard Deviation (bps)
1	-13.3333	6.6372
3	-7.5352	5.9266
6	0.3016	0.7937
12	2.3771	6.6486
24	0.9736	5.7837
36	-1.2565	2.5624
60	-0.1157	5.2012
84	2.1626	4.2657
120	-0.0610	0.8739
240	0.8163	4.0693
360	-1.0173	3.2993

### 4.1.3 Forecasting and Simulation

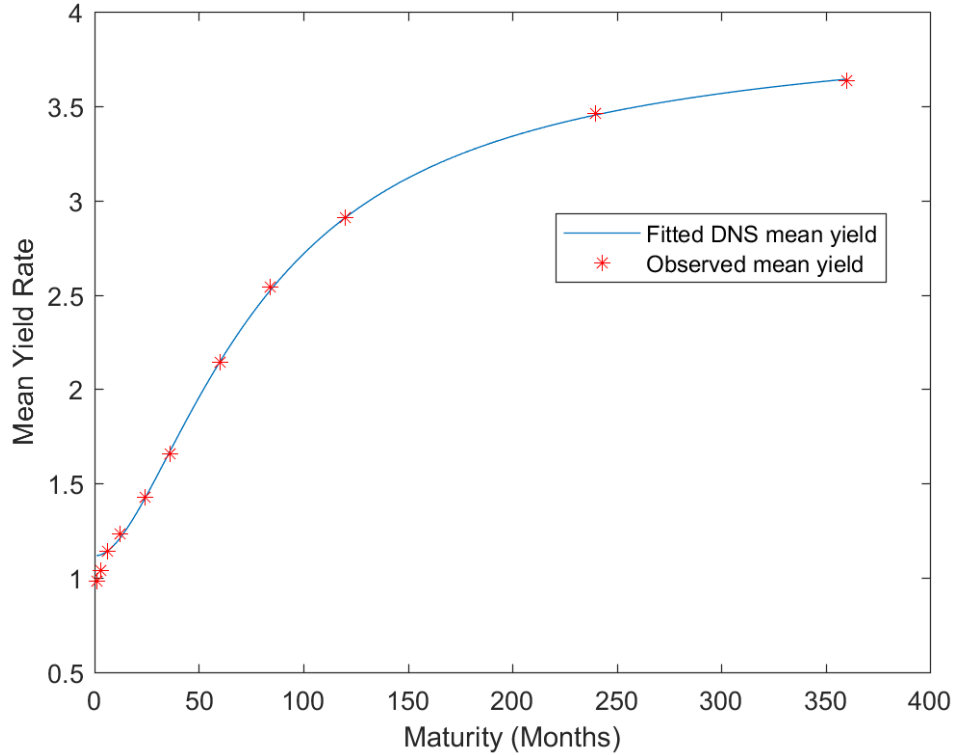
Having estimated the model, we then forecast and simulate the future term structure of interest rates and the associated zero coupon bond prices over a 20 year time horizon. The forecasting of zero coupon bond prices is achieved as follows:

1. Forecast the level, slope and curvature factors  $L_t^F$ ,  $S_t^F$ ,  $C_t^F$  for years  $t = 1, 2, \dots, 20$  from the estimated DNS nominal interest rate model.
2. Substitute the forecast factors into the yield function to forecast the term structure of interest rates.

$$y_t^F(\tau) = L_t^F + S_t^F \left( \frac{1 - e^{-\lambda\tau}}{\lambda\tau} \right) + C_t^F \left( \frac{1 - e^{-\lambda\tau}}{\lambda\tau} - e^{-\lambda\tau} \right). \quad (4.6)$$

3. Compute the associated zero coupon bond price forecasts:

$$P^F(t, T) = e^{(-y_t^F(T-t)(T-t))}. \quad (4.7)$$

**Figure 4.3:** Observed and fitted nominal mean yields, October 2006 to May 2018

The simulation of zero coupon bond prices follows a similar procedure.

1. Simulate the level, slope and curvature factors  $L_t^{[i]}$ ,  $S_t^{[i]}$ ,  $C_t^{[i]}$  for years  $t = 1, 2, \dots, 20$  and for simulation paths  $i = 1, 2, \dots, 5000$  from the estimated DNS nominal interest rate model.
2. Substitute the simulated factors into the yield function to simulate the term structure of interest rates.

$$y_t^{[i]}(\tau) = L_t^{[i]} + S_t^{[i]} \left( \frac{1 - e^{-\lambda\tau}}{\lambda\tau} \right) + C_t^{[i]} \left( \frac{1 - e^{-\lambda\tau}}{\lambda\tau} - e^{-\lambda\tau} \right). \quad (4.8)$$

3. Compute the associated zero coupon bond price simulations:

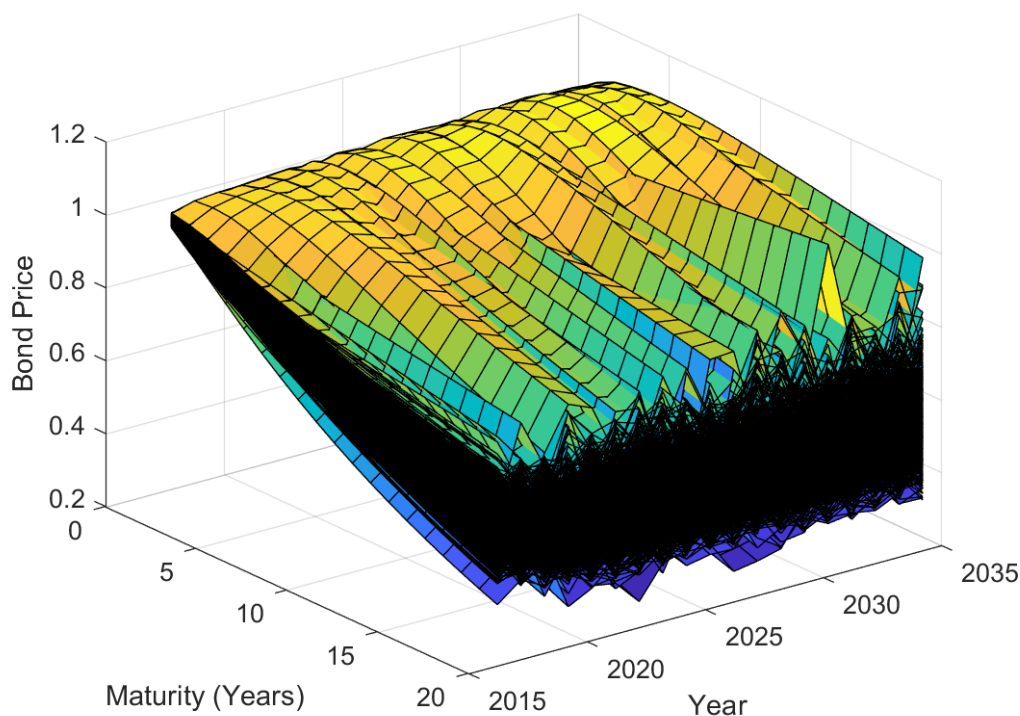
$$P^{[i]}(t, T) = e^{(-y_t^{[i]}(T-t)(T-t))}. \quad (4.9)$$

Indeed, one of the key advantages associated with the affine term structure of interest rate modelling framework is the availability of explicit closed-form solutions to future yield rates and zero coupon bond prices which can be expressed as a function of the underlying factors.

Figure 4.4 shows the simulated future nominal bond prices over the 20 year simulation horizon for maturities of up to 20 years. From this surface plot, one of the key limitations of modelling nominal interest rates using the dynamic Nelson

Siegel model becomes apparent: there is a small probability that certain simulations could produce negative nominal interest rates and hence the zero coupon prices may not be monotonically decreasing with respect to the term to maturity for all simulation paths. However, as is evident from Figure 4.4, this probability is, in practice, quite small.

**Figure 4.4:** Simulated nominal bond prices over a 20 year simulation horizon



## 4.2 Real Interest Rate Model

The modelling of real interest rates broadly reflects the nominal interest rate modelling framework described in Section 4.1.

### 4.2.1 Model Specification

The real interest rate model incorporates three latent time-varying factors:

- $L_t^R$ : a level factor for the real yield curve,
- $S_t^R$ : a slope factor for the real yield curve, and
- $C_t^R$ : a curvature factor for the real yield curve.

The risk neutral  $Q$  dynamics of the factors are

$$\begin{bmatrix} dL_t^R \\ dS_t^R \\ dC_t^R \end{bmatrix} = - \begin{bmatrix} 0 & 0 & 0 \\ 0 & \lambda^R & -\lambda^R \\ 0 & 0 & -\lambda^R \end{bmatrix} \begin{bmatrix} L_t^R \\ S_t^R \\ C_t^R \end{bmatrix} dt + \begin{bmatrix} \sigma_1^R & 0 & 0 \\ 0 & \sigma_2^R & 0 \\ 0 & 0 & \sigma_3^R \end{bmatrix} \begin{bmatrix} dW_t^{Q,L^R} \\ dW_t^{Q,S^R} \\ dW_t^{Q,C^R} \end{bmatrix}, \quad (4.10)$$

where

- $\lambda^R$  is the Nelson Siegel parameter,
- $\sigma_1^R$ ,  $\sigma_2^R$  and  $\sigma_3^R$  are the factor volatility parameters, and
- $W_t^{Q,L^R}$ ,  $W_t^{Q,S^R}$  and  $W_t^{Q,C^R}$  are Wiener processes under the risk neutral measure.

Invoking the Girsanov theorem (Girsanov, 1960), the real-world measure  $P$  factor dynamics are shown to be

$$\begin{bmatrix} dL_t^R \\ dS_t^R \\ dC_t^R \end{bmatrix} = \begin{bmatrix} k_1^R & 0 & 0 \\ 0 & k_2^R & 0 \\ 0 & 0 & k_3^R \end{bmatrix} \left[ \begin{bmatrix} \theta_{1,R} \\ \theta_{2,R} \\ \theta_{3,R} \end{bmatrix} - \begin{bmatrix} L_t^R \\ S_t^R \\ C_t^R \end{bmatrix} \right] dt + \begin{bmatrix} \sigma_1^R & 0 & 0 \\ 0 & \sigma_2^R & 0 \\ 0 & 0 & \sigma_3^R \end{bmatrix} \begin{bmatrix} dW_t^{P,L^R} \\ dW_t^{P,S^R} \\ dW_t^{P,C^R} \end{bmatrix}, \quad (4.11)$$

where

- $k_1^R$ ,  $k_2^R$ ,  $k_3^R$ ,  $\theta_1^R$ ,  $\theta_2^R$  and  $\theta_3^R$  are parameters, and
- $W_t^{P,L^R}$ ,  $W_t^{P,S^R}$  and  $W_t^{P,C^R}$  are Wiener processes under the real-world measure.

Given these model dynamics, the zero coupon real bond yield at time  $t$  with  $\tau$  months maturity is given by the yield function

$$y_t^R(\tau) = L_t^R + S_t^R \left( \frac{1 - e^{-\lambda^R \tau}}{\lambda^R \tau} \right) + C_t^R \left( \frac{1 - e^{-\lambda^R \tau}}{\lambda^R \tau} - e^{-\lambda^R \tau} \right). \quad (4.12)$$

## 4.2.2 Model Calibration

To calibrate the real DNS interest rate model, we use monthly real yield observations as published by the U.S. Department of the Treasury<sup>2</sup>. In particular, we fit the period from February 2010 to May 2018 because this provides complete data for the following five maturity terms: 5 years, 7 years, 10 years, 20 years and 30 years.

The empirical data is shown in Figure 4.5. Similarly to the observed nominal interest rate data, the real yield curve also appears to be upward sloping with respect to maturity over the in-sample period. Again, there appears to be higher volatility in the short-term interest rates relative to the long-term rates. Unlike the nominal interest rates, we observe negative bond yields at various different time

**Figure 4.5:** Observed real bond yields from February 2010 to May 2018

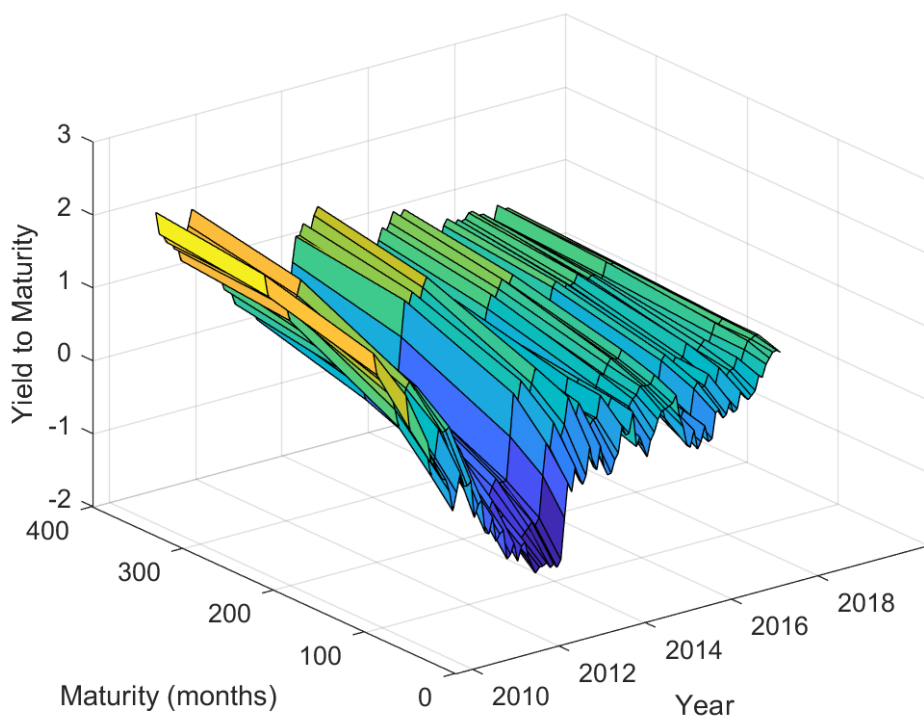


**Figure 4.6:** Fitted real bond yields from February 2010 to May 2018

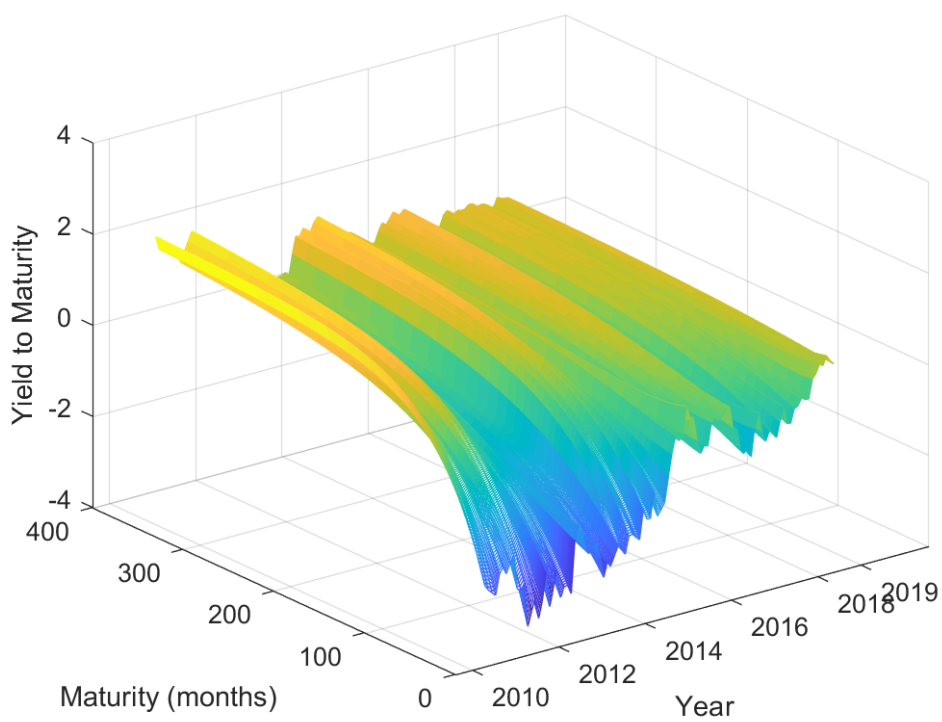


**Table 4.3:** Real interest rate summary statistics

Maturity (months)	Mean	Standard Deviation	Min	Max
60	-0.24	0.57	-1.47	0.72
84	0.08	0.54	-1.20	1.23
120	0.34	0.50	-0.79	1.60
240	0.81	0.46	-0.09	1.99
360	1.05	0.43	0.32	2.16

points, particularly in the 5 year maturity range. The summary statistics for the empirical real yield rates are provided in Table 4.3.

Once more, the Kalman filter (Kalman, 1960) is used to estimate the model. The measurement equation is

$$\vec{y}_t^R = B^R \vec{X}_t^R + \vec{\epsilon}_t^R, \quad \vec{\epsilon}_t^R \sim N_n(\vec{0}, H^R), \quad (4.13)$$

where

$$\vec{y}_t^R = \begin{bmatrix} y_t^R(\tau_1) \\ \vdots \\ y_t^R(\tau_n) \end{bmatrix}, \quad B^R = \begin{bmatrix} 1 & \frac{1-e^{-\lambda^R \tau_1}}{\lambda^R \tau_1} & \frac{1-e^{-\lambda^R \tau_1}}{\lambda^R \tau_1} - e^{-\lambda^R \tau_1} \\ \vdots & \vdots & \vdots \\ 1 & \frac{1-e^{-\lambda^R \tau_n}}{\lambda^R \tau_n} & \frac{1-e^{-\lambda^R \tau_n}}{\lambda^R \tau_n} - e^{-\lambda^R \tau_n} \end{bmatrix}, \quad \vec{X}_t^R = \begin{bmatrix} L_t^R \\ S_t^R \\ C_t^R \end{bmatrix},$$

$$\vec{\epsilon}_t^R = \begin{bmatrix} \epsilon_t^R(\tau_1) \\ \vdots \\ \epsilon_t^R(\tau_n) \end{bmatrix},$$

$H^N$  is the (diagonal) covariance matrix of the normal error terms and  $n = 5$  observed maturities.

The state transition equation is given by

$$[\vec{X}_t^R - \vec{\theta}^R] = \kappa^R [\vec{X}_{t-1}^R - \vec{\theta}^R] - \vec{\eta}_t, \quad \vec{\eta}_t \sim N_3(\vec{0}, Q^R), \quad (4.14)$$

where

$$\vec{\theta}^R = \begin{bmatrix} \theta_L^R \\ \theta_S^R \\ \theta_C^R \end{bmatrix}, \quad \kappa^R = \begin{bmatrix} e^{-\kappa_1^R \Delta t} & 0 & 0 \\ 0 & e^{-\kappa_2^R \Delta t} & 0 \\ 0 & 0 & e^{-\kappa_3^R \Delta t} \end{bmatrix},$$

$$Q^R = \begin{bmatrix} \frac{\sigma_1^2(1-e^{-2\kappa_1^R \Delta t})}{2\kappa_1^R} & 0 & 0 \\ 0 & \frac{\sigma_2^2(1-e^{-2\kappa_2^R \Delta t})}{2\kappa_2^R} & 0 \\ 0 & 0 & \frac{\sigma_3^2(1-e^{-2\kappa_3^R \Delta t})}{2\kappa_3^R} \end{bmatrix}$$

<sup>2</sup><https://home.treasury.gov/>

and  $\Delta t = \frac{1}{12}$  (for monthly data).

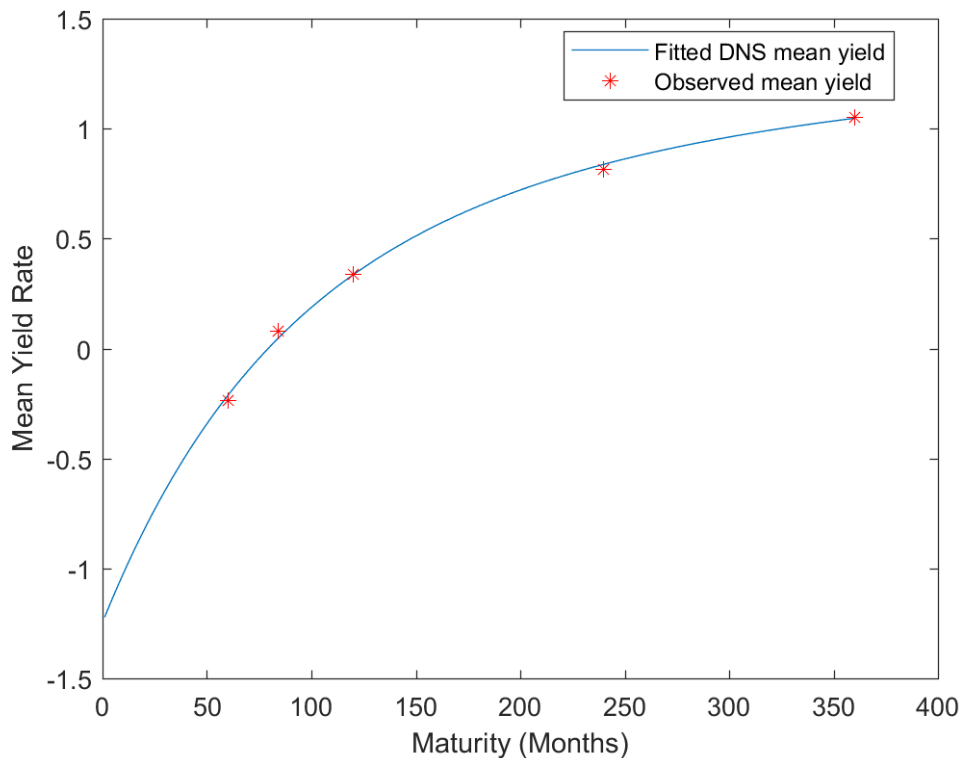
We apply the Kalman filtering technique to the observed real bond yield data and obtain an estimated Nelson Siegel parameter of  $\lambda^R = 0.017$ . The fitted yields are presented in Figure 4.6 and appear to broadly capture the key features of the observed interest rate data.

The mean and standard deviations of the model residuals by maturity are provided in Table 4.4. It appears that the model exhibits a relatively good fit for all observed maturities, as indicated by relatively low residual means and standard deviations. Figure 4.7 compares the observed and empirical mean yield curves and confirms the satisfactory overall fit of the estimated interest rate model.

**Table 4.4:** Real interest rates: residual mean and standard deviation by maturity

Maturity (months)	Mean (bps)	Standard Deviation (bps)
60	-2.4091	5.6250
84	3.1164	6.7812
120	0.0000	0.0000
240	-2.3681	3.3248
360	0.3077	0.8901

**Figure 4.7:** Observed and fitted real mean yields, February 2010 to May 2018

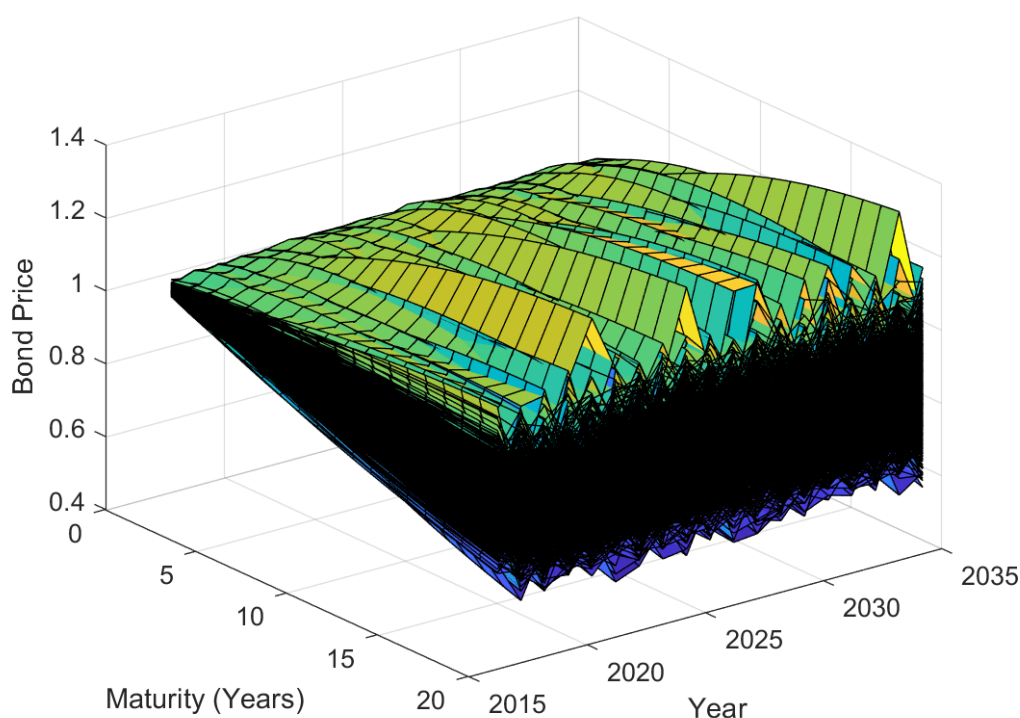


### 4.2.3 Forecasting and Simulation

Having estimated the model, we then forecast and simulate the future term structure of interest rates and the associated zero coupon bond prices over a 20 year time horizon. The forecasting and simulation of bond yields and prices follows the same approach as described in Subsection 4.1.3.

Figure 4.8 shows the simulated future real bond prices over the 20 year simulation horizon for maturities of up to 20 years. Unlike the nominal interest rate case, negative bond yields are acceptable when modelling real interest rates.

**Figure 4.8:** Simulated real bond prices over a 20 year simulation horizon



The simulated and forecasted nominal and real zero coupon bond prices can now be combined with the mortality rate projections developed in Chapter 3 in order to construct the value-based longevity index, as well as to conduct basis risk analyses for retirement income portfolios hedged using the constructed index.

# Chapter 5

## Value-Based Longevity Index and Longevity Risk Hedging

In this chapter, we draw on the simulated and forecast outcomes from the mortality and interest rate modelling frameworks described in Chapters 3 and 4 respectively in order to construct the value-based longevity index and assess its effectiveness when hedging the risks associated with retirement income portfolios. Section 5.1 details the definition and construction of the index. In Section 5.2, we design the hedging strategy by calibrating the optimal notional swap weighting. It is critical to compare the hedge effectiveness associated with the value-based longevity index against that of alternative longevity indices to identify the key drivers of risk in retirement income portfolios – these comparison indices are outlined in the Section 5.3. Section 5.4 presents several basis risk measures to quantify the effectiveness of different hedging indices. Finally, in Section 5.5, we conduct a range of sensitivity analyses to determine the significance of various modelling assumptions and experimental design settings.

### 5.1 Index Construction

We define the value-based longevity index  $I_{x,t}$  as the expected present value of a unit of longevity and inflation-indexed income paid annually in arrears to a cohort aged  $x$  at initial time  $t$ . The index reflects only the expected survival rates, interest rates and inflation. As referenced in Subsection 2.4, BlackRock's CoRI is not a suitable index for longevity hedging purposes because it accounts for the market price of longevity risk as reflected in the current pricing of retirement income products by providers. Therefore, it is not perceived by market participants as an independent, objective representation of longevity outcomes. To overcome this issue, our index does not incorporate any longevity risk premium. Instead, it is up to financial

markets to determine an appropriate price for longevity risk through the setting of forward prices for traded index-linked instruments. Furthermore, in accordance with Chang and Sherris (2018), our index will not account for any expense loading or profit margin.

The value of the index is

$$I_{x,t} = \sum_{i=1}^{\omega-x} S^R(x, t, t+i) \times P_R(t, t+i), \quad (5.1)$$

where

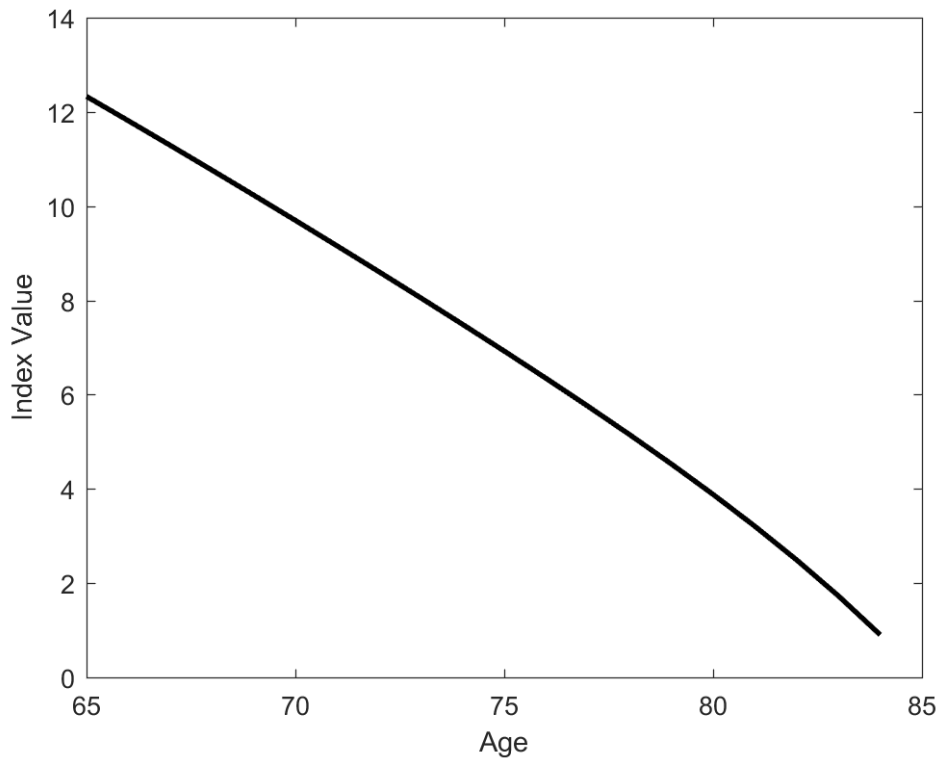
- $\omega$  denotes the age of final payment (assumed to be 85 in our analysis),
- $S^R(x, t, t+i)$  denotes the forecast  $i$  year survival probability of the reference population, and
- $P_R(t, t+i)$  is the forecast time  $t$  price of an inflation-indexed zero coupon bond making a single unit payment at time  $t+i$  as computed from the real DNS interest rate model.

Figure 5.1 shows the initial (that is, time  $t = 0$ ) index values for ages 65 to 84, drawing on survival probabilities generated by the continuous-time mortality model. The index value for age 65 is 12.18. That is, for each 65 year old male who is promised \$1 of inflation-indexed income per year upon survival from ages 66 to 85, a retirement income provider requires \$12.18 worth of investments today.

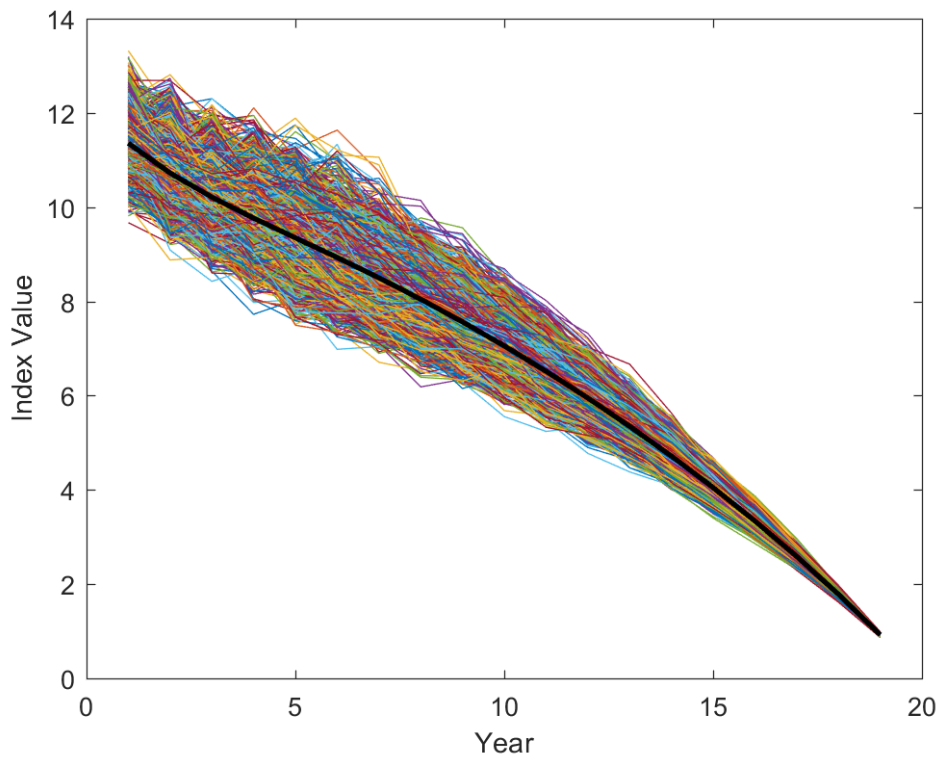
It is also possible to forecast and simulate future index values over time based on mortality and interest rate forecasts and simulations. For example, the forward index values for the cohort initially aged 65 (at time  $t = 0$ ) is represented by the black curve in Figure 5.2. This shows the expected path of the value-based longevity index over the payment period for this particular reference population cohort. A smooth and stable decline is observed.

In reality, mortality, interest rate and inflation factors will differ over time from initial forecasts and hence the evolution of the index will not exactly track its expected pathway. Figure 5.2 also shows 5,000 simulations of the index value for the cohort initially aged 65. We see that although the forward index values remain broadly in the middle of the distribution of simulated paths, there is material variability around the expected value over time. The volatility around the forward values declines over time until the final age is reached.

**Figure 5.1:** Initial index value by age (joint ATSM)



**Figure 5.2:** Forward and simulated index values, (joint ATSM)



## 5.2 Hedging Strategy

Having constructed the value-based longevity index, this section now describes the design of an optimal hedging strategy by retirement income provider using a standardised swap instrument which references the value-based longevity index.

For our hedging analysis, we assume that a retirement income provider is aiming to hedge the risks associated with a closed annuity pool of 65 year old males who are promised \$1 of inflation-indexed income per year upon survival from ages 66 to 85. That is, the fund consists of a single cohort and no subsequent additions to the scheme are made.

The random present value of the retirement income portfolio liability is

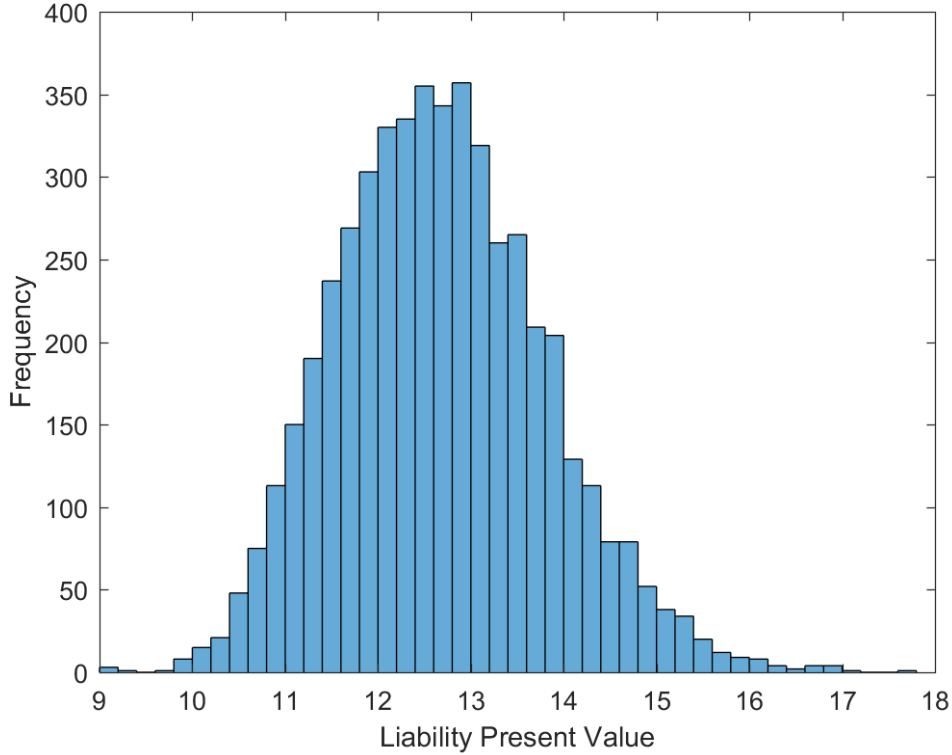
$$PV(\text{Unhedged Portfolio}) = \sum_{i=1}^{\omega-x} l_{x+i,t+i}^B \times P_R(t, t+i), \quad (5.2)$$

where

- $x = 65$  and  $\omega = 85$ .
- the number of surviving annuitants  $l_{x+i,t+i}^B$  (aged  $x+i$  at time  $t+i$ ) is dependent on the simulated book population mortality dynamics generated by the mortality models. However, we also account for sampling basis risk by allowing the number of deaths in any given year to follow a binomial distribution  $D_{x,t}^B \sim \text{Bin}(E_{x,t}^B, q_{x,t}^B)$  (Haberman et al., 2014) where the exposure  $E_{x,t}^B$  is given by the number of surviving annuitants in year  $t$  and the mortality rate parameter  $q_{x,t}^B$  is simulated from the mortality model.
- $P_R(t, t+i)$  is the time  $t$  price of an inflation-indexed zero coupon bond making a single unit payment at time  $t+i$  as computed from the real interest rate model.  $P_R(t, t+i)$  is computed from a single simulation path.

In Figure 5.3, we plot a histogram showing 5,000 simulations of the liability present value for a portfolio with an initial size of 100,000 lives. A degree of positive skewness is apparent, with the simulated distribution exhibiting a heavier right tail.

Assume that an annually-settled index swap trades in the longevity risk transfer market. For a given age  $x$  at initial time  $t$ , the swap references the constructed value-based longevity index  $I_{x,t}$ ; at time  $t+i$ , the fixed leg pays the  $i$  year forward index value  $I_{x+i,t+i}^f$  while the floating leg pays the realised index value  $I_{x+i,t+i}$ . As index values are based on forward-looking cashflows, the final swap payment is made when the initial cohort reaches age  $\omega - 1$ ; not at age  $\omega$  when the final annuity payments are made to surviving policyholders. That is, the swap has an initial maturity term of  $\omega - x - 1$ . Therefore, the longevity, interest rate and inflation risk over the final year of the liability remain unhedged. This mismatch between liability and hedge cashflows constitutes an example of structuring basis risk.

**Figure 5.3:** Liability present value histogram, (joint ATSM, 100,000 lives)

A retirement income provider seeking to hedge their risk exposure would be the fixed leg payer to this index swap. From their perspective, the random present value of the swap instrument is

$$PV(\text{Index Swap}) = \sum_{i=1}^{\omega-x-1} (I_{x+i,t+i} - I_{x+i,t+i}^f) \times P_N(t, t+i), \quad (5.3)$$

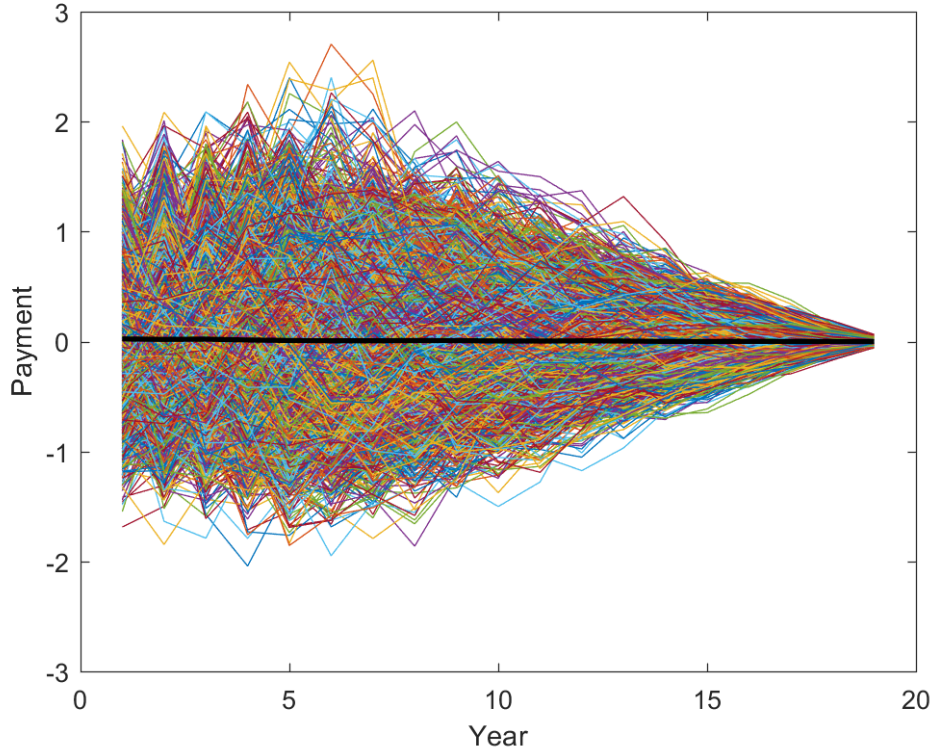
where

- $x = 65$  and  $\omega = 85$ .
- $I_{x+i,t+i}^f$  denotes the forward index value. It is computed from central forecasts.
- $I_{x+i,t+i}$  denotes the realised index value. Its computation entails two distinct steps. The initial phase involves the simulation of a single mortality intensity and interest rate path up until time  $t+i$ . In the second stage, conditional on the mortality and interest rate realisations in the first phase, central forecasts from time  $t+i$  onwards are computed to derive the realised index value  $I_{x+i,t+i}$ .
- $P_N(t, t+i)$  is the time  $t$  price of a nominal zero coupon bond making a single unit payment at time  $t+i$ .  $P_N(t, t+i)$  is simulated from the nominal interest rate model.

The simulated swap payment paths received by the fixed leg payer over the 19 year swap term is shown in Figure 5.4. Although individual swap payment paths can

be volatile, the average swap payment, as depicted by the black line, remains very close to zero. This reflects the fact that forward index values are simply assumed to follow the expected values with no risk or profit premiums priced in to the forward values. As reflected in Figure 5.2, the variability of swap payments is highest in the early years of the hedge and steadily decreases over the term of the swap.

**Figure 5.4:** Simulated swap payments (joint ATSM)



When a retirement income provider hedges their exposure using the swap instrument, they effectively combine the hedging instrument with their exposed portfolio. Therefore, the random present value of the retirement income provider's hedged portfolio is given by the sum of the the present values of the two components.

$$\begin{aligned}
 PV(\text{Hedged Portfolio}) &= PV(\text{Unhedged Portfolio}) + PV(\text{Index Swap}) \\
 &= \sum_{i=1}^{\omega-x} l_{x+i,t+i}^B \times P_R(t, t+i) + w_0 \sum_{i=1}^{\omega-x-1} (I_{x+i,t+i} - I_{x+i,t+i}^f) \times P_N(t, t+i), \quad (5.4)
 \end{aligned}$$

where  $w_0$  refers to the notional amount of the longevity swap. Following the suggested framework in Li et al. (2017), we estimate  $w_0$  using numerical optimisation with an objective to minimise the variance of the hedged portfolio's present value, obtaining a solution of  $w_0 = 0.3268$ . Since the analysis is based on a static hedging framework, the swap weight is calibrated at the outset and thereafter does not require periodic rebalancing or recalibration in response to evolving market conditions or mortality experience. In contrast, under a dynamic hedging regime,  $w_0$  is

recalibrated each time the portfolio is rebalanced. Ngai and Sherris (2011) note that static hedging is more appropriate and practical given the lack of liquidity in the longevity risk transfer market.

## 5.3 Comparison Against Other Longevity Indices

Inspired by Chang and Sherris (2018), we compare the hedge outcomes associated with the value-based longevity index to two other longevity indices which we also construct. The purpose of these comparisons is to attribute the risks associated with retirement income portfolios into longevity risk, interest rate risk and inflation risk components.

### 5.3.1 Survival Index

We define the index  $I_{x,t}^0$  as the expected survival probability of a cohort aged  $x$  in year  $t$ . The survival index value is

$$I_{x,t}^0 = \sum_{i=1}^{\omega-x} S^R(x, t, t+i), \quad (5.5)$$

where

- $\omega$  denotes the age of final payment, and
- $S^R(x, t, t+i)$  denotes the forecast  $i$  year survival probability of the reference population.

### 5.3.2 Value-Based Longevity Index without Inflation-Indexation

We define the index  $I_{x,t}^1$  as the expected present value of a unit of longevity-indexed income paid annually in arrears to a cohort aged  $x$  in year  $t$ . The index value is

$$I_{x,t}^1 = \sum_{i=1}^{\omega-x} S^R(x, t, t+i) \times P_N(t, t+i), \quad (5.6)$$

where

- $\omega$  denotes the age of final payment,
- $S^R(x, t, t+i)$  denotes the forecast  $i$  year survival probability of the reference population.
- $P_N(t, t+i)$  is the forecast time  $t$  price of a nominal zero coupon bond making a single unit payment at time  $t+i$  as computed from the nominal interest rate model.

The risk coverage of the various constructed longevity indices is summarised in Table 5.1 below.

**Table 5.1:** Risk coverage of different longevity indices

Index	Longevity Risk	Interest Rate Risk	Inflation Risk
$I_{x,t}^0$	✓		
$I_{x,t}^1$	✓	✓	
$I_{x,t}$	✓	✓	✓

Based on this table, the attribution of risk can be outlined as follows:

- The risk reduction achieved by hedging the retirement income portfolio using  $I_{x,t}^0$  as the reference index represents the impact of longevity risk.
- The additional risk reduction achieved by hedging the retirement income portfolio using  $I_{x,t}^1$  as the reference index (relative to a hedge referencing the index  $I_{x,t}^0$ ) represents the impact of interest rate risk.
- The additional risk reduction achieved by hedging the retirement income portfolio using  $I_{x,t}$  as the reference index (relative to a hedge referencing the index  $I_{x,t}^1$ ) represents the impact of inflation risk.

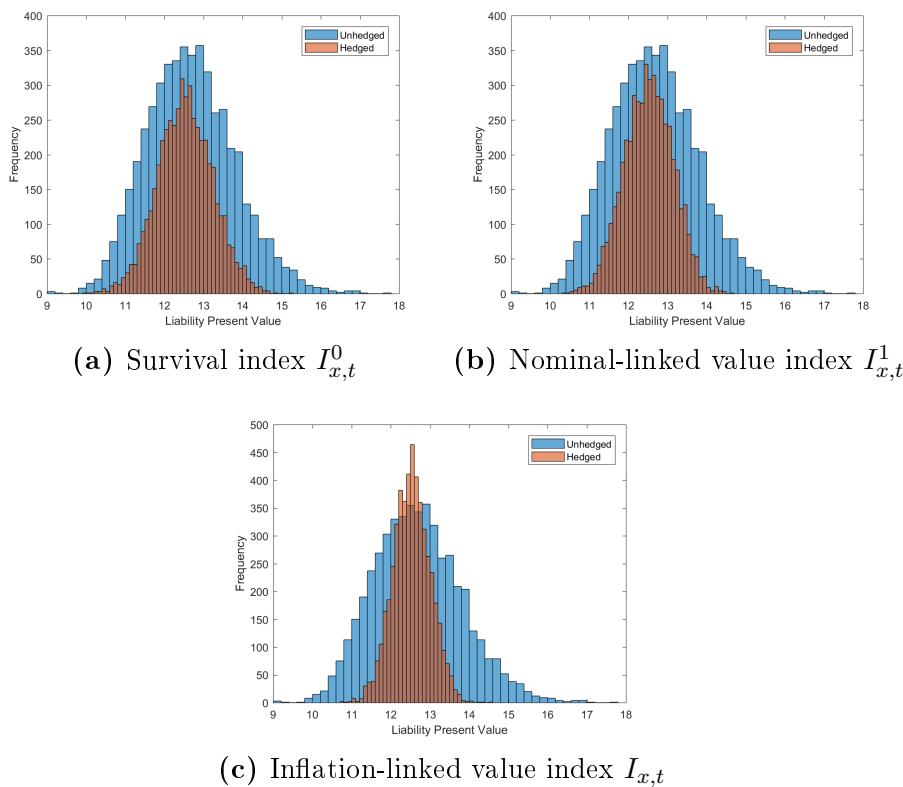
## 5.4 Basis Risk Analysis

Having calibrated the longevity swap instrument following the framework described in Section 5.2, it is critical to assess the effectiveness of the hedging strategy. We initially adopt graphical risk reduction representations as visualisation can be a very efficient way to communicate the effectiveness of hedging strategies to a variety of different stakeholders. Following Coughlan (2009), we plot the simulated liability distributions to obtain a preliminary overview of the degree of risk reduction achieved by the index-based hedge, as well as the other comparison indices described in Section 5.3.

In Figure 5.5, the blue histograms represent the present value of the *unhedged* portfolio liability outcomes, while the overlaid orange histograms represent the net present value of the *hedged* liability outcomes (that is, the sum of the unhedged liability outcomes and the weighted index swap outcomes). These diagrams represent annuity pools with 100,000 initial members. For all three indices, we observe a reduction in the volatility of liability valuations once the index swaps have been taken into account. However, it is also apparent that when the liability is hedged

with reference to the inflation-indexed value-based longevity index  $I_{x,t}$  (Figure 5.5c), the hedged distribution becomes materially narrower relative to the two alternate longevity indices.

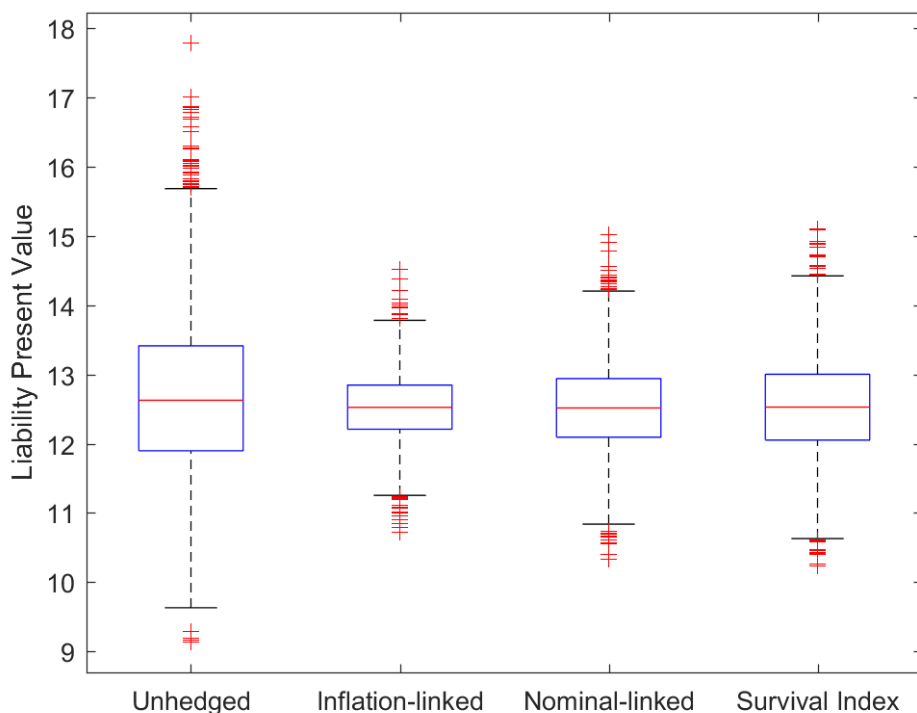
**Figure 5.5:** Hedged and unhedged liability present value distributions by hedging index (joint ATSM, 100,000 lives)



We also present a box and whisker plot of the simulated liability present value outcomes in Figure 5.6. In all four simulated distributions, the median outcome as indicated by the central mark is relatively similar. However, once we examine the 25<sup>th</sup> and 75<sup>th</sup> percentiles of the liability distribution (represented by the lower and upper edges of the box respectively), we note that variability is materially reduced when comparing the inflation-linked hedge against the unhedged liability as well as the two other alternate hedging indices. Furthermore, the outliers associated with the simulated net liability outcomes (indicated by the red crosses) are much less extreme in the case of the inflation-linked value-based longevity index, confirming the observations inferred from the histograms in Figure 5.5.

However, although graphical representations can provide an adequate understanding of hedging efficiency, in order to systematically evaluate the hedge effectiveness of the inflation-indexed value-based longevity index relative to the other longevity indices, quantitative risk measures must also be examined. Therefore, we investigate the summary statistics of the simulated liability present value distributions, as presented in Table 5.2. From these figures, it is evident that the

**Figure 5.6:** Hedged and unhedged liability present value box and whisker plots by hedging index (joint ATSM, 100,000 lives)



minimum and maximum outcomes are much less extreme and the variance of the liability present value distribution is materially reduced by hedging. Indeed, given the approximate normality of the distributions observed in Figure 5.5, we conduct an F-test for equality of two variances to formally examine whether the variance of the liability present value is reduced when hedged against the inflation-linked value index relative to the two other indices. Against a one-sided alternative, we are able to reject the null hypothesis at all reasonable significance levels ( $p$ -value  $< 0.0001$ ) and conclude that the variance of the hedged liability tied to the inflation-linked value index is lower than that of both other indices at a statistically significant level.

**Table 5.2:** Summary statistics: hedged and unhedged liability present value outcomes by hedging index (joint ATSM, 100,000 lives)

Hedging Index	Minimum	Maximum	Mean	Variance
Unhedged	9.10	17.25	12.59	1.23
Survival index $I_{x,t}^0$	9.80	14.73	12.44	0.46
Nominal-linked value index $I_{x,t}^1$	10.36	14.84	12.44	0.33
Inflation-linked value index $I_{x,t}$	10.87	14.18	12.44	0.20

The Longevity Risk Reduction (LRR) metric is also well established in the liter-

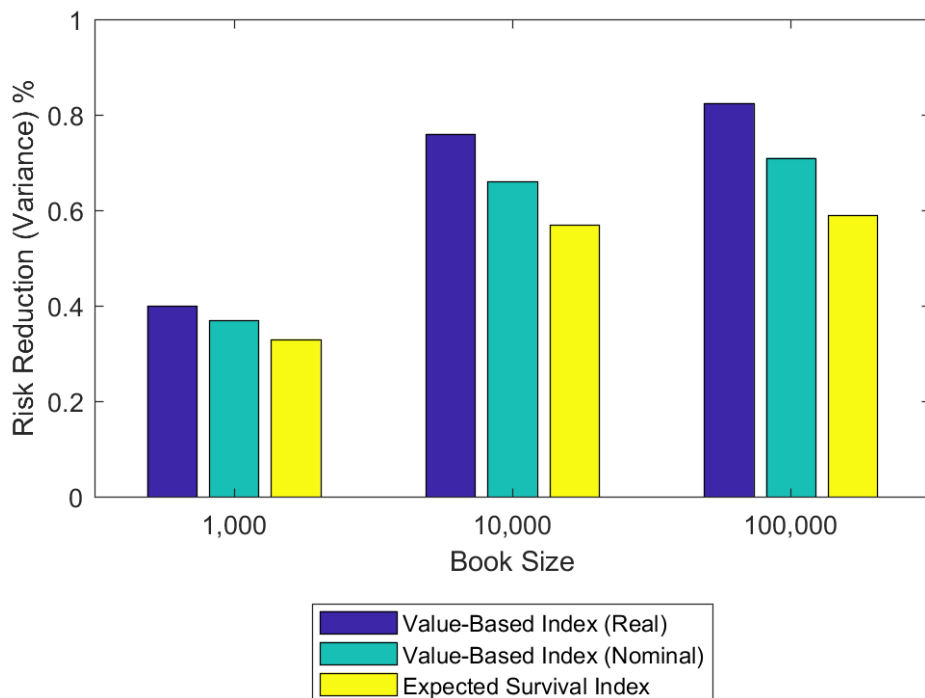
ature as a robust indicator of hedging performance for longevity-linked instruments (see, for example, Coughlan et al., 2011; Li et al., 2017). Note that some authors refer to the LRR metric using alternate terms such as “hedge efficiency” (Chang and Sherris, 2018). Following Cairns et al. (2014), we define our LRR measure based on the percentage reduction in variance of the liability present value:

$$\text{Longevity Risk Reduction} = \left(1 - \frac{\text{var}(\text{Hedged Portfolio})}{\text{var}(\text{Unhedged Portfolio})}\right) \times 100\%, \quad (5.7)$$

where  $\text{var}(\text{Unhedged Portfolio})$  and  $\text{var}(\text{Hedged Portfolio})$  refer to the variance of the retirement income provider’s net position before and after the hedge has been applied, respectively.

In Figure 5.7, we show the LRR attained by the various indices across three different book sizes. It is apparent that all indices are ineffective at book sizes of 1,000 policyholders due to sampling basis risk. Once the portfolio size increases to 10,000 and eventually 100,000 policyholders, all three indices exhibit a much improved hedging performance. However, the LRR associated with the inflation-linked value-based longevity index remains materially superior to the other indices at all book sizes, with the magnitude of the out-performance found to be higher in larger portfolios. However, it should be noted that even in a particularly large portfolio of 100,000 annuitants, the inflation-indexed value-based longevity index does not provide a perfect hedge (LRR of 82.47%). Demographic basis risk remains a factor, while the structuring basis risk associated with the final year of the liability remaining unhedged also impacts the outcome.

The differences between the hedging outcomes associated with the three indices also provide an indication as to the relative impact of the three identified risk sources. For example, the additional risk reduction attained using the inflation-linked value index as opposed to the value index linked to nominal interest rates is 10.3% in a book of 100,000 policyholders. Therefore, when hedging annuity exposures where payments are tied to price levels, an index that reflects the inflation-linked nature of these obligations provides a material advantage over indices that fail to account for inflation. Similarly, we observe a difference of over 22% between the inflation-linked value index and the standard survival rate index, suggesting that retirement income providers who pursue survivor swaps when hedging inflation-linked liabilities would experience significant basis risk due to the inability of survival indices to account for inflation or interest rate risk.

**Figure 5.7:** Longevity risk reduction: % reduction in variance (joint ATSM)

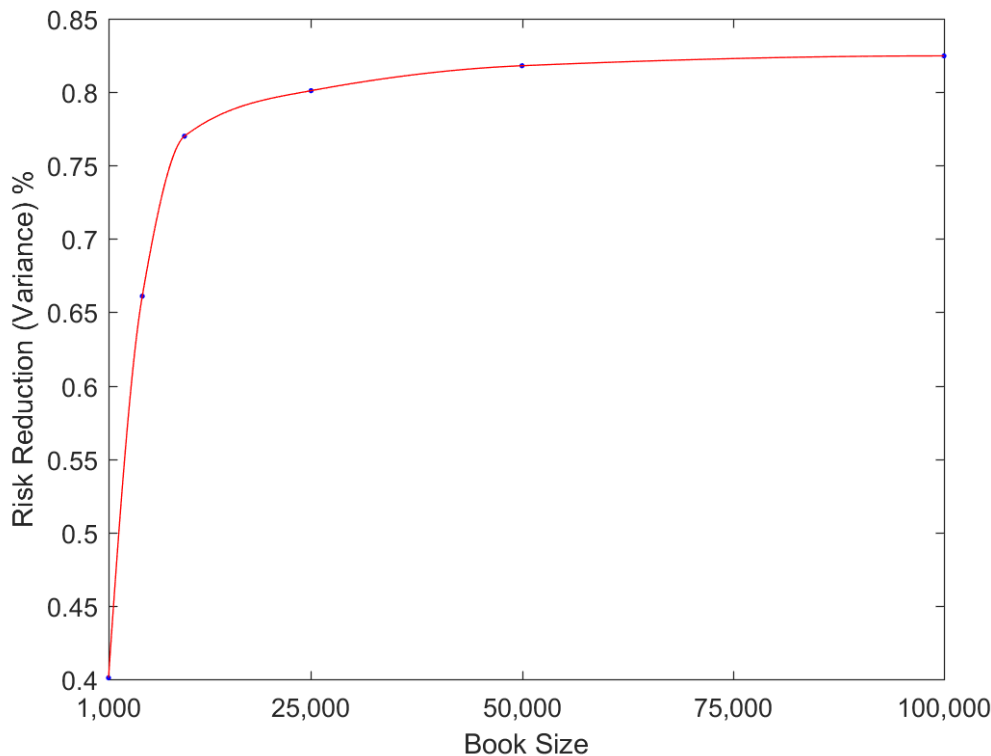
## 5.5 Sensitivity Analysis

It is critical to assess the significance of various modelling assumptions and experimental design settings. Following the template of Li et al. (2017), robustness checks are performed on various aspects of the modelling framework and methodological process to examine the potential impact of different assumption settings on hedge outcomes. In each of the following cases, one key experimental variable is changed, while all other factors and settings are held constant.

### 5.5.1 Book Size

It is well established in the literature (see, for example, Villegas et al., 2017; Li et al., 2017; Chang and Sherris, 2018) that the effectiveness of index-based longevity hedges are greater for larger book sizes. Indeed, this is also evidenced in our analysis. It occurs because in larger retirement income portfolios, sampling basis risk lacks the sufficient leverage to materially impact aggregate hedge outcomes. To more closely examine the relationship between portfolio size and longevity risk reduction, we test our hedging framework utilising the inflation-linked value-based longevity index in portfolio sizes of 1,000, 5,000, 10,000, 25,000, 50,000 and 100,000 lives. The LRR outcomes attained at these book sizes are plotted in Figure 5.8.

It appears that while hedge efficiency improves at a significant rate up until about

**Figure 5.8:** Hedge efficiency by book size (joint ATSM)

10,000 lives, the impact of sampling basis risk on portfolio hedging outcomes becomes progressively smaller for larger pension pools, with minimal marginal benefits extracted when increasing the book size beyond 50,000 lives.

### 5.5.2 Discrete-Time Mortality Model

In order to evaluate the potential impact of model risk on hedging outcomes, we repeat our analysis using the simulation and forecasting results generated by the discrete-time M7-M5 mortality model described in Section 3.2. This facilitates the comparison of the two mortality modelling frameworks and bridges the literature gap between continuous-time and discrete-time multi-population mortality modelling techniques. As in the previously presented example, we assume that a retirement income provider is aiming to hedge the risks associated with a pool of 65 year old males who are promised \$1 of inflation-indexed income per year upon survival from ages 66 to 85. In this analysis, the simulated interest rate paths are controlled from the results presented for the continuous-time analysis.

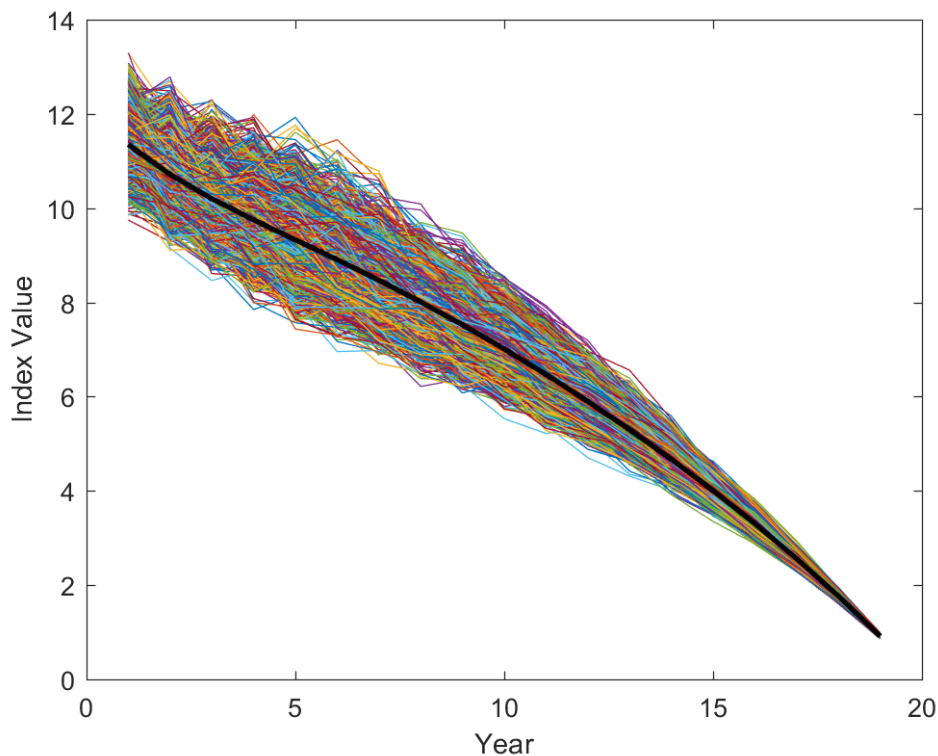
The plot of forward and simulated index values are provided in Figure 5.9. We note consistent features to the corresponding plot for the joint ATSM in Figure 5.2:

- the forward/expected index values (represented by the black curve) declines in a smooth, predictable manner and remains towards the centre of the distri-

bution of simulated index values, and

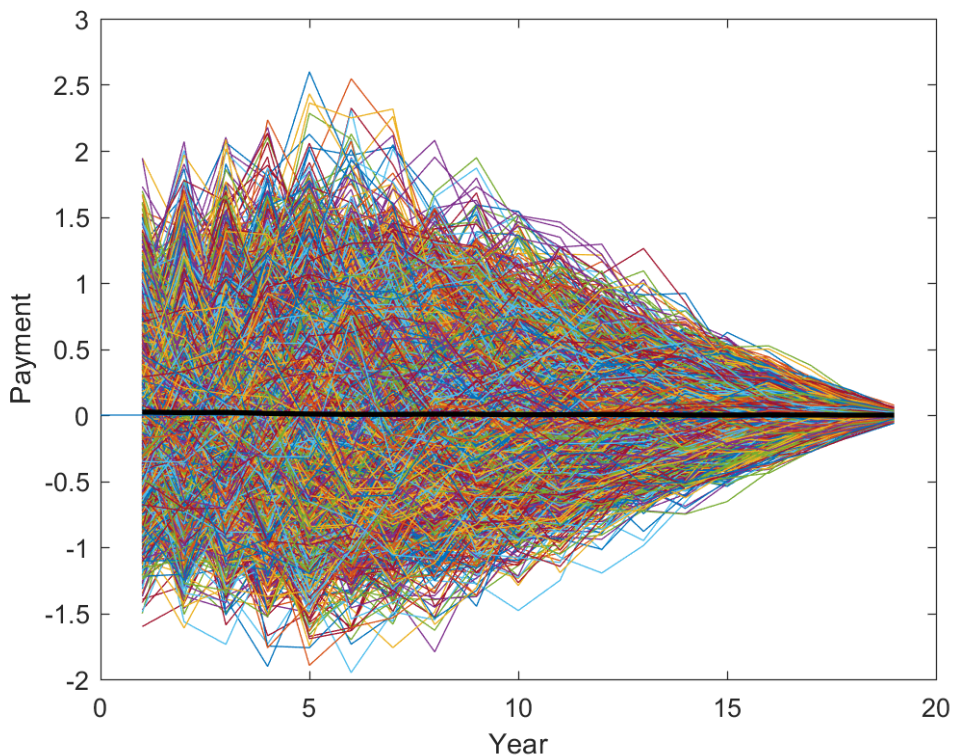
- the simulated index values show a material degree of variation about the forward values, with the variation highest in the early years and gradually declining over time.

**Figure 5.9:** Forward and simulated index values, (M7-M5 model)



The graph of simulated net swap payments made by the fixed leg payer is presented in Figure 5.10. As with the joint ATSM, the average swap payment (the black line) remains effectively zero throughout the term of the swap, reflecting the setting of forward values to the expected index values.

The histogram showing 5,000 simulated liability present value outcomes for a portfolio of 100,000 initial policyholders is presented in Figure 5.11. As was the case for the continuous-time joint ATSM, a degree of positive skewness is evident in the distribution. Figure 5.12 indicates the liability present value histograms once they have been hedged to the various longevity indices, while Figure 5.13 presents the associated box and whisker plots. From these graphical representations, in addition to the LRR metrics presented in Figure 5.14 and the summary statistics detailed in Table 5.3, we do not observe a material difference between the continuous and discrete-time mortality modelling frameworks in the analysis of hedge effectiveness. For example, for the inflation-linked value-based longevity index, the observed LRR

**Figure 5.10:** Simulated swap payments (M7-M5 model)

metric is 83.42% for a portfolio size of 100,000 with an associated swap weight parameter of  $w_0 = 0.3307$  – highly comparable to the corresponding values of 82.47% and  $w_0 = 0.3268$  from the joint ATSM.

**Table 5.3:** Summary statistics: hedged and unhedged liability present value outcomes by hedging index (M7-M5 model, 100,000 lives)

Hedging Index	Minimum	Maximum	Mean	Variance
Unhedged	9.13	17.79	12.68	1.26
Survival index $I_{x,t}^0$	9.87	14.94	12.51	0.50
Nominal-linked value index $I_{x,t}^1$	10.21	14.74	12.54	0.38
Inflation-linked value index $I_{x,t}$	10.72	14.52	12.52	0.23

Having estimated both a continuous-time and a discrete-time mortality modelling framework, we are also able to examine the stability of hedging outcomes when the alternate model is used to calibrate the notional swap parameter  $w_0$ . That is, we can estimate the swap weight using the discrete-time mortality model and use this weighting to compute the hedging outcomes associated with the value-based longevity index under the continuous-time mortality framework (and vice versa). We find that the sensitivity of risk reduction outcomes to this variation in hedge calibration method is very limited. As shown in Table 5.4, for the continuous-time

**Figure 5.11:** Liability present value distributions histogram, (M7-M5 model, 100,000 lives)

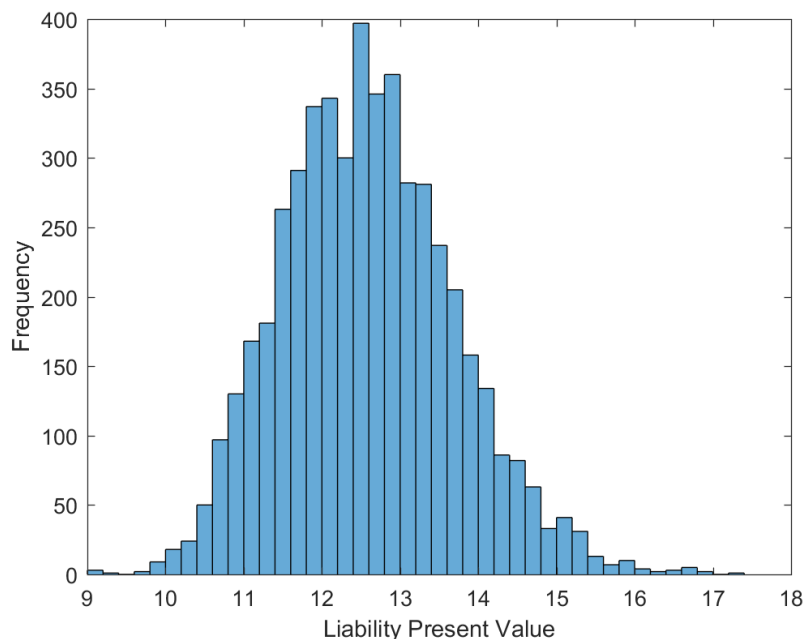
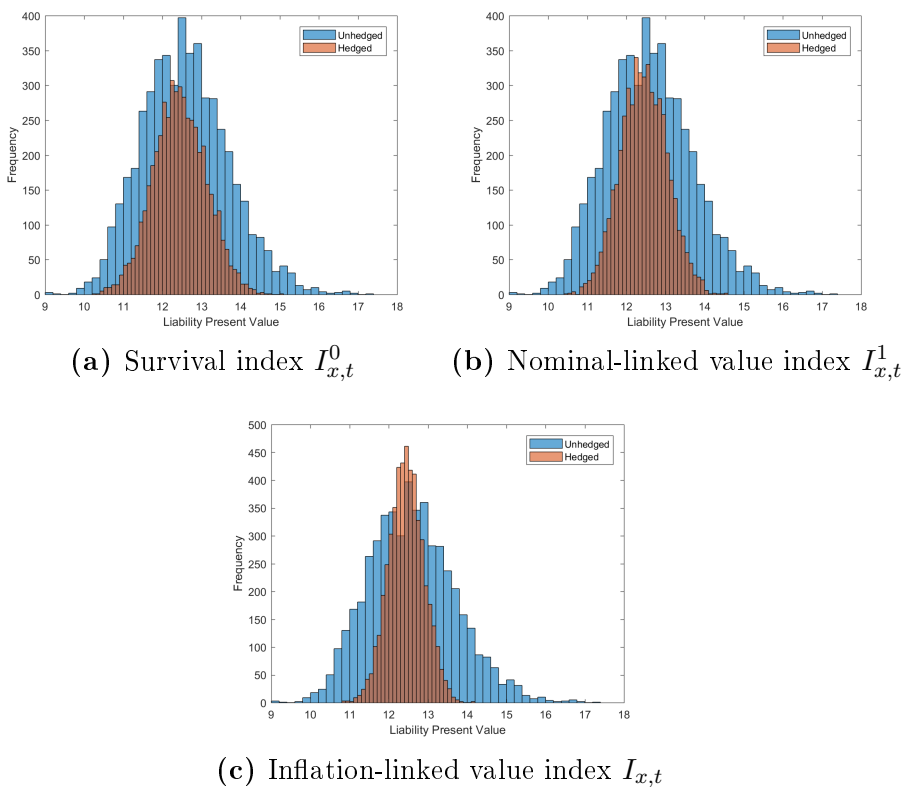
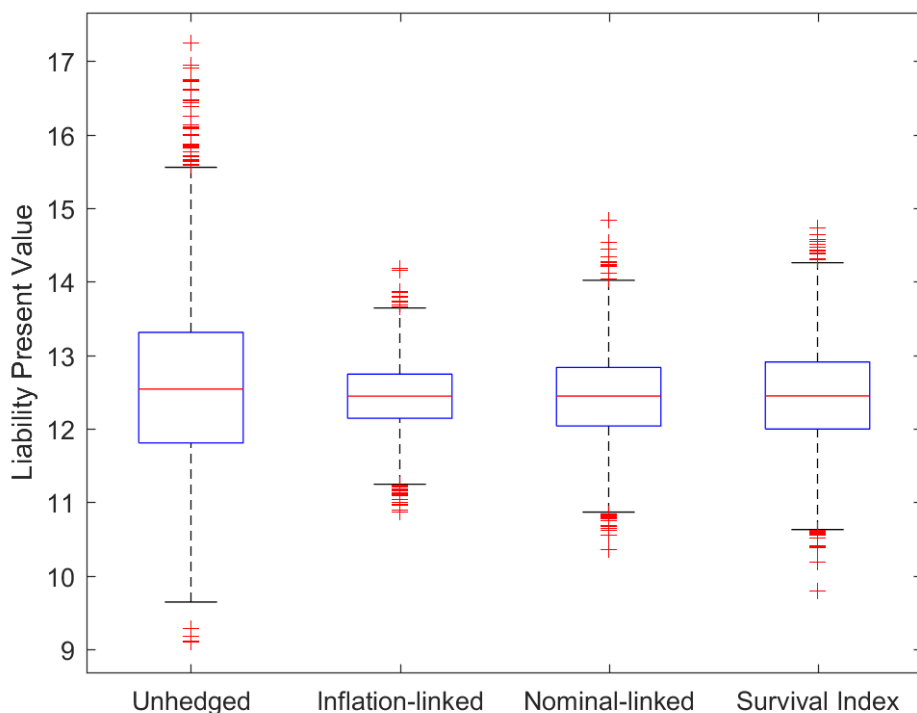


**Figure 5.12:** Hedged and unhedged liability present value distributions by hedging index (M7-M5 model, 100,000 lives)



and discrete-time mortality models, the reduction in hedging efficiency is minimal when the other model is used to compute  $w_0$  – a result that is not unexpected

**Figure 5.13:** Hedged and unhedged liability present value box and whisker plots by hedging index (M7-M5 model, 100,000 lives)



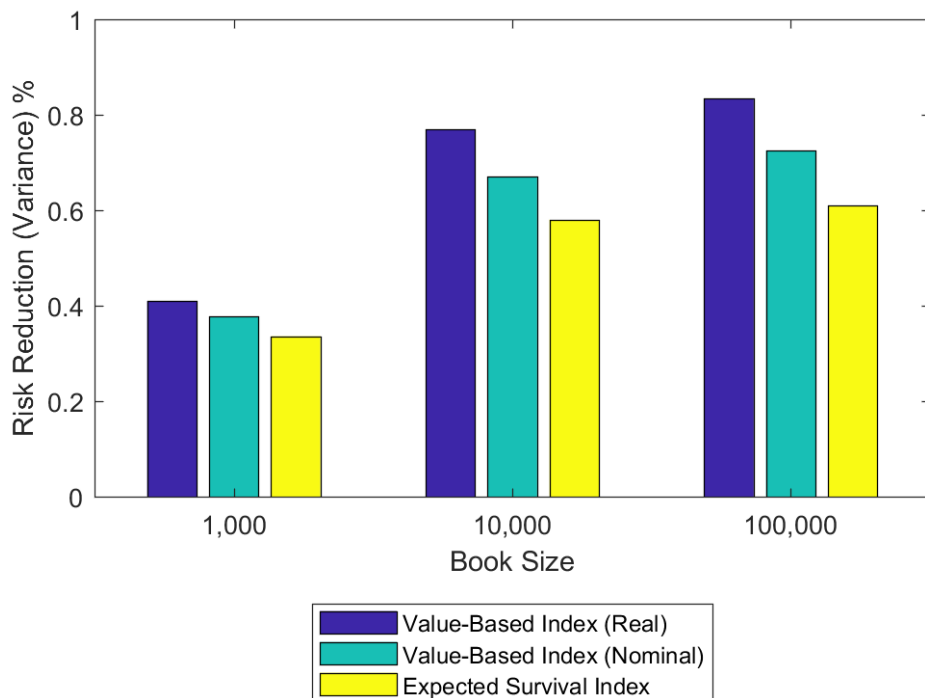
given the similar swap weight parameters obtained by the two different mortality modelling frameworks.

**Table 5.4:** Model hedge effective comparison (% reduction in variance, 100,000 lives)

	Joint ATSM	M7-M5 model
$w_0$ calibrated by same model	82.47%	83.42%
$w_0$ calibrated by alternate model	82.13%	83.21%

### 5.5.3 Extending to Age 90

The book population mortality dataset is derived from state-level statistics obtained from the CDC. One of the limitations of this approach is that the CDC's deaths and exposure data does not extend beyond age 85, meaning that the retirement income portfolios analysed in the previous sections represent pools of term annuities where the final payment occurs at age 85 as we lack the requisite data at older ages to reliably train the mortality models. However, it is at these older ages where longevity risk is most significant as the future improvement in mortality rates is more unpredictable.

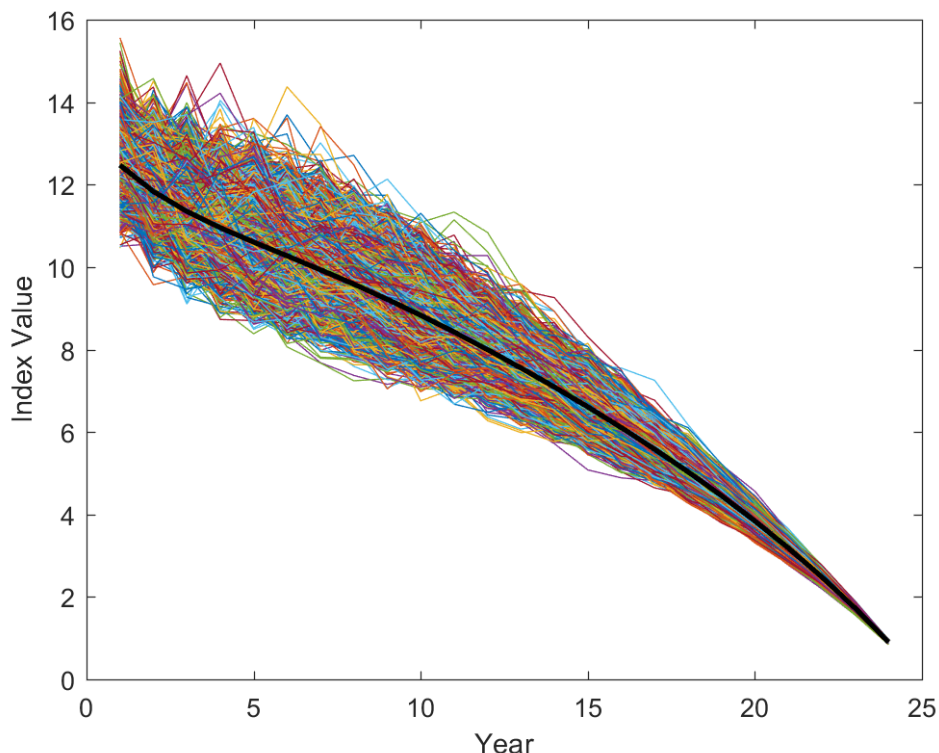
**Figure 5.14:** Longevity risk reduction: % reduction in variance (M7-M5 model)

Therefore it is informative to extend our analysis beyond age 85 using the estimated parameters of the continuous-time joint ATSM in conjunction with the simulated mortality factors to generate future mortality rate simulations despite our inability to observe empirical book population mortality data at these older age ranges. In particular, we extend our basis risk analysis to retirement income portfolios where members receive \$1 of inflation-indexed income per annum upon survival from ages 66 to 90, reflecting the age range considered by the LBRWG publications.

The graph of simulated and forward index values for the reference population cohort initially aged 65 is presented in Figure 5.15. Figure 5.16 shows the associated net swap payments made by the payer of the fixed leg to an index swap with a 24 year term. As with the case of swap cashflows for a cohort whose promised payments cease at age 85, the average swap payment remains effectively zero at all future years when the age range is extended to 90.

The liability present value histogram for an annuity pool whose promised payments now extend to age 90 is presented in Figure 5.18. When these liabilities are hedged using the inflation-linked value-based longevity index swap instrument, the liability present value once again shows a material reduction in volatility relative to the unhedged portfolio. The computed LRR measure is 79.38%. Therefore, this does represent a minor decrease relative to the analyses ceasing at age 85 (LRR measures of 82.47% and 83.42% when computed using the continuous and discrete-time

**Figure 5.15:** Forward and simulated index values (joint ATSM extended to age 90)



mortality modelling frameworks, respectively). A possible explanation is that over longer time horizons, demographic and sampling basis risk attain greater leverage to materially impede hedging performance. However, given that the joint ATSM has not been trained on ages beyond 85, the results presented in this sensitivity analysis are subject to a degree of estimation risk.

In this chapter, we have demonstrated that the universal value-based longevity index facilitates superior hedging outcomes relative to standard survival rate indices, such as those examined by the LBRWG. Furthermore, we have used this index to attribute the risks arising from retirement income portfolios into longevity risk, interest rate risk and inflation risk components. Finally, we have conducted a range of sensitivity analyses on the hedging results, demonstrating that our findings can vary among retirement income portfolios of differing size, but are robust across different age ranges and mortality modelling frameworks.

**Figure 5.16:** Simulated swap payments (joint ATSM extended to age 90)

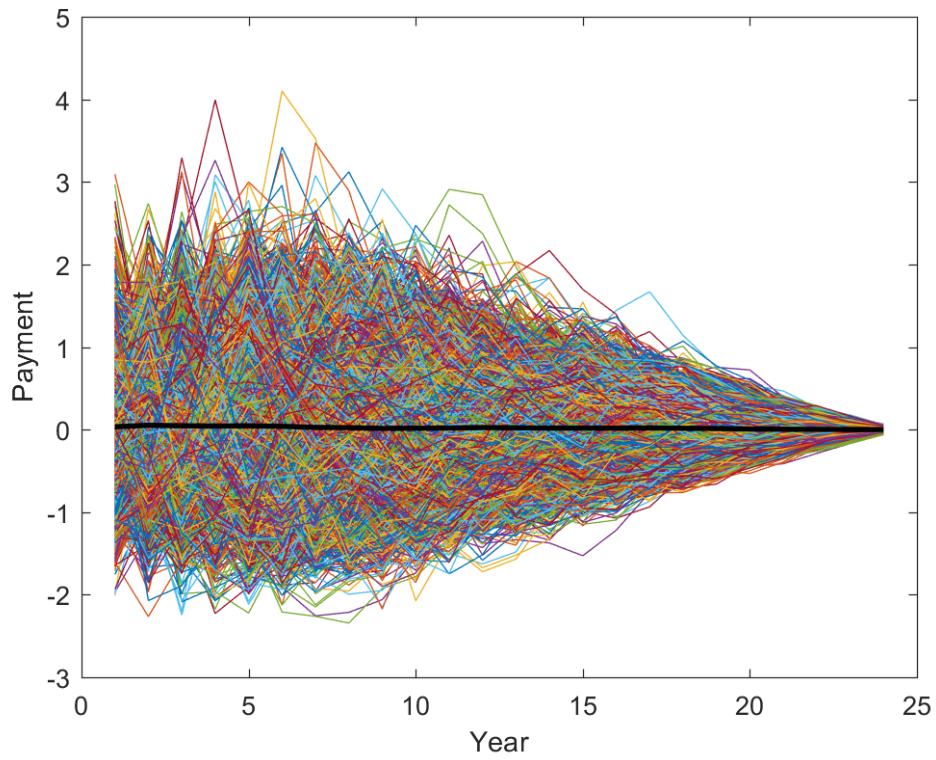


**Figure 5.17:** Liability present value histogram (joint ATSM extended to age 90, 100,000 lives)

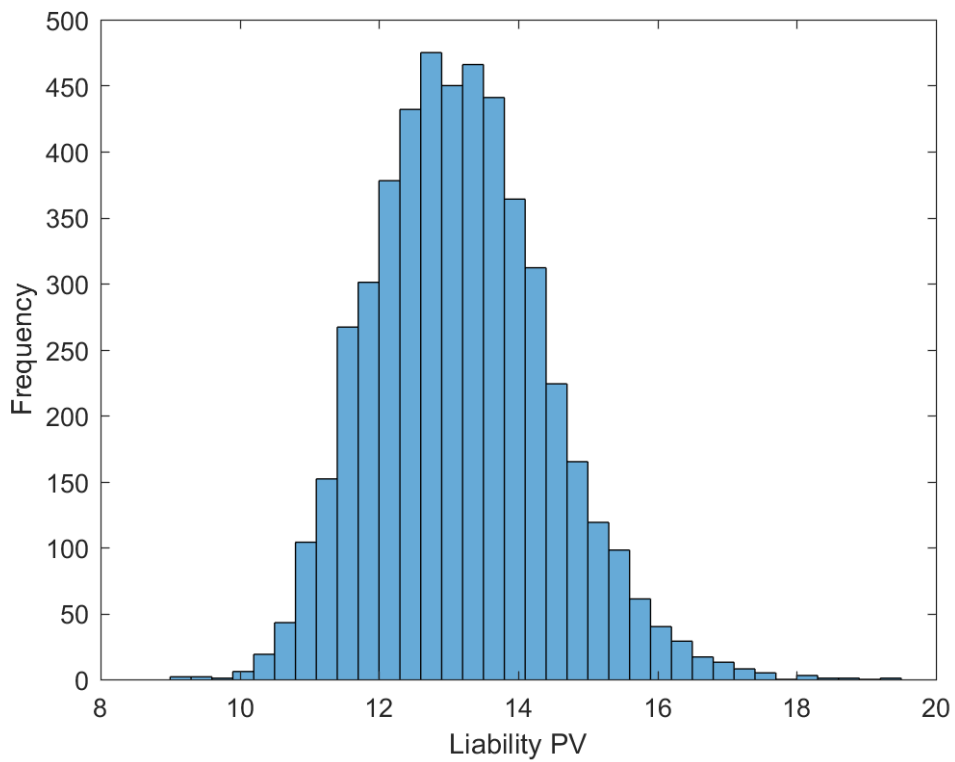
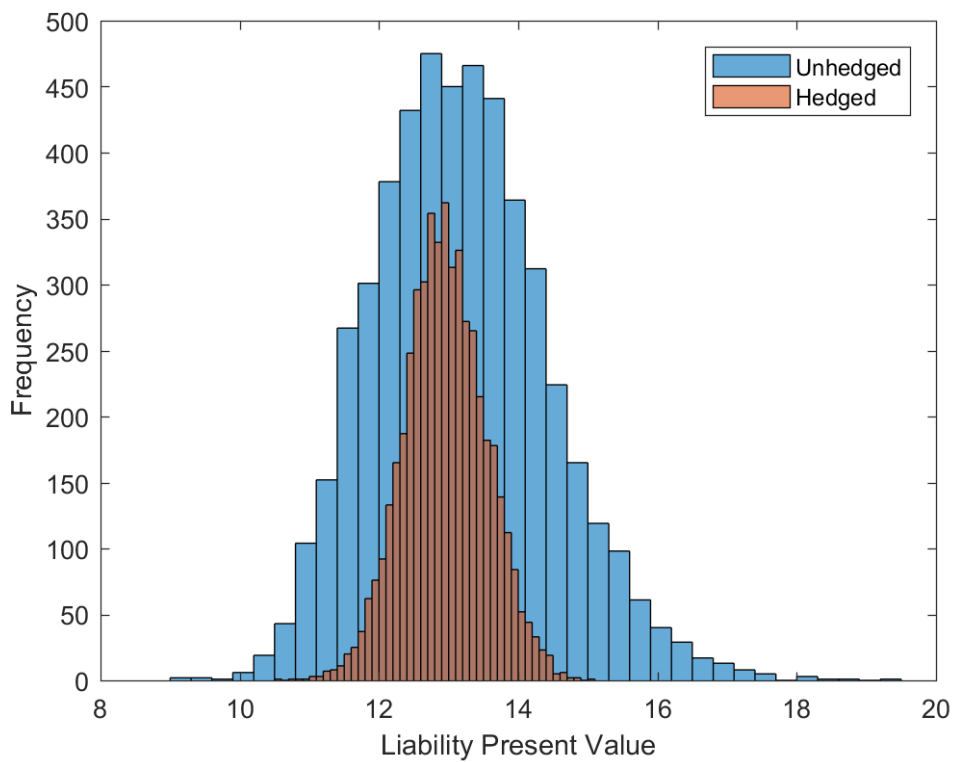


**Figure 5.18:** Hedged and unhedged liability present value distributions – inflation-linked value index (joint ATSM extended to age 90, 100,000 lives)



# Chapter 6

## Conclusion

This chapter concludes this thesis by reiterating our key research findings and contributions to the literature. We also explain the theoretical and practical limitations of our research methodology and identify potential avenues for future research to extend our work.

### 6.1 Key Contributions

In this thesis, we have made a threefold contribution to the literature. These contributions are motivated by the fundamental aim of supporting and accelerating the practice of index-based longevity hedging for retirement income portfolio risk exposures.

#### 6.1.1 Construction of a Universal Value-Based Longevity Index

We have constructed a universal value-based longevity index whose functionality is illustrated with the aid of U.S. economic and mortality data. The index is defined as the expected present value of a unit of longevity and inflation-indexed income, thereby incorporating both interest rate and inflation risk unlike other value-based longevity indices constructed in the literature. This contribution demonstrates how the market can design an index that closely tracks the value of longevity-linked liabilities – a critical requirement for the development of a viable, liquid longevity risk transfer market.

Furthermore, the construction of the value-based longevity index has facilitated the attribution of risk arising from retirement income portfolios into distinct longevity risk, interest rate risk and inflation risk components.

### **6.1.2 Decomposed Longevity Basis Risk Quantification for Hedge Comparisons**

We have also drawn on key aspects of the LBRWG’s longevity basis risk quantification framework to demonstrate that hedges referencing the value-based longevity index generate material reductions in basis risk relative to survivor swap instruments based on standard mortality rate indices such as the Lifemetrics Index. Indeed, the minimisation and robust quantification of longevity basis risk represents a critical element in establishing the credibility of longevity-linked securities as viable risk management instruments for retirement income providers. Additionally, the application of the LBRWG’s basis risk quantification framework to a value-based longevity index marks the filling of another key gap in the literature.

### **6.1.3 Comparison of Continuous-Time and Discrete-Time Multi-Population Mortality Modelling Frameworks**

Our third contribution is the comparison of the continuous-time multi-population mortality modelling techniques introduced by Xu et al. (2017) to the discrete-time M7-M5 multi-population mortality model advocated by the LBRWG. Despite the differing approaches developed by these authors for modelling the relationship between the mortality patterns of multiple populations, our analysis indicates that the two frameworks suggest relatively similar outcomes when hedging retirement income portfolios by means of index-based swap instruments.

Ultimately by making these contributions to the literature, our research has the potential to support the transition towards index-based longevity hedging. This is of critical importance since index-based longevity hedging represents arguably the most realistic prospect for a viable and liquid longevity risk transfer market, given all of the complexities associated with indemnity-based longevity hedges.

## **6.2 Limitations and Areas for Future Research**

### **6.2.1 Book Population Data**

Our book population is constructed from a synthetic dataset under the assumption that the aggregation of high income states sufficiently approximates the demographics of a typical retirement income portfolio. This approach has been opted for on account of being unable to obtain time series deaths and exposure data for U.S. annuity holders. However, this is clearly an imperfect method of obtaining book population data. Future research that is able to engage authentic retirement income portfolio mortality data would further enhance the credibility of index-based

longevity hedging as a viable long-term solution for the management of longevity risk.

Furthermore, given that longevity risk is most significant and unpredictable at the oldest ages, annuitant mortality datasets that extend beyond age 85 would facilitate a more robust evaluation of value-based index hedging frameworks for whole-of-life retirement income stream products.

## 6.2.2 Application to Realistic Retirement Income Portfolios

In our research methodology, the longevity hedging strategy considers a closed portfolio where all members are aged  $x$  years at initial time  $t$  and are of the same gender. That is, the fund consists of a single cohort of 65 year old males with no subsequent additions to the scheme over time.

This is not reflective of retirement income portfolios in practice which consist of both males and females and a range of different ages, while also remaining open for new members to join. Such scenarios would require more complex hedging methods involving multiple different longevity swap contracts and more intensive hedge calibration and optimisation techniques. Therefore, our research methodology is limited in the sense that, although we demonstrate that the value-based longevity index is materially superior to mortality rate indices for hedging purposes, the context in which we conduct our analyses is a highly simplified version of real-life retirement income portfolios. There is scope for future research to extend the hedging framework to book portfolios that are more analogous to those in practice.

## 6.2.3 Dynamic Hedging

The approach in this thesis represents a static hedging framework. That is, a strategy that is constructed at the outset and does not require periodic rebalancing or recalibration in response to evolving market conditions or mortality experience. Ngai and Sherris (2011) note that static hedging is more appropriate and practical given the lack of liquidity in the longevity risk transfer market. However, as the market for longevity-linked instruments continues to develop and mature over time, there is potential to further reduce longevity basis risk in a dynamic hedging framework which offers greater flexibility. Therefore, the performance of index-based longevity hedging using value-based longevity indices within a dynamic hedging framework remains an area for future research. Furthermore, comparisons between the outcomes of dynamic and static hedging strategies may also be of interest for retirement income providers.

## 6.2.4 Incorporation of the Longevity Risk Premium

We do not account for the market price of longevity risk in our research. In practice, counterparties to longevity hedging transactions would require a risk premium to compensate them for absorbing a retirement income provider's longevity risk exposure. Although risk premiums do not affect the computation of the value-based longevity index nor the degree of basis risk from associated hedges, the incorporation of the the market price of longevity risk into the hedging framework would allow retirement income providers to more informatively analyse the trade off between the lower cost of index-based longevity hedging against the residual basis risk exposure.

## 6.2.5 Further Sensitivity Analyses

There is scope to incorporate further sensitivity analyses into our research. For example, Li et al. (2017) also model the potential impact of structural changes in mortality, mortality jumps and alternate data fitting periods on the degree of risk reduction achieved by standardised index-based longevity hedges. More broadly, one could consider other national populations in addition to the U.S. in future works.

# References

- D. Anderson and S. Baxter. Longevity risk transfer. In *The Palgrave Handbook of Unconventional Risk Transfer*, pages 375–434. Springer, 2017.
- Artemis. Bt pension scheme in record £16 billion longevity swap transaction. <http://www.artemis.bm/blog/2014/07/04/bt-pension-scheme-in-record-16-billion-longevity-swap-transaction/>, 2014.
- Artemis. Longevity swaps and longevity risk transfer transactions. [www.artemis.bm/library/longevity\\_swaps\\_risk\\_transfers.html](http://www.artemis.bm/library/longevity_swaps_risk_transfers.html), 2018.
- P. Barrieu, H. Bensusan, N. El Karoui, C. Hillairet, S. Loisel, C. Ravanelli, and Y. Salhi. Understanding, modelling and managing longevity risk: key issues and main challenges. *Scandinavian actuarial journal*, 2012(3):203–231, 2012.
- E. Biffis. Affine processes for dynamic mortality and actuarial valuations. *Insurance: Mathematics and Economics*, 37(3):443–468, 2005.
- C. Blackburn and M. Sherris. Consistent dynamic affine mortality models for longevity risk applications. *Insurance: Mathematics and Economics*, 53(1):64–73, 2013.
- BlackRock. The BlackRock CoRI Retirement Indexes. <https://www.blackrock.com/cori/fact-sheets>, 2018.
- D. Blake and W. Burrows. Survivor bonds: Helping to hedge mortality risk. *Journal of Risk and Insurance*, pages 339–348, 2001.
- D. Blake, A. Cairns, K. Dowd, et al. Still living with mortality: the longevity risk transfer market after one decade. <https://www.actuaries.org.uk/documents/still-living-mortality-longevity-risk-transfer-market-after-one-decade>, 2018.

- D. P. Blake, A. De Waegenare, R. D. MacMinn, and T. Nijman. Longevity risk and capital markets: The 2008-2009 update. *Insurance: Mathematics and Economics*, 46(1):135–138, 2009.
- A. Cairns, K. Dowd, D. Blake, and G. D. Coughlan. Longevity hedge effectiveness: A decomposition. *Quantitative Finance*, 14(2):217–235, 2014.
- A. J. Cairns, D. Blake, and K. Dowd. A two-factor model for stochastic mortality with parameter uncertainty: theory and calibration. *Journal of Risk and Insurance*, 73(4):687–718, 2006.
- A. J. Cairns, D. Blake, and K. Dowd. Modelling and management of mortality risk: a review. *Scandinavian Actuarial Journal*, 2008(2-3):79–113, 2008.
- A. J. Cairns, D. Blake, K. Dowd, G. D. Coughlan, D. Epstein, A. Ong, and I. Balevich. A quantitative comparison of stochastic mortality models using data from england and wales and the united states. *North American Actuarial Journal*, 13(1):1–35, 2009.
- A. J. Cairns, D. Blake, K. Dowd, G. D. Coughlan, D. Epstein, and M. Khalaf-Allah. Mortality density forecasts: An analysis of six stochastic mortality models. *Insurance: Mathematics and Economics*, 48(3):355–367, 2011.
- Centers for Disease Control and Prevention. Underlying cause of death, 1999-2016 request. <https://www.cdc.gov/>, 2018.
- W.-S. Chan, J. S.-H. Li, and J. Li. The cbd mortality indexes: Modeling and applications. *North American Actuarial Journal*, 18(1):38–58, 2014.
- W.-S. Chan, J. S. Li, K. Q. Zhou, and R. Zhou. Towards a large and liquid longevity market: A graphical population basis risk metric. *The Geneva Papers on Risk and Insurance-Issues and Practice*, 41(1):118–127, 2016.
- Y. Chang and M. Sherris. Longevity risk management and the development of a value-based longevity index. *Risks*, 6(1):10, 2018.
- G. Coughlan. Longevity risk transfer: Indices and capital market solutions. *The Handbook of Insurance-Linked Securities*, pages 261–281, 2009.
- G. Coughlan. Hot topics in risk management: Longevity hedging. In *Paper presented at the Actuarial Profession’s Risk and Investment Conference, June*, pages 21–23, 2009a.

- G. Coughlan, D. Epstein, A. Sinha, and P. Honig. q-forwards: Derivatives for transferring longevity and mortality risks. *JPMorgan Pension Advisory Group, London, July, 2, 2007*.
- G. D. Coughlan, M. Khalaf-Allah, Y. Ye, S. Kumar, A. J. Cairns, D. Blake, and K. Dowd. Longevity hedging 101: A framework for longevity basis risk analysis and hedge effectiveness. *North American Actuarial Journal*, 15(2): 150–176, 2011.
- S. H. Cox and Y. Lin. Natural hedging of life and annuity mortality risks. *North American Actuarial Journal*, 11(3):1–15, 2007.
- Deutsche Börse. Deutsche Börse Xpect – Club Vita Indices Longevity risk of specific pensioner groups. <http://www.xpect-index.com/>, 2012.
- F. X. Diebold and C. Li. Forecasting the term structure of government bond yields. *Journal of econometrics*, 130(2):337–364, 2006.
- K. Dowd. Survivor bonds: a comment on blake and burrows. *Journal of Risk and Insurance*, 70(2):339–348, 2003.
- K. Dowd, D. Blake, A. J. Cairns, and P. Dawson. Survivor swaps. *Journal of Risk and Insurance*, 73(1):1–17, 2006.
- K. B. Dunn and J. J. McConnell. Valuation of gnma mortgage-backed securities. *The Journal of Finance*, 36(3):599–616, 1981.
- A. V. Egorov, H. Li, and D. Ng. A tale of two yield curves: Modeling the joint term structure of dollar and euro interest rates. *Journal of Econometrics*, 162(1):55–70, 2011.
- I. V. Girsanov. On transforming a certain class of stochastic processes by absolutely continuous substitution of measures. *Theory of Probability & Its Applications*, 5(3):285–301, 1960.
- G. Graziani. Longevity risk—a fine balance. *Special Issue on Pension and Longevity Risk Transfer for Institutional Investors*, 2014(1):35–27, 2014.
- S. Haberman, P. Millosovich, V. Kaishev, A. Villegas, S. Baxter, A. Gaches, S. Gunnlaugsson, and M. Sison. Longevity basis risk a methodology for assessing basis risk. <https://www.actuaries.org.uk/documents/longevity-basis-risk-methodology-assessing-basis-risk>, 2014.
- Human Mortality Database. USA - Complete Data Series. [www.mortality.org/](http://www.mortality.org/), 2018.

Institute and Faculty of Actuaries. Longevity risk policy summary. <https://www.actuaries.org.uk/documents/policy-summary-longevity-risk-december-2015>, 2015.

International Monetary Fund. Global financial stability report. *World Economic and Financial Surveys*, 2012.

Joint Forum. Longevity risk transfer markets: market structure, growth drivers and impediments, and potential risks. <https://www.bis.org/publ/joint31.pdf>, 2013.

J.P. Morgan. LifeMetrics: A toolkit for measuring and managing longevity and mortality risks. [https://www.jpmorgan.com/cm/BlobServer/lifemetrics\\_technical.pdf?blobcol=urldata&blobtable=MungoBlobs&blobkey=id&blobwhere=1158472448701&blobheader=application%2Fpdf](https://www.jpmorgan.com/cm/BlobServer/lifemetrics_technical.pdf?blobcol=urldata&blobtable=MungoBlobs&blobkey=id&blobwhere=1158472448701&blobheader=application%2Fpdf), 2007.

R. E. Kalman. A new approach to linear filtering and prediction problems. *Journal of Basic Engineering*, 82(1):35–45, 1960.

J.-P. Lee and M.-T. Yu. Valuation of catastrophe reinsurance with catastrophe bonds. *Insurance: Mathematics and Economics*, 41(2):264–278, 2007.

R. D. Lee and L. R. Carter. Modeling and forecasting us mortality. *Journal of the American Statistical Association*, 87(419):659–671, 1992.

J. Li and S. Haberman. On the effectiveness of natural hedging for insurance companies and pension plans. *Insurance: Mathematics and Economics*, 61: 286–297, 2015.

J. Li, J. S.-H. Li, L. Tickle, and C. I. Tan. Assessing basis risk for longevity transactions. <https://www.actuaries.org.uk/documents/longevity-basis-risk-phase-2-report>, 2017.

J. S.-H. Li and M. R. Hardy. Measuring basis risk in longevity hedges. *North American Actuarial Journal*, 15(2):177–200, 2011.

J. S.-H. Li, R. Zhou, and M. Hardy. A step-by-step guide to building two-population stochastic mortality models. *Insurance: Mathematics and Economics*, 63:121–134, 2015.

N. Li and R. Lee. Coherent mortality forecasts for a group of populations: An extension of the lee-carter method. *Demography*, 42(3):575–594, 2005.

Life and Longevity Markets Association. Technical note: The s-forward. [www.llma.org](http://www.llma.org), 2010.

- J. Loeys, N. Panigirtzoglou, and R. M. Ribeiro. Longevity: A market in the making. [https://www.jpmorgan.com/cm/BlobServer/lifemetrics\\_technical.pdf?blobcol=urldata&blobtable=MungoBlobs&blobkey=id&blobwhere=1158472448701&blobheader=application%2Fpdf](https://www.jpmorgan.com/cm/BlobServer/lifemetrics_technical.pdf?blobcol=urldata&blobtable=MungoBlobs&blobkey=id&blobwhere=1158472448701&blobheader=application%2Fpdf), 2007.
- H. Markowitz. Portfolio selection. *The Journal of Finance*, 7(1):77–91, 1952.
- J. Mosher and P. Sagoo. Longevity: Parallels with the past. <http://www.theactuary.com/archive/old-articles/part-4/longevity-3A-parallels-with-the-past/>, 2011.
- A. Ngai and M. Sherris. Longevity risk management for life and variable annuities: The effectiveness of static hedging using longevity bonds and derivatives. *Insurance: Mathematics and Economics*, 49(1):100–114, 2011.
- J. Oeppen and J. W. Vaupel. Broken limits to life expectancy. <http://science.sciencemag.org/content/296/5570/1029>, 2002.
- R. Ribeiro and V. di Pietro. Longevity risk and portfolio allocation. <https://www.jpmorgan.com/cm/BlobServer/longevityrisk.pdf?blobcol=urldata&blobtable=MungoBlobs&blobkey=id&blobwhere=1158542080885&blobheader=application%2Fpdf>, 2009.
- M. Sherris. Australian longevity index: A technical note. <https://www.business.unsw.edu.au/research-site/australianinstituteofpopulationageingresearch-site/Documents/M.%20Sherris%20-%20Australian%20Longevity%20Index%20-%20A%20Technical%20Note.pdf>, 2009.
- Small Area Income and Poverty Estimates Program. Saipе datasets. <https://www.census.gov/en.html>, 2018.
- P. Sweeting. Longevity indices and pension fund risk. <https://kar.kent.ac.uk/47883/>, 2010.
- C. I. Tan, J. Li, J. S.-H. Li, and U. Balasooriya. Parametric mortality indexes: From index construction to hedging strategies. *Insurance: Mathematics and Economics*, 59:285–299, 2014.
- K. Tan, D. Blake, and R. MacMinn. Longevity risk and capital markets: The 2013-14 update. [https://uwaterloo.ca/center-of-actuarial-excellence/sites/ca.center-of-actuarial-excellence/files/uploads/files/longevity\\_9\\_editorial\\_ime\\_final.pdf](https://uwaterloo.ca/center-of-actuarial-excellence/sites/ca.center-of-actuarial-excellence/files/uploads/files/longevity_9_editorial_ime_final.pdf), 2015.

Towers Watson. Longevity hedging the next stop on your ldi journey. <https://www.towerswatson.com/DownloadMedia.aspx?media=%7B5D249CF2-99D5-42CF-8D8D-B3EF349427F9%7D>, 2013.

Trading Risk. JP Morgan longevity swap unlocks UK annuity market. <https://www.trading-risk.com/articles/61877/jpmorgan-longevity-swap-unlocks-uk-annuity-market>, 2008.

A. M. Villegas, S. Haberman, V. K. Kaishev, and P. Millosovich. A comparative study of two-population models for the assessment of basis risk in longevity hedges. *ASTIN Bulletin: The Journal of the IAA*, 47(3):631–679, 2017.

M. Wadsworth. The pension annuity market: Further research into supply and constraints. *Association of British Insurers, London*, 2005.

R. Wehrhahn. Longevity bonds or securitizing longevity. <http://slideplayer.com/slide/10968001/>, 2005.

Willis Towers Watson. Global pension assets study 2018. <https://www.willistowerswatson.com/-/media/WTW/Images/Press/2018/01/Global-Pension-Asset-Study-2018-Japan.pdf>, 2018.

S. Wills and M. Sherris. Securitization, structuring and pricing of longevity risk. *Insurance: Mathematics and Economics*, 46(1):173–185, 2010.

Y. Xu, M. Sherris, and J. Ziveyi. Market price of longevity risk for a multi-cohort mortality model with application to longevity bond option pricing. In *Workshop: Risk: Modelling*, 2017.